

A Novel Statistical Framework for Assessment of Intraspecific Haplotype

Sampling Completeness

by

Jarrett D. Phillips

A Thesis
presented to
The University of Guelph

In partial fulfilment of requirements
for the degree of
Doctor of Philosophy
in
Computational Sciences

Guelph, Ontario, Canada

©Jarrett D. Phillips, April, 2021

ABSTRACT

A NOVEL STATISTICAL FRAMEWORK FOR ASSESSMENT INTRASPECIFIC HAPLOTYPe SAMPLING COMPLETENESS

Jarrett Daniel Phillips
University of Guelph, 2019

Co-Advisors:
Dr. Daniel Gillis and Dr. Robert Hanner

The problem of determining adequate sample sizes necessary for studies of biodiversity conservation and management is a challenging one that has received some attention in recent years. One particular area where the probing of sampling completeness is of utmost priority is DNA barcoding. Because species show remarkable genomic marker variation within and among taxa, along with differing evolutionary and life histories, knowing how many specimens of a given species likely need to be collected to observe the majority of standing COI haplotype diversity present within animal species is complex question to answer. Estimates of specimen sample sizes for DNA barcoding range from a single to hundreds of individuals per species (but typically around 5-10 individuals). However, due to obstacles surrounding project funding and species rarity, often just one or two specimens per species can be reasonably collected. In addition, numerous other factors, especially sequence quality and integrity, hinder the accurate and reliable estimation of specimen sample sizes from existing species-level sequence data found in large DNA repositories.

Here, a deep examination of the genetic specimen sample size problem (GSSSP) is undertaken. Specifically, a novel nonparametric stochastic local search optimization algorithm based on trends in species haplotype accumulation curves, herein called HACS_{im}

(**Haplotype Accumulation Curve Simulator**) is introduced. The method, available as an R package, is tested on a variety of both hypothetical and real animal species mined from the Barcode of Life Data Systems (BOLD). Through a detailed statistical simulation study, the approach is demonstrated to work well across all examined scenarios. As HACSim makes numerous simplifying assumptions that are unlikely to hold well in practice, such as panmixia (random mating), future work in incorporating elements of population structure is imperative.

In addition, it is argued that DNA barcoding currently lacks in statistical rigor needed to robustly estimate the DNA barcode gap. A number of accessible statistical solutions revolving around sample sizes needed for gap assessment, as well as visualization and inference are offered in this regard.

ACKNOWLEDGEMENTS

First and foremost, I would like to acknowledge the support and guidance of my coadvisors, Drs. Dan Gillis and Bob Hanner for their encouragement over the years. In addition, thanks go out to all current and past members of the Gillis and Hanner Lab groups, particularly Rob Young for all the fun times that were had throughout the journey.

Secondly, I wish to thank Dr. Deb Stacey and Dr. Graham Taylor for serving on my advisory committee, graciously reading my individual manuscripts and the current thesis, as well as engaging in stimulating discussion during my many committee meetings and graduate seminars over the past four and a half or so years.

Third, I would like to recognize the tremendous efforts of both Steven French and Scarlett Bootsma for their interest and willingness to learn about the inner workings of the HACSim algorithm and assist with coding, debugging and simulation as part of their fourth year thesis projects.

Fourth, thanks to Sally Adamowicz and Rodger Gwiazdowski for providing valuable edits and comments to individual chapters, published or otherwise, found within this thesis.

Fifth, a big shout out goes out to graduate students in the Adamowicz, Hebert Hajibabaei and Steinke Labs for their friendships throughout the years, especially Jacopo D'Ercole and Mike Wright.

I sincerely apologize in advance to those whom I may have missed in acknowledging here. Just know that whatever your contribution, no matter how big or small, to my success in this endeavour, Thank You!

Lastly, I would like to thank my family for their love and encouragement throughout my journey into the vast unknown that is doctoral study. Now they can finally stop constantly asking: “When are you going to get your PhD.??”

This work was supported in part by a Graduate Excellence Entrance (GEE) Scholarship. Other sources of funding came from various travel grants which greatly aided the ability to attend and present my research at the 7th and 8th International Barcode of Life (iBOL) Conferences held in Kruger National Park, South Africa and Trondheim, Norway in 2017 and 2019 respectively.

Table of Contents

List of Tables	viii
List of Figures	x
1 Introduction	1
1.0.1 Thesis Overview	1
1.0.2 Thesis Statement	2
2 Incomplete estimates of genetic diversity within species: Implications for DNA barcoding	4
2.1 Introduction	6
2.2 Current Methods	11
2.2.1 Methods to Assess Haplotype Variation	11
Haplotype Diversity	11
Haplotype Networks	12
Haplotype Accumulation Curves	13
2.2.2 Sampling Models for Genetic Diversity Prediction	15
2.2.3 DNA Barcoding	17
2.2.4 The Importance of Sampling to DNA Barcoding	19
2.2.5 Consideration of Species' Life Histories	23
2.3 Key Findings	25
2.3.1 DNA Barcoding and Sample Size: Past Studies	25
2.4 Case Study: Phillips <i>et al.</i> (2015)	31
2.4.1 Model Assumptions	31
2.4.2 Mathematical Details	33
2.4.3 Application to Ray-finned Fishes	37
2.5 Future Prospects	39

3 HACSim: An R package to estimate intraspecific sample sizes for genetic diversity assessment using haplotype accumulation curves	45
3.1 Introduction	48
3.1.1 Background	48
3.1.2 Motivation	52
3.2 Methods	53
3.2.1 Haplotype Accumulation Curve Simulation Algorithm	53
Algorithm Functions	53
Algorithm Parameters	56
How Does HACSim Work?	61
3.3 Results	68
3.3.1 Application of HACSim to Hypothetical Species	69
Equal Haplotype Frequencies	69
Unequal Haplotype Frequencies	71
3.3.2 Application of HACSim to Real Species	74
Lake Whitefish (<i>Coregonus clupeaformis</i>)	74
Deer tick (<i>Ixodes scapularis</i>)	80
Scalloped hammerhead (<i>Sphyrna lewini</i>)	85
3.4 Discussion	89
3.4.1 Initializing HACSim and Overall Algorithm Behaviour	89
3.4.2 Additional Capabilities and Extending Functionality of HACSim . .	91
3.4.3 Summary	94
3.5 Conclusions	98
4 Solving the genetic specimen sample size problem for DNA barcoding with a local search optimization algorithm	102
4.1 Introduction	105
4.1.1 Background	105
4.1.2 Phillips <i>et al.</i> 's (2020) Haplotype Sampling Model	108
4.1.3 Assessing the Computational and Statistical Performance of HACSim	113
Background	113
Theory	114
4.1.4 Outline of the Current Study	119
4.2 Methods	119
4.2.1 Hypothetical Species	120
4.2.2 Real Species	122
Pea aphid (<i>Acyrtosiphon pisum</i>)	123
Common mosquito (<i>Culex pipiens</i>)	124
Gypsy Moth (<i>Lymantria dispar</i>)	125
4.2.3 Simulation Study	126
4.2.4 Statistical Analysis	128

4.3	Results and Discussion	130
4.3.1	Effect of Population Size	130
4.3.2	Algorithm Runtimes	134
4.4	Conclusion	135
5	Lack of statistical rigor in DNA barcoding likely invalidates the presence of a true species' barcode gap	165
6	Conclusion	166
6.0.1	Thesis Summary	166
References		169
A	Additional Information Accompanying Chapter 3	183
B	Additional Information Accompanying Chapter 4	184
C	Derivation of Approximate Confidence Interval for Sampling Sufficiency (θ) (Equation 3.3)	185

List of Tables

3.1	Parameters inputted (first 7) and outputted (last six) by <code>HAC.sim()</code> and <code>HAC.simrep()</code> , along with their definitions. Range refers to plausible values that each parameter can assume within the haplotype accumulation curve simulation algorithm. [and] indicate that a given value is included in the range interval; whereas, (and) indicate that a given value is excluded from the range interval. Simulation progress can be tracked through setting <code>progress = TRUE</code> within <code>HACHypothetical()</code> or <code>HACReal()</code> . Users can optionally specify that a file be created containing all information outputted to the R console (via the argument <code>filename</code> , which can be named as the user wishes).	57
4.1	Mean proportion of observed unique haplotypes found over 50 replications of the simulation study for hypothetical species. In all cases, HACSim was run 100 times. Estimates correspond to the solid red horizontal lines depicted in confidence interval plots found within Figures 15-23 and Supplemental Information accompanying the present article.	157
4.2	Mean proportion of observed unique haplotypes found over 50 replications of the simulation study for real species. In all cases, HACSim was run 100 times. Estimates correspond to the solid red horizontal lines depicted in confidence interval plots found within the Supplemental Information accompanying the present article.	158
4.3	Bonferroni-corrected Dunn's post-hoc test results at the 0.83% significance level for comparison of population size <i>versus</i> haplotype frequency distribution in hypothetical species. Note: KW test statistics, <i>p</i> -values and statistical significance for Scenario I could not be calculated.	159
4.4	Bonferroni-corrected Dunn's post-hoc test results at the 0.83% significance level for comparison of population size <i>versus</i> haplotype frequency distribution in real species.	160
4.5	Characteristics of local optima found by HACSim for hypothetical species..	161

4.6	Characteristics of local optima found by HACSim for real species. For some species, distinct optima were located for different population sizes. * corresponds to a population size of 1000 and ** to population sizes of 10000, 100000 and 10000000.	162
4.7	Coverage probabilities and 95% Clopper-Pearson confidence intervals for hypothetical species across all assessed population sizes. Calculated probabilities are based on the number of observed local optima found using HACSim. . .	163
4.8	Coverage probabilities and 95% Clopper-Pearson confidence intervals for real species across all assessed population sizes. Calculated probabilities are based on the number of observed local optima found using HACSim. . .	164

List of Figures

2.1 Longfin damselfish (<i>Stegastes diencaeus</i>) TCS [139] haplotype network depicting an overall skewed distribution of observed haplotypes. Sizes of circles reflect the number of DNA sequences contained within each vertex. Tick marks indicate the number of mutational differences separating sampled haplotypes. DNA barcode sequence data used in the generation of the network were taken from supplemental material accompanying Phillips <i>et al.</i> [118]. The software PopArt [84] was used to create the haplotype network.	13
2.2 Graphical depiction of Phillips <i>et al.</i> 's [118] sampling model as described in detail within the main text. The <i>x</i> -axis is meant to depict the number of specimens sampled, whereas the <i>y</i> -axis is meant to convey the cumulative number of unique haplotypes uncovered for every additional individual that is randomly sampled. N and H refer to specimen and haplotype numbers that are observed for a given species. N^* is the total sample size that is needed to capture all H^* haplotypes that exist for a species.	36
3.1 Modified haplotype network from Phillips <i>et al.</i> [116]. Haplotypes are labelled according to their absolute frequencies such that the most frequent haplotype is labelled “1”, the second-most frequent haplotype is labelled “2”, <i>etc.</i> and is meant to illustrate that much species locus variation consists of rare haplotypes at very low frequency (typically only represented by 1 or 2 specimens). Thus, species showing such patterns in their haplotype distributions are probably grossly under-represented in public sequence databases like BOLD and GenBank.	54

3.2 Schematic of the HACS _{im} optimization algorithm (setup, initialization and iteration). Shown is a hypothetical example for a species mined from a biological sequence database like BOLD or GenBank with $N = 5$ sampled specimens (DNA sequences) possessing $H^* = 5$ unique haplotypes. Each haplotype has an associated numeric ID from 1- H^* (here, 1-5). Haplotype labels are randomly assigned to cells on a two-dimensional spatial array (ARRAY) with <code>perms</code> rows and N columns. All haplotypes occur with a frequency of 20%, (<i>i.e.</i> , <code>probs</code> = (1/5, 1/5, 1/5, 1/5, 1/5)). Specimen and haplotype information is then fed into a black box to iteratively optimize the likely required sample size (N^*) needed to capture a proportion of at least p haplotypes observed in the species sample.	61
3.3 Iterative extrapolation algorithm pseudocode for the computation of taxon sampling sufficiency employed within HACS _{im} . A user must input N , H^* and <code>probs</code> to run simulations. Other function arguments required by the algorithm have default values and are not necessary to be inputted unless the user wishes to alter set parameters.	63
3.4 Graphical depiction of the iterative extrapolation sampling model as described in detail herein. The figure is modified from Phillips <i>et al.</i> [116]. The x -axis is meant to depict the number of specimens sampled, whereas the y -axis is meant to convey the cumulative number of unique haplotypes uncovered for every additional individual that is randomly sampled. N_i and H_i refer respectively to specimen and haplotype numbers that are observed at each iteration (i) of HACS _{im} for a given species. N^* is the total sample size that is needed to capture all H^* haplotypes that exist for a species.	65
3.5 Graphical output of <code>HAC.sim()</code> for a hypothetical species with equal haplotype frequencies. A: Iterated haplotype accumulation curve. B: Corresponding haplotype frequency barplot. For the generated haplotype accumulation curve, the 95% confidence interval for the number of unique haplotypes accumulated is depicted by gray error bars. Dashed lines depict the observed number of haplotypes (<i>i.e.</i> , RH^*) and corresponding number of individuals sampled found at each iteration of the algorithm. The dotted line depicts the expected number of haplotypes for a given haplotype recovery level (here, $p = 95\%$) (<i>i.e.</i> , pH^*). In this example, $R = 100\%$ of the $H^* = 10$ estimated haplotypes have been recovered for this species based on a sample size of only $N = 100$ specimens.	70
3.6 Initial graphical output of <code>HAC.sim()</code> for a hypothetical species having three dominant haplotypes. In this example, initially, only $R = 83.3\%$ of the $H^* = 10$ estimated haplotypes have been recovered for this species based on a sample size of $N = 100$ specimens.	72

3.7 Final graphical output of <code>HAC.sim()</code> for a hypothetical species having three dominant haplotypes. In this example, upon convergence, $R = 95.4\%$ of the $H^* = 10$ estimated haplotypes have been recovered for this species based on a sample size of $N = 180$ specimens.	73
3.8 Initial haplotype frequency distribution for $N = 235$ high-quality lake whitefish (<i>Coregonus clupeaformis</i>) COI barcode sequences obtained from BOLD. This species displays a highly-skewed pattern of observed haplotype variation, with Haplotype 1 accounting for c. 91.5% (215/235) of all sampled records.	77
3.9 Initial graphical output of <code>HAC.sim()</code> for a real species (Lake whitefish, <i>C. clupeaformis</i>) having a single dominant haplotype. In this example, initially, only $R = 73.8\%$ of the $H^* = 15$ estimated haplotypes for this species have been recovered based on a sample size of $N = 235$ specimens. The haplotype frequency barplot is identical to that of Fig. 3.8	79
3.10 Final graphical output of <code>HAC.sim()</code> for Lake whitefish (<i>C. clupeaformis</i>) having a single dominant haplotype. Upon convergence, $R = 95.8\%$ of the $H^* = 15$ estimated haplotypes for this species have been uncovered with a sample size of $N = 604$ specimens.	80
3.11 Initial haplotype frequency distribution for $N = 349$ high-quality deer tick (<i>Ixodes scapularis</i>) COI barcode sequences obtained from BOLD. In this species, Haplotypes 1-8 account for c. 51.3% (179/349) of all sampled records.	82
3.12 Initial graphical output of <code>HAC.sim()</code> for a real species (Deer tick, <i>I. scapularis</i>) having eight dominant haplotypes. In this example, initially, only $R = 78.7\%$ of the $H^* = 83$ estimated haplotypes for this species have been recovered based on a sample size of $N = 349$ specimens. The haplotype frequency barplot is identical to that of Fig. 3.11	84
3.13 Final graphical output of <code>HAC.sim()</code> for deer tick (<i>I. scapularis</i>) having eight dominant haplotypes. Upon convergence, $R = 95.4\%$ of the $H^* = 83$ estimated haplotypes for this species have been uncovered with a sample size of $N = 803$ specimens.	84
3.14 Initial haplotype frequency distribution for $N = 171$ high-quality scalloped hammerhead (<i>Sphyrna lewini</i>) COI barcode sequences obtained from BOLD. In this species, Haplotypes 1-3 account for c. 87.7% (150/171) of all sampled records.	87
3.15 Initial graphical output of <code>HAC.sim()</code> for a real species (Scalloped hammerhead, <i>S. lewini</i>) having three dominant haplotypes. In this example, initially, only $R = 82.6\%$ of the $H^* = 12$ estimated haplotypes for this species have been recovered based on a sample size of $N = 171$ specimens. The haplotype frequency barplot is identical to that of Fig. 3.14	88

3.16 Final graphical output of <code>HAC.sim()</code> for scalloped hammerhead (<i>S. lewini</i>) having three dominant haplotypes. Upon convergence, $R = 95.6\%$ of the $H^* = 12$ estimated haplotypes for this species have been uncovered with a sample size of $N = 414$ specimens.	89
4.1 Initial haplotype frequency distribution for $N = 356$ high-quality Pea aphid (<i>Acyrtosiphon pisum</i>) COI barcode sequences obtained from BOLD. This species displays a highly-skewed pattern of observed haplotype variation, Haplotype 1 accounts for c. 96.6% (344/356) of all sampled records.	141
4.2 Initial haplotype frequency distribution for $N = 217$ high-quality Common mosquito (<i>Culex pipiens</i>) COI barcode sequences obtained from BOLD. In this species, Haplotype 1 accounts for c. 84.3% (183/217) of all sampled records.	142
4.3 Initial haplotype frequency distribution for $N = 365$ high-quality Gypsy moth (<i>Lymantria dispar</i>) COI barcode sequences obtained from BOLD. In this species, Haplotypes 1-5 account for c. 70.4% (257/365) of all sampled records.	142
4.4 Frequency plot showing all located local optima and the number of times each was found by <code>HACSim</code> for Scenario II (1 dominant haplotype).	143
4.5 Frequency plot showing all located local optima and the number of times each was found by <code>HACSim</code> for Scenario III (2 dominant haplotypes).	143
4.6 Frequency plot showing all located local optima and the number of times each was found by <code>HACSim</code> for Scenario IV (3 dominant haplotypes).	144
4.7 Frequency plot showing all located local optima and the number of times each was found by <code>HACSim</code> for Pea aphid (<i>Acyrtosiphon pisum</i>).	144
4.8 Frequency plot showing all located local optima and the number of times each was found by <code>HACSim</code> for Lake whitefish (<i>Coregonus clupeaformis</i>).	145
4.9 Frequency plot showing all located local optima and the number of times each was found by <code>HACSim</code> for Common mosquito (<i>Culex pipiens</i>).	145
4.10 Frequency plot showing all located local optima and the number of times each was found by <code>HACSim</code> for Deer tick (<i>Ixodes scapularis</i>).	146
4.11 Frequency plot showing all located local optima and the number of times each was found by <code>HACSim</code> for Gypsy moth (<i>Lymantria dispar</i>).	146
4.12 Frequency plot showing all located local optima and the number of times each was found by <code>HACSim</code> for Scalloped hammerhead shark (<i>Sphyraena lewini</i>).	147

- 4.13 Plot showing all located local optima and the proportion of observed haplotypes captured for Scenario II (1 dominant haplotype) with 95% confidence intervals for a population size of 10000. The mean proportion across 50 replications is depicted as a black dot. The mean proportion across all located local optima is displayed as a solid red horizontal line. The thickness of displayed grey error bars is a construct of `ggplot2` based on the number of local optima and holds no additional meaning in the context of this study. 148
- 4.14 Plot showing all located local optima and the proportion of observed haplotypes captured for Scenario III (2 dominant haplotypes) with 95% confidence intervals for a population size of 10000. The mean proportion across 50 replications is depicted as a black dot. The mean proportion across all located local optima is displayed as a solid red horizontal line. The thickness of displayed grey error bars is a construct of `ggplot2` based on the number of local optima and holds no additional meaning in the context of this study. 149
- 4.15 Plot showing all located local optima and the proportion of observed haplotypes captured for Scenario IV (3 dominant haplotypes) with 95% confidence intervals for a population size of 10000. The mean proportion across 50 replications is depicted as a black dot. The mean proportion across all located local optima is displayed as a solid red horizontal line. The thickness of displayed grey error bars is a construct of `ggplot2` based on the number of local optima and holds no additional meaning in the context of this study. 150
- 4.16 Plot showing all located local optima and the proportion of observed haplotypes captured for Pea aphid (*A. pisum*) with 95% confidence intervals for a population size of 10000. The mean proportion across 50 replications is depicted as a black dot. The mean proportion across all located local optima is displayed as a solid red horizontal line. The thickness of displayed grey error bars is a construct of `ggplot2` based on the number of local optima and holds no additional meaning in the context of this study. 151
- 4.17 Plot showing all located local optima and the proportion of observed haplotypes captured for Lake whitefish (*C. clupeaformis*) with 95% confidence intervals for a population size of 10000. The mean proportion across 50 replications is depicted as a black dot. The mean proportion across all located local optima is displayed as a solid red horizontal line. The thickness of displayed grey error bars is a construct of `ggplot2` based on the number of local optima and holds no additional meaning in the context of this study. 152
- 4.18 Plot showing all located local optima and the proportion of observed haplotypes captured for Common mosquito (*C. pipiens*) with 95% confidence intervals for a population size of 10000. The mean proportion across 50 replications is depicted as a black dot. The mean proportion across all located local optima is displayed as a solid red horizontal line. The thickness of displayed grey error bars is a construct of `ggplot2` based on the number of local optima and holds no additional meaning in the context of this study. 153

- 4.19 Plot showing all located local optima and the proportion of observed haplotypes captured for Deer tick (*I. scapularis*) with 95% confidence intervals for a population size of 10000. The mean proportion across 50 replications is depicted as a black dot. The mean proportion across all located local optima is displayed as a solid red horizontal line. The thickness of displayed grey error bars is a construct of `ggplot2` based on the number of local optima and holds no additional meaning in the context of this study. 154
- 4.20 Plot showing all located local optima and the proportion of observed haplotypes captured for Gypsy moth (*L. dispar*) with 95% confidence intervals for a population size of 10000. The mean proportion across 50 replications is depicted as a black dot. The mean proportion across all located local optima is displayed as a solid red horizontal line. The thickness of displayed grey error bars is a construct of `ggplot2` and thus holds no additional meaning in the context of this study. 155
- 4.21 Plot showing all located local optima and the proportion of observed haplotypes captured for Scalloped hammerhead shark (*S. lewini*) with 95% confidence intervals for a population size of 10000. The mean proportion across 50 replications is depicted as a black dot. The mean proportion across all located local optima is displayed as a solid red horizontal line. The thickness of displayed grey error bars is a construct of `ggplot2` and thus holds no additional meaning in the context of this study. 156

Chapter 1

Introduction

1.0.1 Thesis Overview

This thesis outlines a novel statistical framework for assessment of COI DNA barcode haplotype sampling completeness. Much of the work presented herein reflects a spin-off of research completed at the Master's level in bioinformatics.

Chapter 2 consists of an in-depth literature review of studies conducted to date pertaining to sample size estimation for DNA barcoding, as well as the need for further research in this area. A case study assessing haplotype diversity in the ray-finned fishes [118] provides motivation for subsequent work presented and examined in the present thesis.

Chapter 3 details a novel stochastic optimization algorithm called `HACSim` (short for **Haplotype Accumulation Curve Simulator**) that is programmed in the R Statistical Environment [122]. `HACSim` can be employed to calculate likely required specimen sample sizes needed to capture a given fraction of genetic diversity within species based

on iteratively extrapolating species' haplotype accumulation curves. HACSim is applied to various vertebrate and invertebrate taxa of recent interest within the DNA barcoding literature, primarily fishes and arthropods of conservation, medical, and forensic/regulatory importance.

Chapter 4 extends elements discussed in Chapter 3 through delving further into the usability and applicability of HACSim via a detailed statistical simulation study to assess both the validity and overall performance of HACSim and its utility for assessing intraspecific sampling completeness within DNA barcoding studies for a variety of species mined from the Barcode of Life Data Systems (BOLD) [123].

Finally, in Chapter 5, it is argued that DNA barcoding is currently lacking in statistical rigor and that better statistical methods are necessary to more accurately assess standing genetic variation at the species level. Proposed approaches are illustrated through a case study focussing on Pacific fishes of Canada [135].

1.0.2 Thesis Statement

Through the development of a novel stochastic simulation algorithm for the generation of haplotype accumulation curves, the current research will provide a framework that can be employed to determine plausible specimen sample sizes sufficient to quantify levels of haplotypic sampling completeness within species under both uniform and non-uniform haplotype frequency distributions.

Such a framework will be valuable in hopefully promoting a greater degree of statistical thoroughness in future DNA barcoding studies.

Chapter 2

Incomplete estimates of genetic diversity within species: Implications for DNA barcoding

Jarrett D. Phillips^{1,2}, Daniel J. Gillis¹ and Robert H. Hanner^{2,3}

¹School of Computer Science

²Centre for Biodiversity Genomics, Biodiversity Institute of Ontario

³Department of Integrative Biology

ABSTRACT

DNA barcoding has greatly accelerated the pace of specimen identification to the species level, as well as species delineation. Whereas the application of DNA barcoding to the matching of unknown specimens to known species is straightforward, its use for species delimitation is more controversial, as species discovery hinges critically on present levels of haplotype diversity, as well as patterning of standing genetic variation that exists within and between species. Typical sample sizes for molecular biodiversity assessment using DNA barcodes range from 5-10 individuals per species. However, required levels that are necessary to fully gauge haplotype variation at the species level are presumed to be strongly taxon-specific. Importantly, little attention has been paid to determining appropriate specimen sample sizes that are necessary to reveal the majority of intraspecific haplotype variation within any one species.

In this paper, we present a brief outline of the current literature and methods on intraspecific sample size estimation for the assessment of COI DNA barcode haplotype sampling completeness. The importance of adequate sample sizes for studies of molecular biodiversity is stressed, with application to a variety of metazoan taxa, through reviewing foundational statistical and population genetic models, with specific application to ray-finned fishes (Chordata: Actinopterygii). Finally, promising avenues for further research in this area are highlighted.

2.1 Introduction

One of the most fundamental problems underpinning much of modern molecular biodiversity research is the issue of determining optimal levels of sampling effort that are required in order to adequately characterize biological sequence variation at the species level. Molecular genetic studies of biodiversity that utilize mitochondrial DNA (mtDNA) marker variation for the purpose of characterizing existing species genetic diversity are particularly sensitive to sample sizes. Four fundamental evolutionary forces act to alter the genetic composition of species populations: migration/gene flow, mutation, natural selection and random genetic drift. The effect of genetic drift on species populations is most evident when population sizes are small, as in the case of a recent bottleneck or founder event, resulting in the rapid loss of genetic diversity. Species differ in both their evolutionary histories and in their geographic distributions; therefore, the question of accurately determining how many samples to include in order to observe a wide range of species genetic variation has been an ongoing area of interest and research. This is an important question deserving of more attention. Accurate determination of within-species (intraspecific) sample sizes for mtDNA diversity estimation permits detailed analyses to be undertaken at the phylogenetic and phylogeographic levels in order to infer key biological processes such as isolation, dispersal and speciation [8, 38, 51]. Aside from addressing purely biological questions, the issue of determining optimal sampling strategies and sample sizes for genetic variation assessment at the species level also manifests at applied socioeconomic scales, particularly in the detection of food or natural health product fraud

and in the monitoring of aquatic and terrestrial ecosystems [76].

Within the field of biodiversity science, researchers have long recognized the importance of sampling design in order to achieve a study's objectives. According to Lindblom [86], well-developed sampling designs within the field of molecular biodiversity science should be formulated around three basic areas: research study questions, research study aims and taxonomic focus. In addition to these three areas, Costa *et al.* [32] point to further considerations: planning the number and geographical distribution of specimens to be sampled, the category and number of genetic loci to be examined, and the spatial distribution and number of individuals to be sampled within each species' population. While there is a lack of clear sampling guidelines currently in place for optimal spatio-temporal assessment of species populations, Pante *et al.* [108] argues that such schemes should be guided by adequate coverage of both the putative geographic/ecologic range of the species under study, as well as potentially closely related species over its entire range. Given that much of species spatio-temporal metadata is not reported alongside genetic data, such assessments become problematic unless community standards and practices are improved [58, 100, 138]. Where this becomes particularly important is in the development and design of species-specific real-time Polymerase Chain Reaction (qPCR) primers and probes, for integration within environmental DNA (eDNA) assays for instance. This is especially the case if such tools are to be continuously implemented within regulatory or forensic settings such as the Canadian Food Inspection Agency (CFIA) [129] and the United States Food and Drug Administration (USFDA),

as the success of such methods depends greatly on the extent of geographic coverage of species genetic diversity.

The overall goal of sampling is to make inferences concerning a population of interest based only on information contained within finite samples drawn from the larger population. This is done through estimating population parameters such as the population mean (μ) using the sample mean (\bar{x}). One example, relevant to molecular population genetics, is the calculation of average pairwise distances based on Nei's estimator of nucleotide diversity (π) [103]. Under the Frequentist statistical paradigm, the minimum sample size that is required to estimate a population mean, from a Normal distribution, is given by [2]

$$n \geq \left(\frac{z_{\alpha/2}\sigma}{d} \right)^2 \quad (2.1)$$

where $z_{\alpha/2}$ is the appropriate critical value to estimate μ with a level of significance of $1-\alpha$, σ^2 is the population variance and d is the desired margin of error. From the above equation, the required minimum sample size is controlled by the experimenter through the margin of error. A smaller margin of error results in a larger value of n . Similarly, predicting n with a higher level of accuracy can be achieved through narrowing d . Sample sizes that are computed from the above equation serve as a baseline requirement prior to conducting any quantitative study of interest. Depending on the sampling scheme, for instance stratified sampling, other formulas exist for the appropriate calculation of necessary sample sizes.

In determining the most appropriate sample size required for a particular study, a crude rule of thumb that is often used in statistics and other scientific disciplines pertains to the use of a sample size of at least $n = 30$ when making comparisons among study groups or when deciding to use probabilities derived from the Standard Normal distribution [30]. Unfortunately, adequate sample sizes, while widely viewed as being central to a given biodiversity research study, are often neglected in practice [85]. In such cases, this may be due to, for example, costs associated with or resources required for adequate specimen collection [20, 72, 97].

Statistical power analysis can be employed to help shed light on sample sizes required in order to detect a given effect prior to carrying out a scientific study. Power, which is defined as the complement of the Type II error rate (β), depends on four factors: effect size (ES), significance level/Type I error rate (α), sample size (n) and population standard deviation (σ) through the proportionality [36]

$$(1 - \beta) \propto \frac{ES \times \alpha \times \sqrt{n}}{\sigma}. \quad (2.2)$$

Effect size is the difference between an observed quantity and one hypothesized under a null distribution. Larger deviations lead to greater power to detect real effects. It is easily seen from the above proportionality that larger values of effect size, significance level and sample size all generate higher levels of statistical power; whereas, increasing population standard deviation results in loss of power. Together with the sample size

equation discussed previously (Equation 1), many factors are at play in determining the most appropriate sample size needed for a given study.

Any sampling scheme that is carried out will be subject to systematic error. Sampling (ascertainment) bias is an important factor to consider in this regard because it can lead to under- or overestimation of population parameters. Ascertainment bias describes the tendency of certain individuals to be less likely sampled than others [112] and is common in molecular biodiversity studies (*e.g.*, [59, 97, 99, 149]). This can occur, for example, when sampling is restricted to certain geographic regions [97] or to particular species (*e.g.*, those known to be of conservation importance) [59]. Sampling bias can be minimized through increasing the geographic breadth of a study, in addition to targeting representative taxa with large specimen sample sizes.

The present review briefly examines current approaches for species genetic variation assessment as it relates to the estimation of intraspecific sample sizes for DNA barcoding. Specifically, the focus will be on COI DNA barcode haplotype sampling completeness. Few studies have focused on DNA barcode sample size prediction for wide-ranging taxa in this regard. Here, methods of haplotype variation assessment are first covered. This is then followed by an examination of existing studies, with particular consideration of important findings to date within the literature. Finally, promising new avenues for further research are explored.

2.2 Current Methods

2.2.1 Methods to Assess Haplotype Variation Haplotype Diversity

Genetic diversity is manifested within species in several ways. One way is through haplotype variation. While there are many different definitions of what constitutes a haplotype, in the broadest sense, a haplotype is a unique DNA sequence that differs from others at one or more basepair positions within and between species. Nei's [102] haplotype diversity (h), which is a widely-used approach to measuring genetic variation within species populations, is given by the equation

$$h = \frac{n}{n-1} \left(1 - \sum_i p_i^2 \right). \quad (2.3)$$

where p_i is the frequency of the i^{th} haplotype in the sample. Two interpretations of h are that it expresses the probability of observing a previously unseen haplotype upon sampling a new individual [145] or that it represents the probability that two haplotypes, selected at random from a sample of n DNA sequences, are distinct [52]. Haplotype diversity can also be quantified using the absolute number of haplotypes (H). Both h and H are greatly affected by levels of sampling intensity within species. In particular, undersampling can cause these measures to become under- or overestimated [52]. Several other approaches are in wide use to aid researchers in assessing levels of standing genetic variation existing within species populations. Two of these are haplotype networks and haplotype

accumulation curves.

Haplotype Networks

A widely-used approach to assessing levels of genetic variation within and between species is through the construction of haplotype networks [139]. Haplotype networks accurately represent differences existing among sampled haplotypes through grouping identical DNA sequences within the same vertex. The size of a given vertex is proportional to the number of DNA sequences it contains. Divergent haplotypes are connected via edges that display the number of mutational differences separating adjacent vertices.

Haplotype networks are appealing because they can be used to infer potential cryptic diversity within a taxon or interspecific hybridization between allopatric (*i.e.*, reproductively-isolated) species, but interpretation can sometimes become difficult when multiple species cluster together into one or multiple nodes or subnetworks [60, 63, 152] or when ambiguous/missing nucleotide data are present within DNA sequences (*e.g.*, Ns or gaps (-)) [78]. While haplotype networks, such as the one shown in **Figure 2.1**, cannot give a direct indication of the level of sampling completeness for a given species, the presence of numerous rare haplotypes suggests gross undersampling of intraspecific genetic variation (or alternatively PCR/sequencing error).

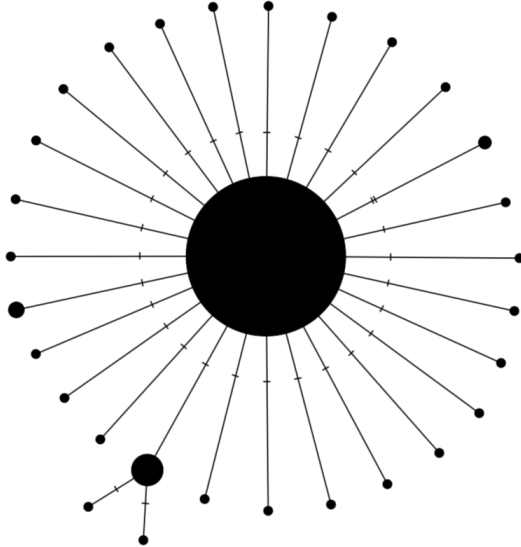


Figure 2.1: Longfin damselfish (*Stegastes diencaeus*) TCS [139] haplotype network depicting an overall skewed distribution of observed haplotypes. Sizes of circles reflect the number of DNA sequences contained within each vertex. Tick marks indicate the number of mutational differences separating sampled haplotypes. DNA barcode sequence data used in the generation of the network were taken from supplemental material accompanying Phillips *et al.* [118]. The software PopArt [84] was used to create the haplotype network.

Haplotype Accumulation Curves

Assessing the completeness of intraspecific haplotype sampling can be carried out through generating haplotype accumulation curves. Such curves are analogous to rarefaction curves used in studies of species richness [53] and depict the degree of asymptotic behaviour as a function of both the number of specimens sampled and the cumulative mean number of haplotypes accumulated. Initially, accumulation curves will increase very rapidly since many new haplotypes will be captured for a given species with minimal sampling effort, but haplotype recovery slows drastically as sampling depth is increased because many haplotypes that are found will have already been observed

previously. Thus, species curves showing rapid saturation strongly suggest that the majority of haplotype diversity has been uncovered; whereas, those curves displaying little to no evidence of reaching an asymptote indicate that further sampling is required [159]. Deciding whether a species should be further sampled can be deduced from the magnitude of the slopes calculated using a fixed number of points occurring on the end of the curve (e.g., ten in the case of [118, 155]). Slopes near or below a predefined threshold, for example, 0.01 (*i.e.*, equivalent to observing one new haplotype for every 100 DNA sequences), suggest that additional sampling is unlikely to reveal any new haplotypes; whereas, those species curves with slopes above 0.1 (*i.e.*, observing one new haplotype for every 10 DNA sequences) strongly indicate that further sampling is necessary [72].

One obvious problem that arises in the use of haplotype accumulation curves to gauge species genetic diversity and levels of sampling effort, however, is the fact that the functional form of such curves is not known and can differ widely across taxa [118]. Furthermore, deciding on appropriate curve slope thresholds necessary for adequate sampling coverage are largely arbitrary [72]. While various parametric model curve-fitting approaches, such as the power, negative exponential and Michaelis-Menten functions, have been heavily employed and debated in the literature to model species-area relationships [34, 141] or species richness, no single approach yet exists that can be readily applied to determine sample sizes that are likely required for intraspecific genetic variation assessment.

A second, lesser-investigated issue, relates to the fact that haplotype accumulation curves are not spatially-explicit. Thus, it becomes difficult to account for correlations that may exist at the subpopulation or higher taxonomic levels. This has been noted in past studies of species richness employing species accumulation and rarefaction curves (*e.g.*, [15, 27, 140]).

2.2.2 Sampling Models for Genetic Diversity Prediction

In addition to qualitative approaches to assessing standing genetic variation within species, a number of quantitative models to estimate required sample sizes for overall genetic diversity assessment have been proposed. These include Frequentist, Bayesian and coalescent models.

Holt *et al.* [71] reviewed several Frequentist and Bayesian statistical methods of sample size determination for intraspecific haplotype diversity assessment that are most informative over large geographic ranges. The authors note that a lower bound on the probability of sampling a dominant haplotype in a sample of size n with significance level α is given by the inequality

$$p \geq \sqrt[n]{\alpha} \tag{2.4}$$

Grewe *et al.* [54] employed an equivalent approach to Holt *et al.*'s [71] study through utilizing a binomial sampling model to determine the minimum sample size required to

assess mtDNA variation in Lake Ontario lake trout (*Salvelinus namaycush*) stocks according to the equation

$$n = \frac{\ln(1 - \beta)}{\ln(1 - p)} \quad (2.5)$$

where p is the frequency of a given haplotype and β is the desired confidence level. The authors found that $n = 60$ individuals are likely needed to be randomly sampled in order to observe a single haplotype having a frequency of at least $p = 5\%$ with $\beta = 95\%$ confidence. It is worth noting that this figure increases to *c.* 460 individuals for a haplotype occurring at frequency of 1% with 99% confidence [54]. This marked increase in sample size is not surprising given that one would need to sample many more individuals in order to be certain that the majority of rare haplotypes have been uncovered. It is important to note, however, that Grewe *et al.* [54] sampled individuals from six different but highly divergent trout strains, each displaying high degrees of population substructure. Population subdivision likely will have an effect on the estimation of required sample sizes needed to gauge levels of standing genetic variation at the species level.

Similar magnitudes of sample sizes were found by Austerlitz *et al.* [7], who employed coalescent theory [80], in order to determine the probability of adequately sampling all genetic variation of a species with sample size n . Coalescent theory attempts to trace the lineage of an ancestral allele (termed the Most Recent Common Ancestor, MRCA) backwards in time within a gene genealogy. Under a geometric distribution, this probability

is given by the equation [7]

$$p = \frac{n - 1}{n + 1}. \quad (2.6)$$

From the above equation, only $n = 39$ individuals are required to be sampled at random in order to observe $p = 95\%$ of all genetic diversity for a species. It should be noted however that even with increasing sample sizes, one's confidence in having sampled all of a species genetic diversity approaches closely, but never actually reaches, 100% [7]. This is illustrated by the finding that the required sample size increases to $n = 1999$ individuals necessary to observe $p = 99.9\%$ of the total genetic diversity that exists for a given species using Equation (6). This can be explained by the fact that individual haplotypes for a given species become much more difficult to recover as the intensity of specimen sampling is increased because intraspecific genetic variation is expected to increase as a result. The coalescent, as a large-scale sampling model, has found wide application in DNA-based approaches to species identification and delimitation, most notably DNA barcoding [73].

2.2.3 DNA Barcoding

Since its conception in 2003, DNA barcoding [65] has risen to become the largest taxonomically-driven biodiversity initiative to date aimed at identifying and cataloging all assemblages of multicellular life on the planet. DNA barcoding is a genomic technique that relies on DNA sequence variation within short, standardized gene regions in order

to rapidly identify specimens to the level of species and to discover new species. The ideal DNA barcode is one that is found in all organisms, readily distinguishes between taxa, and is easily amplified, sequenced and aligned. In animals, the agreed-upon marker of choice for taxon assignment is a *c.* 650 basepair (bp) fragment from the 5' end of the mitochondrial-encoded cytochrome *c* oxidase subunit I (COI) gene. Mitochondrial loci like COI are particularly suitable as genetic markers for DNA barcoding because they are fast evolving, highly conserved across taxa, present in high copy number, haploid, maternally inherited, lack introns, display few insertion-deletion (indel) mutations, and experience little to no gene recombination [65, 67].

The primary goal of DNA barcoding has been to develop a publicly accessible species reference sequence library to aid in the identification of unknown specimens and accelerate the discovery of potentially undescribed taxa. Obtaining adequate sample sizes for building accurate and reliable specimen reference libraries has culminated in the development of the Barcode of Life Data Systems (BOLD; <http://www.boldsystems.org>) [123] as the largest collection of user-curated species sequence data specifically for DNA barcoding currently available on the World Wide Web. At present (as of May 1, 2018), BOLD holds over six million DNA barcode records from over 250,000 named species. Certain taxa are well represented in BOLD with upwards of hundreds of barcode sequences for some species. Despite this, barcode reference libraries within BOLD remain largely incomplete, even for the most well-sampled taxa such as fishes and insects. As such, comprehensive coverage of species genetic diversity is still decades away [149]. Wilkinson *et al.* [149] points to strong

ascertainment bias as the most likely explanation for this. In the early days of BOLD, DNA barcode sequence acquisition was high, due to the fact that over 75% of taxon records were mined from already well-established sequence databases such as GenBank [149].

2.2.4 The Importance of Sampling to DNA Barcoding

DNA barcoding works in practice because interspecific (between-species) variation is usually much greater than intraspecific (within-species) divergence [92, 137]. While this observed ‘barcoding gap’ [92] is a necessary criterion for successful taxonomic resolution using distance-based methods, it may not be a sufficient one for other molecular approaches (*e.g.*, those employing tree- or character-based techniques). Cases are well documented where considerable overlap/separation between (maximum) intraspecific variation and (minimum) interspecific divergence exists [69, 73]. Undersampling can greatly exaggerate the existence of the barcode gap. The inclusion of small sample sizes over large geographic ranges has the effect of obscuring existing mitochondrial sequence diversity at the species level since the finding of divergent haplotypes may be the result of poorly sampled panmictic (*i.e.*, randomly-mating) intraspecific variation [29]. Compared to regional scales, with increasing sampling effort across wider spatial scales, intraspecific variation is expected to increase whereas interspecific divergence will decrease in effect since more closely-related species will tend to be found due to allopatric speciation being a dominant mode of diversification [13, 114].

How much variation is actually needed to separate species is not known with certainty

because intraspecific sampling has generally been limited to narrow geographic locales. Hebert *et al.* [65] proposed that barcode sequences exhibiting at least 2% nucleotide divergence should be designated as being from distinct species. Intraspecific distances larger than 2% suggest the presence of cryptic species, whereas those smaller than 2% is evidence for evolutionarily young species with a recent origin (*i.e.*, retention of ancestral polymorphisms due to incomplete lineage sorting), hybridization/introgression or inadequate taxonomy (*e.g.*, cryptic species or species synonymy) [73]. In BOLD, query sequences are matched to reference barcodes based on a genetic distance heuristic of 1% [123]. The use of such threshold estimates for species separation is arbitrary and is often applied to a wide variety of taxa, regardless of species life histories. A later estimate of ten times the mean intraspecific distance (the so-called ‘10× rule’) was given by Hebert *et al.* [69]. Unlike the previously suggested estimate of 2% sequence divergence, the 10× rule makes use of all available taxon sequences within a dataset in order to calculate an appropriate limit for species separation. Despite this, the 10× rule has been met with criticism: Collins and Cruickshank [31] suggest consideration of the maximum intraspecific distance and the minimum interspecific divergence (*i.e.*, nearest neighbour distance) for each species under investigation. The use of lower thresholds for species discovery may falsely inflate existing genetic diversity, whereas the adoption of higher cutoffs would likely be too conservative for reliable detection of cryptic species [5]. It is well understood however that the most appropriate cutoff necessary to accurately diagnose species on the basis of sequence variation is strongly taxon-dependent [67, 70, 92] and will

become more precise with increased sampling effort.

DNA barcoding has its roots in the historic disciplines of Darwinian evolutionary theory, population genetics and phylogenetics: the coalescent is a modern interpretation that reconciles these domains [126]. While genetic distance-based approaches to species delimitation are commonplace within barcoding studies because they scale well to large taxon datasets, early-proposed arbitrary separation methods like the 2% or 10 \times rule completely ignore evolutionary relationships that exist among closely-related species. Objective tools for the delimitation of species are well known and generally fall into three overlapping categories: phylogenetic, coalescent, and phylogenetic-coalescent [73]. The well-known neighbour-joining clustering method was advocated for in the early barcoding literature as a means of confirming the presence of reciprocal monophyly across sampled taxa. More recently, novel bioinformatic algorithms, most notably distance-based approaches such as Automatic Barcode Gap Discovery (ABGD; [121]) and tree-based methods including variants of the Generalized Mixed Yule Coalescent (GMYC; [95, 119]) have been put forth in order to facilitate species separation, an otherwise daunting task for even the most highly-skilled and knowledgeable taxonomist. ABGD is a nonparametric technique of partitioning species on the basis of the barcode gap using DNA sequences. On the other hand, GMYC is a likelihood-based method that relies on the premise that bifurcation (*i.e.*, fully-resolved branching) within ultrametric species trees is indicative of speciation/diversification events, and therefore suggests the presence of undescribed taxa. A key factor in the success of such methods is sample size, and few groups have been

so extensively inventoried [73]. For example, GMYC is especially prone to the under- or overestimation of putative species, which can be magnified due to differences in effective population sizes as well as historical versus contemporaneous patterns of migration/gene flow among subpopulations [88, 109]. Thus, sufficient sampling is paramount. Often, researchers would like to know whether all unique haplotypes within a lineage or deme have been adequately sampled; unfortunately, this is complicated by the fact that the majority of species are both geographically-widespread and rare. As a result, given that ascertainment and operational biases are inevitable [99], an extensive sampling of all local populations that comprise a given species is unrealistic, even under the best situations (*e.g.*, strong research budget, easy access to sampling locations). Thus, whenever possible, a more comprehensive sampling of study sites is required in order avoid false positives/negatives and to reveal divergent haplotypes that may have been missed with spatially-narrower sampling routines [95]. Incorporation of coalescent and population genetics theory can aid in informing researchers on broad macro-level processes that may be at play in shaping trends seen within haplotype accumulation curves on the basis of extant patterns of intraspecific genetic diversity.

The Barcode Index Number framework for animals, first introduced by Ratnasingham and Hebert [124], represents a potentially novel approach to addressing the issue of sample sizes necessary for barcoding initiatives. The BIN system partitions COI barcodes into distinct Operational Taxonomic Units (OTUs) on the basis of the REfined Single Linkage (RESL) clustering algorithm and Markov clustering [124]. BINs comprise high-quality

sequences linked to BARCODE compliant records. The BARCODE standard currently in place stipulates that only barcode sequences with read lengths of at least 500 bp and containing less than 1% ambiguous nucleotides are designated unique BIN clusters [58]. While BINs generally show high concordance with actual biological species, they can be further employed to gauge instances of suspected cryptic species diversity, especially in the cases where intraspecific distances are not clearcut. Species that fall into two separate BINs (termed a SPLIT) is evidence that they are being overlumped. Further, the occurrence of rare BINs (*i.e.* those represented by a single specimen) may be the result of limited sampling [64, 75]. Stand-alone BINs may also reflect sequencing errors in the form of very low-frequency (VLF) variants or cryptic pseudogenes [136, 137]. Increased sampling coverage can be beneficial in such instances, as true biological variation is less likely to be misidentified as artificial biological variation and unintentionally flagged as potential VLFs.

2.2.5 Consideration of Species' Life Histories

Life history traits, particularly those pertaining to reproductive strategies and sex determination, in well-studied metazoan taxa such as fishes, insects and herpetofauna, are presumed to play a significant role in observed patterns of mtDNA barcode sequence variation at the species level. For instance, the high occurrence of haplodiploidy, a mode of inheritance whereby females develop from fertilized eggs (hence are diploid), while males arise from unfertilized eggs (therefore are haploid), is common across many insect

orders such as Hymenoptera, and may explain the large abundances and varying (effective) population sizes seen in representative species that ultimately drives speciation and hybridization [68]. Similar “exceptions to the rule”, such as (asexual) modes of parthenogenesis (*e.g.*, unfertilized eggs producing female-only offspring in Squamata such as species of whiptail lizards), or paternal/biparental organelle inheritance in bivalve molluscs (*e.g.*, mussels of the genus *Mytilus*), will likely help inform researchers on the required level of sampling depth needed to fully characterize broad ranges of COI haplotype diversity in taxa that do not otherwise conform to traditional mtDNA inheritance patterning (*i.e.*, strictly maternal lineage), and thus prevent the naïve implementation of recommendations of any one statistical approach employed in the calculation of intraspecific sample sizes for accurate specimen assignment and rapid species delineation. As an example, because parthenogenetic species display lower standing genetic diversity compared to fully sexually-reproducing species (as a result of being exact clones of their parent due to lack of chromosomal recombination) [12], haplotype frequencies aside, the observation of the faster approach of haplotype accumulation curves to an asymptote is expected. Thus, species exhibiting such mechanisms will require reduced levels of sampling effort. Such a result can be invoked through consideration of Muller’s ratchet, as the irreparable accumulation of deleterious mutations that are fixed by genetic drift within asexual genomes directly limits the ability of a species to survive and reproduce [48, 98].

2.3 Key Findings

2.3.1 DNA Barcoding and Sample Size: Past Studies

The ability of DNA barcodes to uncover levels of standing genetic variation within species is strongly influenced by the scale of specimen sampling, which has been recognized as a major barrier to the success of DNA barcoding since its early days [69, 92, 144]. In spite of this, global barcoding efforts have only been partially successful in capturing the full extent of COI barcode variation in animals due to the majority of studies forgoing deep taxon sampling in favour of maximizing the number of different taxa sampled [91, 159]. Sample sizes of a few individuals per species (typically in the range of 5-10, but one or two specimens is not uncommon since these are often the only representatives available, either due to unclear species boundaries or limited geographic sampling of intraspecific variation) are widespread in barcoding studies [56, 91, 159]. Recommended sample sizes currently in place are by no means sufficient since species abundance is often skewed geographically/ecologically. For example, five specimens per species per FAO (Food and Agriculture Organization) region was initially suggested by the Fish Barcode of Life (FISHBOL; [143]) initiative, but the sampling of up to 25 individuals or more may be necessary for some species exhibiting widespread distribution patterns [10, 134]. Similarly, in assessing haplotype and nucleotide COI variation across wide-ranging animal taxa, Goodall-Copestake *et al.* [52] note that a sample size of five individuals per species population was adequate to differentiate between extremes of h , but as many as 25 specimens would need to be collected in order to achieve maximum accuracy. Jin *et al.*

[77], and Matz and Nielsen [91] both point to a sample size of 12 specimens, whereas Ross *et al.* [127] suggest that sampling five or more reference barcodes is sufficient for accurate species identification. Bias toward low sample sizes observed for most species may be the result of many factors (see Bucklin *et al.* [18] for a concise summary in marine metazoa), including the presence of cryptic diversity, amplification of non-functional gene copies (*i.e.*, pseudogenes/nuclear-mitochondrial inserts (NUMTs)), contamination by foreign DNA from other species (*e.g.*, bacterial symbionts such as *Wolbachia*), insertion-deletion (indel) mutations, or errors arising from PCR/sequencing runs [52]. Molecular diagnosis of specimens to the species level using DNA barcoding is not definitive; numerous technical sources of error exist that can hamper the ability of reliable taxon assignment, in particular, misidentifications, sequencing errors and lack of taxonomic metadata (*e.g.*, inclusion of GPS coordinates, record linkage to a voucher specimen). While such factors are likely to occur infrequently for interspecific barcodes, this is not the case for intraspecific datasets. Taken together, biases in sample sizes will likely be considerable. In certain cases, the occurrence of biological phenomena can lead to problems encountered later on in the lab, specifically during the sequence amplification stage using PCR. A well-known example of this is the symbiotic association of the bacterium *Wolbachia* with insects. Integration of *Wolbachia* within host genomes of various Hymenoptera, Diptera and Lepidoptera can cause fluctuations in intraspecific distances [130] and thus, observed haplotype diversity between infected and uninfected hosts [25]. Misamplification of host sequences for bacterial symbionts is widely encountered, as is the amplification of

pseudogenes/NUMTs. Technical sources of error such as expert taxonomic misidentifications, sequence contamination, as well as errors arising from the amplification/sequencing process can be controlled, and can be minimized to a degree. Two critical steps in avoiding such issues are: (1) the construction of an NJ tree in order to pinpoint potentially misidentified specimens and/or sequence contaminants (as opposed to solely being used in the establishment of reciprocal monophyly, as argued by Collins and Cruickshank [31]) and (2) the careful inspection of BOLD specimen trace files in order to resolve noisy sequence regions that inflate estimates of standing genetic variation through the introduction of functional (heteroplasmic) sequence variation (as in *e.g.*, Hebert *et al.*, [66]) and/or nonexistent low-frequency species haplotypes occurring in high abundance [136]. The effect of these on generated haplotype accumulation curves is delayed saturation to an asymptote due to larger required sample sizes. Combined with initially large numbers of specimens within intraspecific data sets (*e.g.*, $N > 100$), this effect can be quite substantial. As BOLD is ever-evolving, in part due to the sheer volume of DNA barcode sequences being added on a daily basis, it is crucial that suspected errors within taxon records be dealt with in a timely manner (*e.g.*, through community users flagging problematic records for closer examination by submitters), so that sequence integrity is not compromised. While the issue of determining adequate sample sizes for molecular species diagnosis has largely been aimed at animal taxa, Liu *et al.* [87] explored optimal sample sizes needed for plant DNA barcoding. It was found that relatively small sample sizes were adequate to recover sequence variation in slowly evolving genes (2 or 3 sequences per

species population for matK); whereas, higher numbers are necessary for rapidly evolving markers (minimum of 10, 8 and 6 individuals per population for trnH-psbA, trnL-trnF and ITS respectively) [87]. Further, the authors found that a sample size of 8-10 individuals per species across the entire geographic range appears sufficient for *Taxus* barcoding. Unfortunately, such small sample sizes, likely the result of low information content due to the high presence of sequence artifacts (*e.g.*, indels within mitochondrial/plastid markers), often lack discriminatory power that is needed for accurate identification of specimens on the basis of genetic polymorphism with DNA barcodes.

To date, few studies explicitly exploring simulated sample sizes for DNA barcoding in wide ranging animal taxa have been conducted. One of the first studies to examine the issue of sample sizes for DNA barcoding via haplotype accumulation curves was conducted by Zhang *et al.* [159] using a modified form of the Michaelis-Menten equation. Using this method, the authors found that the random sampling of 250-1188 individuals from the Costa Rican skipper butterfly (*Astraptes fulgerator*) cryptic species complex are likely needed in order to detect 95% of all genetic diversity for this species based on an initial sample size of 407 individuals. Conversely, the same authors found that 156-1985 specimens were needed to retrieve 95% of COI variation using simulated island [153] and stepping-stone [79] coalescent models across three distinct subpopulations and under varying effective population sizes. In addition, a sample size outlier of only 47 individuals was found for one subpopulation of *A. fulgerator* butterflies. The authors note that this may be due to the low level of genetic variation observed in this population: only two

haplotypes were observed across 14 sampled individuals. In contrast, a later study on European diving beetles undertaken by Bergsten *et al.* [13] found that based on 419 sampled *Agabus bipustulatus* specimens, a sample size of 250 specimens was required to be randomly sampled across its range to achieve 95% haplotype recovery. On the other hand, 70 individuals of the same species was necessary to be sampled in order to recover 95% of COI variation when geographic dispersion between a new sample and the closest previous sample was maximized using resampling simulation.

Not all studies find evidence for greatly broadening the scope of comprehensive specimen sampling. Luo *et al.* [90] demonstrate the utility of the Central Limit Theorem (CLT), employing a simple resampling scheme along with the modified Michaelis-Menten saturation model. The CLT states that the distribution of the sample mean tends toward the (Standard) Normal distribution as the sample size increases. It was found that a minimum sample size of only 20 individuals is needed to provide a reliable estimate of genetic polymorphism at the species level on the basis of observed haplotype numbers. The authors note however that sample sizes should be as large as possible, even though new haplotypes will tend to be observed with lower frequency. Compared to present sample size range of 5-10 specimens per species, a slightly larger minimum sample size range of 11-15 individuals per species was recommended by Yao *et al.* [154] for widely-distributed coastal and inland aquatic salt-tolerant plant species of the families Poaceae and Chenopodiaceae across seven different genera, based on results obtained through resampling procedures and nonparametric Mann-Whitney *U* tests.

Though not devoted to estimating sample sizes for mitochondrial genes such as COI, using resampling simulation, Hale *et al.* [57] found that a sample size of 25-30 individuals was sufficient to accurately estimate microsatellite allele frequencies in hypothetical populations of hairy wood ants (*Formica lugubris*), kakis (*Himantopus novaezelandia*), black-browed albatrosses (*Thalassarche melanophris*) and red squirrels (*Sciurus vulgaris*). The sampling of 25-30 individuals per species for the assessment of genetic diversity via microsatellite loci was also recommended by Pruett and Winker [120] in an earlier study of song sparrows (*Melospiza melodia*). A more recent simulation study examining minimum sample sizes for accurate estimation of genetic diversity from a large number of single nucleotide polymorphism (SNP) markers in the terrestrial Amazonian plant *Amphirrhox longifolia* found that sample sizes beyond eight are sufficient for genetic diversity assessment and as few as two individuals are needed in order to obtain good estimates of population differentiation [101]. These studies clearly point to the need for large sample sizes in multilocus population genetic studies for the overall assessment of genetic diversity at the species level.

These examples serve to illustrate the fact that, as is the case for species divergence thresholds, there is no one universal sample size that can accurately recover the majority of intraspecific genetic variation across taxa and it appears likely that varying levels of additional sampling will be required within taxa and across geographic ranges [89]. What seems to be clear is the fact that many previous assessments of sample sizes necessary for DNA barcoding studies have underestimated levels of sampling depth that are actually

needed in order to recover much of the genetic variation that exists at the species level. Such a trend seems most attributable to restricted geographic sampling and unclear species boundaries, limited funding for adequate specimen retrieval, as well as human-mediated mechanisms such as errors accrued during the amplification/sequencing process.

2.4 Case Study: Phillips *et al.* (2015)

Phillips *et al.* [118] wished to estimate *sampling sufficiency* (θ) — the sample size at which accuracy is maximized and above which no additional sampling information is likely to be gained. This was applied in the context of haplotype accumulation curves in order to determine the point on the x -axis where curve saturation first becomes evident. If such an estimate exists, it would provide a useful stopping rule for specimen sampling [118]. That is, if a lower bound for specimen sample size exists, then it would provide the best estimate of sampling sufficiency for a given species.

2.4.1 Model Assumptions

In developing their sampling model, Phillips *et al.* [118] made several important assumptions, which together form a baseline “perfect-world” scenario for further exploration of specimen/haplotype sampling. These are:

- that specimen sampling is carried out randomly and without replacement from an infinitely large, panmictic population with constant size

- that species haplotypes are both biologically real and unique; and
- that species haplotypes occur with equal frequency.

In the first assumption, the contribution of genetic drift is presumed to be negligible and it is assumed that population structure is absent. Luo *et al.* [90] presumed a constant population size, as well as an absence of natural selection, when calculating intraspecific sample sizes for their simulation study. The argument was that a limited number of individuals would be available in species populations undergoing contraction and that coalescence may not be evident. With regard to the second assumption, DNA barcodes are presumed to be of sufficiently high quality such that they are free of both ambiguous and missing nucleotide bases, which can lead to overestimation of observed and total haplotype numbers through creating artificial haplotype variation within species [6, 33, 118, 136, 137].

Assumptions 1 and 3 were employed by Dixon [38] in proposing a method to assess the extent of haplotype sampling completeness utilizing a Bayesian statistical framework based on the use of Stirling numbers. It was noted that the probability of all haplotypes being observed for a species becomes less accurate if the assumptions of random sampling and equal haplotype frequencies are not met and that the presence of rare species haplotypes will lead to overestimation of overall sampling completeness. Similarly, Phillips *et al.* [118] hypothesized that the presence of rare haplotypes within species will lead to inflation of total sample sizes. Further, as noted by Dixon [38], evolutionary mechanisms such

as isolation-by-distance, which describes the variation in genetic composition of species populations with increasing geographic distance, will likely cause the true extent of sampling effort to be overestimated. In exploring coalescent simulations, Luo *et al.* [90] treated barcode sequences as panmictic. In this way, all specimens can be regarded as being sampled from a single geographic region. Such an assumption is not uncommon within DNA barcoding studies, which are often geographically-focused [31]. While Luo *et al.* [90] did not consider spatial heterogeneity within their simulation study, it was proposed that stratified sampling, where individuals are repetitively sampled without replacement from a pre-selected number of strata, can be employed, with the added assumption that gene flow can largely be ignored.

2.4.2 Mathematical Details

Phillips *et al.* [118] derived a simple Method of Moments [113] estimator in order to predict adequate specimen sample sizes necessary to uncover the majority of cytochrome *c* oxidase subunit I (COI) DNA barcode haplotype diversity existing within animal species according to the equation

$$N^* = \left\lceil \frac{NH^*}{H} \right\rceil. \quad (2.7)$$

Above, N^* is considered an estimate of θ , the true sampling sufficiency, which, under the Frequentist statistical paradigm, is a fixed but unknown parameter. The quantity $\left\lceil \frac{N}{H} \right\rceil$

is the number of specimens represented by each haplotype ($\lceil x \rceil$ is the ceiling function applied to a number x , evaluated by rounding up to the nearest integer). Since haplotypes are assumed to be sampled with equal frequency from a species population, in a sample of $N = 100$ sequences comprising $H = 10$ distinct haplotypes, it is expected that each haplotype is represented by 10 specimens [118]. H^* is found using the equation

$$H^* = \sum_{i=1}^H i = \frac{H(H + 1)}{2} \quad (2.8)$$

where N is the number of DNA sequences observed for a given species, H is the number of observed haplotypes and H^* is the estimated total number of haplotypes (both observed and unobserved) for a species. The above estimator is similar to estimators of total species richness used widely in ecological settings (*e.g.*, the Chao1 estimator of abundance [24]). The central idea around the above estimator is that the majority of haplotypes within a species are rare, being represented by only one (singleton) individual. Thus, once such haplotypes have been accounted for in a species sample, few additional unduplicated haplotypes are likely to be observed, since the majority of remaining haplotypes will be dominant (duplicates) in the population (*i.e.* being represented by two or more specimens); thus, species comprising many singleton haplotypes should be expected to require larger sample sizes in order to capture most of the existing genetic variation for a given species of interest [118, 151].

Phillips *et al.* [118] also proposed both absolute and relative “measures of sampling

closeness” in order to quantify the extent of specimen and haplotype sampling effort. These quantities are as follows:

- Mean number of haplotypes sampled: H
- Mean number of haplotypes not sampled: $H^* - H$
- Proportion of haplotypes sampled: $\frac{H}{H^*}$
- Proportion of haplotypes not sampled: $\frac{H^* - H}{H^*}$
- Mean number of individuals not sampled: $N^* - N$

The above equations, which are central to Phillips *et al.*'s [118] sampling model, can be depicted graphically as follows (**Figure 2.2**).

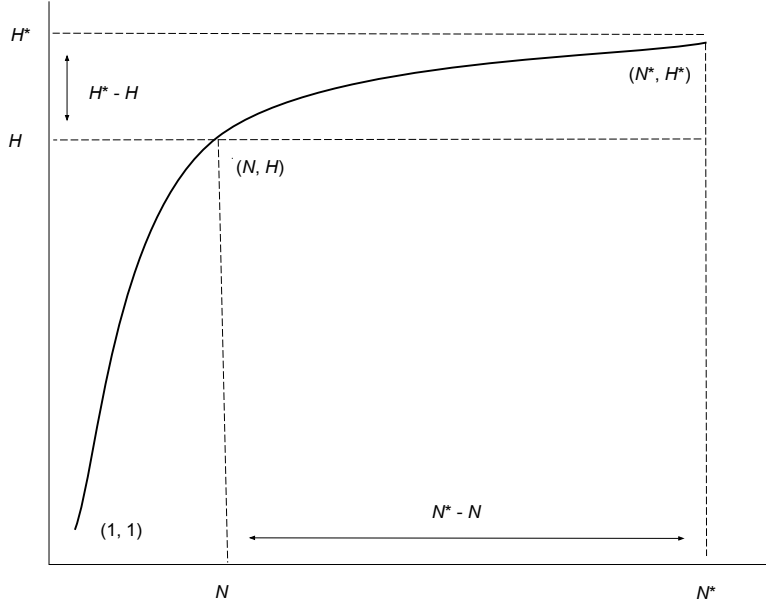


Figure 2.2: Graphical depiction of Phillips *et al.*'s [118] sampling model as described in detail within the main text. The x -axis is meant to depict the number of specimens sampled, whereas the y -axis is meant to convey the cumulative number of unique haplotypes uncovered for every additional individual that is randomly sampled. N and H refer to specimen and haplotype numbers that are observed for a given species. N^* is the total sample size that is needed to capture all H^* haplotypes that exist for a species.

Figure 2 resembles the general shape of a saturated haplotype accumulation curve for a hypothetically well-sampled species. The point labelled (N, H) on the curve reflects the current level of sampling effort that has been expended for a given species (*i.e.*, as found in BOLD). The goal is to extrapolate the curve to the point (N^*, H^*) in order to observe the value on the x -axis (*i.e.*, N^*) at which levelling off toward an asymptote (on the y -axis) first becomes evident (*i.e.*, at the value of H^*). Here, $N^* - N$ is the number of additional specimens that must be randomly sampled in order to observe $H^* - H$ additional haplotypes for a given species. If H is equal to H^* , then N^* will be equal to N , and no further sampling

is necessary; otherwise, if H is less than H^* , then N^* will be greater than N , and additional sampling will be required. The curve in **Figure 2** passes through the point (1, 1), which is due to the fact that the sampling of a single individual of a given species corresponds to observing one unique haplotype for that species.

2.4.3 Application to Ray-finned Fishes

Phillips *et al.* [118] investigated levels of existing COI haplotype variation in 18 species of ray-finned fishes (Chordata: Actinopterygii) represented by a minimum of 60 individuals in accordance with Grewe *et al.* [54]. Results showed that 147-5379 specimens likely must be randomly sampled to uncover all predicted haplotype diversity in the selected species (between 3-528 total haplotypes) [118]. Sample size estimates obtained by Phillips *et al.* [118] are comparable in magnitude to those of Zhang *et al.* [159], but not in the case of Luo *et al.* [90], which are closer to practical sample sizes for DNA barcoding. Further, haplotype accumulation curves displayed evidence of reaching an asymptote for only 3/18 examined species: Chinook salmon (*Oncorhynchus tshawytscha*), Rockfish (*Sebastodes* sp.) and Siamese fighting fish (*Betta splendens*) based on significance testing of curve slopes with a one-sided *t*-test using the last 10 points on the end of accumulation curves [118]. Of note is the haplotype accumulation curve for Chinook salmon, which appeared to show premature saturation despite only 12 out of an estimated total of 78 haplotypes being found for the species. At the time of publication of Phillips *et al.*'s [118] study, *Sebastodes* sp. was linked to a single BIN. The BIN system is inherently dynamic: as more sequences

are added within BOLD, specimens assigned to a single BIN may be allocated to multiple BINs or multiple existing BINs may be coalesced into a single BIN. This is especially the case as species boundaries become clearer or taxonomic revisions are made. As an example, the genus *Sebastes* is a highly speciose group, thought to have undergone an adaptive radiation as recently as 8-9 million years ago [135]. This fact could explain the low haplotype diversity observed for this species (two haplotypes across 98 individuals). Such findings may be due to the underlying assumptions of the model, which are likely to be over-simplistic, particularly that of equality of intraspecific haplotype frequencies. Further, the proposed estimator for the calculation of total haplotype diversity (H^*) (Equation 6) may be a gross overestimate. Despite not being realistic for populations of real species, the reason for adopting a uniform distribution of haplotypes was due to mathematical convenience, in order to make calculations of sample size as simple and as straightforward as possible. This is commonly done in practice, since determining the true distribution of species haplotypes is likely strongly dependent on species under study. Thus, values of N^* are likely overestimates of the true number of specimens that must be randomly sampled in order to observe most haplotype variation that exists for a species [118]. Phillips *et al.* [118] argue that the use of a limited number of points in the calculation of curve slopes may not be adequate; the authors argue that a fixed proportion of curve points should instead be used. Further, through successively targeting the last 20-15%, 15-10% and the last 10% of species haplotype accumulation curves, in order to observe a statistically-significant change in slope values, the precise point of saturation can be localized [118].

Determining the precise point corresponding to haplotype accumulation curves reaching an asymptote (*i.e.*, having a slope near zero) is difficult. One way this can be accomplished is through employing numerical techniques, specifically iteration. Such methods work by repeatedly recycling computed values into an algorithm; that is, current values are used as starting values to the next iteration until convergence to a solution is achieved. One way this can be realized is through iterating Equation (7) along with the equations for the “measures of sampling closeness” proposed by Phillips *et al.* [118]. This seems to be the most logical way forward in better ascertaining at what level specimen sampling is deemed sufficient and thus, when further collection of specimens should be ceased.

2.5 Future Prospects

The present review explores the issue of sampling in DNA barcoding from the perspective of computational and statistical methodologies. Key sample size studies in the barcoding literature were examined in detail. A lack of consensus exists in the most appropriate number of specimens that must be targeted in order to uncover the majority of haplotype diversity that exists at the species level for a variety of taxa. This question is similar to the problem of calculating species divergence thresholds for taxon delimitation and is strongly dependent on species abundances, life histories and geographic coverage. To date, few studies exploring sample sizes for DNA barcoding have been conducted. Existing studies ([118, 159]) appear to point to the comprehensive sampling of hundreds to

thousands of specimens in order to capture a wide range of standing genetic variation for a given species based on asymptotic behaviour of haplotype accumulation curves.

In order to thoroughly examine the issue of determining specimen sample sizes that are necessary for full assessment of COI DNA barcode haplotype sampling completeness within animal species, relaxation of assumptions inherent in Phillips *et al.*'s [118] sampling model is necessary. Specifically, subsequent approaches should investigate the following:

1. relaxing the assumption of uniformity of species haplotype frequencies;
2. loosening the assumption of panmixia within species; and,
3. testing both above assumptions in tandem.

The incorporation of population structure into models of haplotype sampling is not straightforward, as sampling strategies for DNA barcoding are quite variable and highly dependent on the taxa under study. Thus, this necessitates the introduction of a more spatially-explicit systematic sampling (*e.g.*, phylogeographic) of species genetic variation across distinct taxon boundaries and along phenotypic gradients (*i.e.*, clines). The view of DNA barcoding metaphorically as a “molecular transect”, along which a wide range of intraspecific haplotype diversity can be uncovered, is fitting. Within-species genetic variation has been limited to over-representation of deep sampling of a single or a few populations. If the ultimate goal is to account for levels of standing genetic variation with species, then constraining taxon sampling to narrow geographic regions is not ideal, as this

can be considered a form of pseudo-replication. This seems to be an issue of nestedness in sampling and while some depth of sampling within a population is certainly warranted, it cannot be conflated with depth of sampling across populations within a species. In addition, future research should aim to answer the question: is there an optimal threshold for specimen sampling above which no new DNA barcode haplotype variation is likely to be observed for a species? While it should be possible to find this limit for already well-sampled taxa based on trends seen in haplotype accumulation curves, the use of haplotype accumulation curves to estimate sample sizes that are required for full assessment of COI DNA barcode haplotype sampling completeness has only been tested in one previous study (Zhang *et al.* [159]). Phillips *et al.* [118] expanded on previous studies through proposing a simple and easily implemented method to estimate specimen sample sizes for a number of ray-finned fish species, which are among the most densely sampled to date within BOLD. Sample size optimization for the identification of animal species across wide-ranging geographic scales is key since intraspecific variation within DNA barcodes is not easy to measure, and obtaining large numbers of barcodes that reflect a wide range of intraspecific genetic divergence is sometimes challenging [14]. In addition to being able to report likely required specimen sample sizes necessary to achieve saturation in species haplotype curves, it would be ideal if DNA barcoding studies could also provide a global measure of geographic dispersion in order to reliably test for cases of isolation-by-distance within species. Unfortunately, no such measure yet exists in this regard, making these kinds of analyses problematic. While model estimates may not be practical, having such

a framework at hand that easily allows for the calculation of lower bounds for sample size offers researchers a glimpse into the most appropriate taxon sample sizes to target, and potentially where those taxa should be sampled. More crucially, the present simulation proposed herein can be employed in order to best determine the proper allocation of sampling effort, time and resources [72]. Such work finds application in studies of metabarcoding [145] as well as more broadly to global climate change [115].

The development of a computational simulation of haplotype accumulation curves, a tool that can greatly aid biodiversity scientists in targeting species that will benefit from increased sampling effort, can be employed in order to build and grow BOLD with statistically defensible taxon records, which ultimately will allow more reliable specimen identification. This work is crucial because many taxon records currently in BOLD are known from only single specimens. Further, such a simulation algorithm could aid in species discovery through providing more reliable estimates of intraspecific sample sizes used in the calculation of the barcode gap. Through developing statistically-relevant sample size estimation tools that capture geographic and genetic variation within and between species, researchers will be able to improve sampling design strategies, which will lead to a better understanding (and improved database) of intra and interspecies genetic variation. As such, new methodologies will fill this void and contribute to the growing literature on sample size estimation for DNA barcoding as well as be implemented as another tool to add to the biodiversity toolbox.

Acknowledgments

We wish to greatly acknowledge the efforts of Rodger Gwiazdowski in providing valuable edits to this manuscript. In addition, comments by Sarah (Sally) Adamowicz improved overall readability and flow of the manuscript considerably. Finally, two anonymous reviewers lent constructive feedback on this work, for which we are greatly appreciative.

This work was supported by a 2016/17 University of Guelph College of Physical and Engineering Science (CPES) Graduate Excellence Entrance Scholarship awarded to JDP.

The Dish With One Spoon Covenant speaks to our collective responsibility to steward and sustain the land and environment in which we live and work, so that all peoples, present and future, may benefit from the sustenance it provides. As we continue to strive to strengthen our relationships with and continue to learn from our Indigenous neighbours, we recognize the partnerships and knowledge that have guided the research conducted in our labs. We acknowledge that the University of Guelph resides in the ancestral and treaty lands of several Indigenous peoples, including the Attawandaron people and the Mississaugas of the Credit, and we recognize and honour our Anishinaabe, Haudenosaunee, and Métis neighbours. We acknowledge that the work presented here has occurred on their traditional lands so that we might work to build lasting partnerships that respect, honour, and value the culture, traditions, and wisdom of those who have lived here since time immemorial.

Author Contributions

JDP conducted the literature review and wrote the manuscript. DJG acted as an advisor in statistics. RHH acted as an advisor in DNA barcoding. All authors contributed to the revision of this manuscript and approved the final version.

Conflict of Interest

None declared.

Chapter 3

HACSim: An R package to estimate intraspecific sample sizes for genetic diversity assessment using haplotype accumulation curves

Jarrett D. Phillips¹, Steven H. French¹, Daniel J. Gillis¹ and Robert H. Hanner^{2,3}

¹School of Computer Science

²Biodiversity Institute of Ontario

³Department of Integrative Biology

ABSTRACT

Assessing levels of standing genetic variation within species requires a robust sampling for the purpose of accurate specimen identification using molecular techniques such as DNA barcoding; however, statistical estimators for what constitutes a robust sample are currently lacking. Moreover, such estimates are needed because most species are currently represented by only one or a few sequences in existing databases, which we can safely assume are undersampled. Unfortunately, sample sizes of 5-10 specimens per species typically seen in DNA barcoding studies are often insufficient to adequately capture within-species genetic diversity.

Here, we introduce a novel iterative extrapolation simulation algorithm of haplotype accumulation curves, called HACSim (**Haplotype Accumulation Curve Simulator**) that can be employed to calculate likely sample sizes needed to observe the full range of DNA barcode haplotype variation that exists for a species. Using uniform haplotype and non-uniform haplotype frequency distributions, the notion of sampling sufficiency θ (the sample size at which sampling accuracy is maximized and above which no new sampling information is likely to be gained) can be gleaned.

HACSim can be employed in two primary ways to estimate specimen sample sizes: (1) to simulate haplotype sampling in hypothetical species, and (2) to simulate haplotype sampling in real species mined from public reference sequence databases like the Barcode of Life Data Systems (BOLD) or GenBank for any genomic marker of interest.

While our algorithm is globally convergent, runtime is heavily dependent on initial sample sizes and skewness of the corresponding haplotype frequency distribution.

3.1 Introduction

3.1.1 Background

Earth is in the midst of its sixth mass extinction event and global biodiversity is declining at an unprecedented rate [23]. It is therefore important that species genetic diversity be catalogued and preserved. One solution to address this mounting crisis in a systematic, yet rapid way is DNA barcoding [65]. DNA barcoding relies on variability within a small gene fragment from standardized regions of the genome to identify species, based on the fact that most species exhibit a unique array of barcode haplotypes that are more similar to each other than those of other species (*e.g.*, a barcode “gap”). In animals, the DNA barcode region corresponds to a 648 bp fragment of the 5’ terminus of the cytochrome *c* oxidase subunit I (COI) mitochondrial marker [65, 67]. A critical problem since the inception of DNA barcoding involves determining appropriate sample sizes necessary to capture the majority of existing intraspecific haplotype variation for major animal taxa [69, 92, 144]. Taxon sample sizes currently employed in practice for rapid assignment of a species name to a specimen, have ranged anywhere from 1-15 specimens per species [52, 77, 91, 127, 154]; however, oftentimes only 1-2 individuals are actually collected. This trend is clearly reflected within the Barcode of Life Data Systems (BOLD) [123], where an overwhelming number of taxa have only a single record and sequence.

A fitting comparison to the issue of adequacy of specimen sample sizes can be made to

the challenge of determining suitable taxon distance thresholds for species separation on the basis of the DNA barcode gap [92]. It has been widely demonstrated that certain taxonomic groups, such as Lepidoptera (butterflies/moths), are able to be readily separated into distinct clusters largely reflective of species boundaries derived using morphology [21]. However, adoption of a fixed limit of 2% difference between maximum intraspecific distance and minimum interspecific (*i.e.*, nearest-neighbour) divergence is infeasible across all taxa [31, 67]. Species divergence thresholds should be calculated from available sequence data obtained through deep sampling of taxa across their entire geographic ranges whenever possible [156]. There is a clear relationship between specimen sample sizes and observed barcoding gaps: sampling too few individuals can give the impression of taxon separation, when in fact none exists [21, 33, 70, 92, 148], inevitably leading to erroneous conclusions [31]. It is thus imperative that barcode gap analyses be based on adequate sample sizes to minimize the presence of false positives. Introducing greater statistical rigour into DNA barcoding appears to be the clear way forward in this respect [21, 90, 104, 116]. The introduction of computational approaches for automated species delimitation such as Generalized Mixed Yule Coalescent (GMYC) [50, 95, 119], Automatic Barcode Gap Discovery (ABGD) [121] and Poisson Tree Processes (PTP; [160]) has greatly contributed to this endeavour in the form of web servers (GMYC, ABGD, PTP) and R packages (GMYC: Species' LImits by Threshold Statistics, splits [47]).

Various statistical resampling and population genetic methods, in particular coalescent simulations, for the estimation of sample sizes, have been applied to Lepidoptera (Costa

Rican skipper butterflies (*Astraptes fulgerator*) [159] and European diving beetles (*Agabus bipustulatus*) [13]. Using Wright's equilibrium island model [153] and Kimura's stepping stone model [79] under varying effective population sizes and migration rates, Zhang *et al.* [159] found that between 156-1985 specimens per species were necessary to observe 95% of all estimated COI variation for simulated specimens of *A. fulgerator*. Conversely, real species data showed that a sample size of 250-1188 individuals is probably needed to capture the majority of COI haplotype variation existing for this species [159]. A subsequent investigation carried out by Bergsten *et al.* [13] found that a random sample of 250 individuals was required to uncover 95% COI diversity in *A. bipustulatus*; whereas, a much smaller sample size of 70 specimens was necessary when geographic separation between two randomly selected individuals was maximized.

Others have employed more general statistical approaches. Based on extensive simulation experiments, through employing the Central Limit Theorem (CLT), Luo *et al.* [90] suggested that no fewer than 20 individuals per species be sampled. Conversely, using an estimator of sample size based on the Method of Moments, an approach to parameter estimation relying on the Weak Law of Large Numbers [113], sample sizes ranging from 150-5400 individuals across 18 species of ray-finned fishes (Chordata: Actinopterygii) were found by Phillips *et al.* [118].

Haplotype accumulation curves paint a picture of observed standing genetic variation that exists at the species level as a function of expended sampling effort [116, 118].

Haplotype sampling completeness can then be gauged through measuring the slope of the curve, which gives an indication of the number of new haplotypes likely to be uncovered with additional specimens collected. For instance, a haplotype accumulation curve for a hypothetical species having a slope of 0.01 suggests that only one previously unseen haplotype will be captured for every 100 individuals found. This is strong evidence that the haplotype diversity for this species has been adequately sampled. Thus, further recovery of specimens of such species provide limited returns on the time and money invested to sequence them. Trends observed from generated haplotype accumulation curves for the 18 actinopterygian species assessed by Phillips *et al.* [118], which were far from reaching an asymptote, corroborated the finding that the majority of intraspecific haplotypes remain largely unsampled in Actinopterygii for even the best-represented species in BOLD. Estimates obtained from each of these studies stand in sharp contrast to sample sizes typically reported within DNA barcoding studies.

Numerical optimization methods are required to obtain reasonable approximations to otherwise complex questions. Many such problems proceed via the iterative method, whereby an initial guess is used to produce a sequence of successively more precise (and hopefully more accurate) approximations. Such an approach is attractive, as resulting solutions can be made as precise as desired through specifying a given tolerance cutoff. However, in such cases, a closed-form expression for the function being optimized is known *a priori*. In many instances, the general path (behaviour) of the search space being explored is the only information known, and not its underlying functional form. In

this paper, we take a middle-ground approach that is an alternative to probing sampling completeness on the basis of haplotype accumulation curve slope measurement. To this end, iteration is applied to address the issue of relative sample size determination for DNA barcode haplotype sampling completeness, a technique suggested by Phillips *et al.* [116]. Given that specimen collection and processing is quite a laborious and costly endeavour [20, 132], the next most direct solution to an otherwise blind search strategy is to employ computational simulation that approximates specimen collection in the field. The main contribution of this work is the introduction of a new, easy-to-use R package implementing a novel statistical optimization algorithm to estimate sample sizes for assessment of genetic diversity within species based on saturation observed in haplotype accumulation curves. Here, we present a novel nonparametric stochastic (Monte Carlo) iterative extrapolation algorithm for the generation of haplotype accumulation curves based on the approach of [118]. Using the statistical environment R [122], we examine the effect of altering species haplotype frequencies on the shape of resulting curves to inform on likely required sample sizes needed for adequate capture of within-species haplotype variation. Proof-of-concept of our method is illustrated through both hypothetical examples and real DNA sequence data.

3.1.2 Motivation

Consider N DNA sequences that are randomly sampled for a given species of interest across its known geographic range, each of which correspond to a single specimen.

Suppose further that H^* of such sampled DNA sequences are unique (*i.e.*, are distinct haplotypes). This scenario leads naturally to the following question: What is N^* , the estimated total number of DNA sequence haplotypes that exist for a species? Put another way, what sample size (number of specimens) is needed to capture the existing haplotype variation for a species?

The naïve approach (adopted by Phillips *et al.* [118]) would be to ignore relative frequencies of observed haplotypes; that is, assume that species haplotypes are equally probable in a species population. Thus, in the absence of any information, the best one can do is adopt a uniform distribution for the number of sampled haplotypes. Such a path leads to obtaining gross overestimates for sufficient sampling [118]. A much better approach uses all available haplotype data to arrive at plausible estimates of required taxon sample sizes. This latter method is explored here in detail.

3.2 Methods

3.2.1 Haplotype Accumulation Curve Simulation Algorithm

Algorithm Functions

Our algorithm, `HACSim` (short for **Haplotype Accumulation Curve Simulator**), consisting of two user-defined R functions, `HAC.sim()` and `HAC.simrep()`, was created to run simulations of haplotype accumulation curves based on user-supplied parameters. The simulation treats species haplotypes as distinct character labels relative to the number of individuals possessing a given haplotype. The usual convention in this

regard is that Haplotype 1 is the most frequent, Haplotype 2 is the next most frequent, *etc.* [55]. A haplotype network represents this scheme succinctly (**Fig. 3.1**).

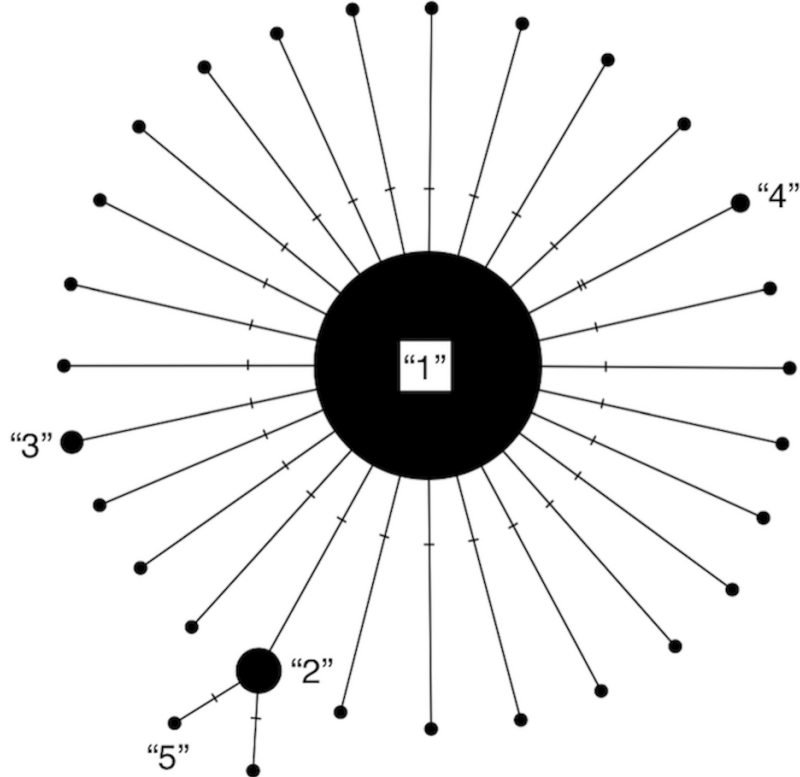


Figure 3.1: Modified haplotype network from Phillips *et al.* [116]. Haplotypes are labelled according to their absolute frequencies such that the most frequent haplotype is labelled “1”, the second-most frequent haplotype is labelled “2”, *etc.* and is meant to illustrate that much species locus variation consists of rare haplotypes at very low frequency (typically only represented by 1 or 2 specimens). Thus, species showing such patterns in their haplotype distributions are probably grossly under-represented in public sequence databases like BOLD and GenBank.

Such an implementation closely mimics that seen in natural species populations, as each character label functions as a unique haplotype linked to a unique DNA barcode sequence. The algorithm then randomly samples species haplotype labels in an iterative fashion with

replacement until all unique haplotypes have been observed. This process continues until all species haplotypes have been sampled. The idea is that levels of species haplotypic variation that are currently catalogued in BOLD can serve as proxies for total haplotype diversity that may exist for a given species. This is a reasonable assumption given that, while estimators of expected diversity are known (*e.g.*, Chao1 abundance) [24], the frequencies of unseen haplotypes are not known *a priori*. Further, assuming a species is sampled across its entire geographic range, haplotypes not yet encountered are presumed to occur at low frequencies (otherwise they would likely have already been sampled).

Because R is an interpreted programming language (*i.e.*, code is run line-by-line), it is slow compared to faster alternatives which use compilation to convert programs into machine-readable format; as such, to optimize performance of the present algorithm in terms of runtime, computationally-intensive parts of the simulation code were written in the C++ programming language and integrated with R via the packages Rcpp [41] and RcppArmadillo [42]. This includes function code to carry out haplotype accumulation (via the function `accumulate()`, which is not directly called by the user). A further reason for turning to C++ is because some R code (*e.g.* nested ‘for’ loops) is not easily vectorized, nor can parallelization be employed for speed improvement due to loop dependence. The rationale for employing R for the present work is clear: R is free, open-source software that it is gaining widespread use within the DNA barcoding community due to its ease-of-use and well-established user-contributed package repository (Comprehensive R Archive Network (CRAN)). As such, the creation and dissemination of

HACSim as a R framework to assess levels of standing genetic variation within species is greatly facilitated.

A similar approach to the novel one proposed here to automatically generate haplotype accumulation curves from DNA sequence data is implemented in the R package `spider` (SPecies IDentity and Evolution in R; [17]) using the `haploAccum()` function. However, the approach, which formed the basis of earlier work carried out by Phillips *et al.* [118], is quite restrictive in its functionality and, to our knowledge, is currently the only method available to generate haplotype accumulation curves in R because `spider` generates haplotype accumulation curves from DNA sequence alignments only and is not amenable to inclusion of numeric inputs for specimen and haplotype numbers. Thus, the method could not be easily extended to address our question. This was the primary reason for the proposal of a statistical model of sampling sufficiency by Phillips *et al.* [118] and its extension described herein.

Algorithm Parameters

At present, the algorithm (consisting of `HAC.sim()` and `HAC.simrep()`) takes 13 arguments as input (**Table 3.1**).

Table 3.1: Parameters inputted (first 7) and outputted (last six) by `HAC.sim()` and `HAC.simrep()`, along with their definitions. **Range** refers to plausible values that each parameter can assume within the haplotype accumulation curve simulation algorithm. $[$ and $]$ indicate that a given value is included in the range interval; whereas, $($ and $)$ indicate that a given value is excluded from the range interval. Simulation progress can be tracked through setting `progress = TRUE` within `HACHypothetical()` or `HACreal()`. Users can optionally specify that a file be created containing all information outputted to the R console (via the argument `filename`, which can be named as the user wishes).

Parameter	Definition	Range
N	total number of specimens/DNA sequences	$(1, \infty)$
H^*	total number of unique haplotypes	$(1, N]$
<code>probs</code>	haplotype probability distribution vector	$(0, 1)$
p	proportion of haplotypes to recover	$(0, 1]$
<code>perms</code>	total number of permutations	$(1, \infty)$
<code>input.seqs</code>	analyze FASTA file of species DNA sequences	TRUE, FALSE
<code>conf.level</code>	desired confidence level for confidence interval calculation	$(0, 1)$
H	cumulative mean number of haplotypes sampled	$[1, H^*]$
$H^* - H$	cumulative mean number of haplotypes not sampled	$[0, H^*)$
$R = \frac{H}{\frac{H^* - H}{H^*}}$	cumulative mean fraction of haplotypes sampled	$(0, 1]$
$\frac{H^*}{N^*}$	cumulative mean fraction of haplotypes not sampled	$[0, 1)$
$N^* - N$	mean specimen sample size corresponding to H^*	$[N, \infty)$
	mean number of individuals not sampled	$[0, N]$

A user must first specify the number of observed specimens/DNA sequences (N) and the number of observed haplotypes (*i.e.*, unique DNA sequences) (H^*) for a given species. Both N and H^* must be greater than one. Clearly, N must be greater than or equal to H^* .

Next, the haplotype frequency distribution vector must be specified. The `probs` argument allows for the inclusion of both common and rare species haplotypes according to user interest (*e.g.*, equally frequent haplotypes, or a single dominant haplotype). The resulting `probs` vector must have a length equal to H^* . For example, if $H^* = 4$, `probs` must contain four elements. The total probability of all unique haplotypes must sum to one.

The user can optionally input the fraction of observed haplotypes to capture p . By default, $p = 0.95$, mirroring the approach taken by both Zhang *et al.* [159] and Bergsten *et al.* [13] who computed intraspecific sample sizes needed to recover 95% of all haplotype variation for a species. At this level, the generated haplotype accumulation curve reaches a slope close to zero and further sampling effort is unlikely to uncover any new haplotypes. However, a user may wish to obtain sample sizes corresponding to different haplotype recovery levels, *e.g.*, $p = 0.99$ (99% of all estimated haplotypes found). In the latter scenario, it can be argued that 100% of species haplotype variation is never actually achieved, since with greater sampling effort, additional haplotypes are almost surely to be found; thus, a true asymptote is never reached. In any case, simulation completion times will vary depending on inputted parameter values, such as `probs`, which controls the skewness of the observed haplotype frequency distribution.

The `perms` argument is in place to ensure that haplotype accumulation curves “smooth out” and tend to H^* asymptotically as the number of permutations (replications) is increased. The effect of increasing the number of permutations is an increase in statistical accuracy and consequently, a reduction in variance. The proposed simulation algorithm outputs a mean haplotype accumulation curve that is the average of `perms` generated haplotype accumulation curves, where the order of individuals that are sampled is randomized. Each of these `perms` curves is a randomized step function (a sort of random walk), generated according to the number of haplotypes found. A permutation size of 1000 was used by Phillips *et al.* [118] because smaller permutation sizes yielded non-smooth (noisy) curves. Permutation sizes larger than 1000 typically resulted in greater computation time, with no noticeable change in accumulation curve behaviour [118]. By default, `perms` = 10000 (in contrast to Phillips *et al.* [118]), which is comparable to the large number of replicates typically employed in statistical bootstrapping procedures needed to ensure accuracy of computed estimates [44]. Sometimes it will be necessary for users to sacrifice accuracy for speed in the presence of time constraints. This can be accomplished through decreasing `perms`. Doing so however will result in only near-optimal solutions for specimen sample sizes. In some cases, it may be necessary to increase `perms` to further smooth out the curves (to ensure monotonicity), but this will increase algorithm runtime substantially.

Should a user wish to analyze their own intraspecific COI DNA barcode sequence data (or sequence data from any single locus for that matter), setting `input.seqs = TRUE`

allows this (via the `read.dna()` function in `ape`). In such a case, a pop-up file window will prompt the user to select the formatted FASTA file of aligned/trimmed sequences to be read into R. When this occurs, arguments for N , H^* and `probs` are set automatically by the algorithm via functions available in the R packages `ape` (Analysis of Phylogenetics and Evolution) [111] and `pegas` (Population and Evolutionary Genetics Analysis System) [110]. Users must be aware however that the number of observed haplotypes treated by `pegas` (via the `haplotype()` function) may be overestimated if missing/ambiguous nucleotide data are present within the final alignment input file. Missing data are explicitly handled by the `base.freq()` function in the `ape` package. When this occurs, R will output a warning that such data are present within the alignment. Users should therefore consider removing sequences or sites comprising missing/ambiguous nucleotides. This step can be accomplished using external software such as MEGA (Molecular Evolutionary Genetics Analysis; [81]). The BARCODE standard [58] was developed to help identify high quality sequences and can be used as a quality filter if desired. Exclusion of low-quality sequences also has the advantage of speeding up computation time of the algorithm significantly.

Options for confidence interval (CI) estimation and graphical display of haplotype accumulation is also available via the argument `conf.level`, which allows the user to specify the desired level of statistical confidence. CIs are computed from the sample $\frac{\alpha}{2}100\%$ and $(1 - \frac{\alpha}{2})100\%$ quantiles of the haplotype accumulation curve distribution. The default is `conf.level = 0.95`, corresponding to a confidence level of 95%. High levels

of statistical confidence (*e.g.*, 99%) will result in wider confidence intervals; whereas low confidence leads to narrower interval estimates.

How Does HACSim Work?

Haplotype labels are first randomly placed on a two-dimensional spatial grid of size $\text{perms} \times N$ (read perms rows by N columns) according to their overall frequency of occurrence (**Fig. 3.2**).

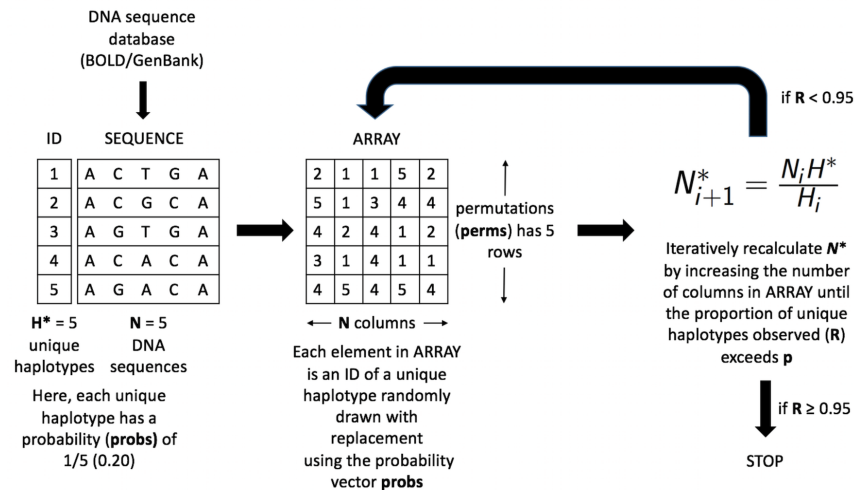


Figure 3.2: Schematic of the HACSim optimization algorithm (setup, initialization and iteration). Shown is a hypothetical example for a species mined from a biological sequence database like BOLD or GenBank with $N = 5$ sampled specimens (DNA sequences) possessing $H^* = 5$ unique haplotypes. Each haplotype has an associated numeric ID from 1- H^* (here, 1-5). Haplotype labels are randomly assigned to cells on a two-dimensional spatial array (ARRAY) with perms rows and N columns. All haplotypes occur with a frequency of 20%, (*i.e.*, **probs** = (1/5, 1/5, 1/5, 1/5, 1/5)). Specimen and haplotype information is then fed into a black box to iteratively optimize the likely required sample size (N^*) needed to capture a proportion of at least p haplotypes observed in the species sample.

The cumulative mean number of haplotypes is then computed along each column (*i.e.*, for every specimen). If all H^* haplotypes are not observed, then the grid is expanded to a size

of `perms` $\times N^*$ and the observed haplotypes enumerated. Estimation of specimen sample sizes proceeds iteratively, in which the current value of N^* is used as a starting value to the next iteration (**Fig. 3.2**). An analogy here can be made to a game of golf: as one aims towards the hole and hits the ball, it gets closer and closer to the hole; however, one does not know the number of times to hit the ball before it lands in the hole. It is important to note that since sample sizes must be whole values, estimates of N^* found at each iteration are rounded up to the next whole number. Even though this approach is quite conservative, it ensures that estimates are adequately reflective of the population from which they were drawn. `HAC.sim()`, which is called internally from `HAC.simrep()`, performs a single iteration of haplotype accumulation for a given species. In the case of real species, resulting output reflects current levels of sampling effort found within BOLD (or another similar sequence repository such as GenBank) for a given species. If the desired level of haplotype recovery is not reached, then `HAC.simrep()` is called to perform successive iterations until the observed fraction of haplotypes captured (R) is at least p . This stopping criterion is the termination condition necessary to halt the algorithm as soon as a “good enough” solution has been found. Such criteria are widely employed within numerical analysis. At each step of the algorithm, a dataset, in the form of a dataframe (called “`d`”) consisting of the mean number of haplotypes recovered (called `means`), along with the estimated standard deviation (`sd`) and the number of specimens sampled (`specs`) is generated. The estimated required sample size (N^*) to recover a given proportion of observed species haplotypes corresponds to the endpoint of the accumulation curve. An indicator message is

additionally outputted informing a user as to whether or not the desired level of haplotype recovery has been reached. The algorithm is depicted in **Fig. 3.3**.

```

Iterative Extrapolation Algorithm to Calculate  $N^*$ 
INPUT:  $N, H^*, \text{probs}, \text{perms}, p, H, R (= \frac{H}{H^*})$ 
OUTPUT:  $N^*$ 
(1) SET  $i = 1$  (initialize iterations);
(2) SET  $N^* = N$  (specify initial guess)
WHILE  $R < p$ 
(3) SET  $i = i + 1$  (update iterations);
(4) SET  $N^*_{i+1} = \frac{N_i H^*}{H_i}$  (compute  $N^*$ );
(5) IF  $N^*_{i+1} = N_i$ , STOP, ELSE return to (3)
END.
```

Figure 3.3: Iterative extrapolation algorithm pseudocode for the computation of taxon sampling sufficiency employed within HACSim. A user must input N, H^* and `probs` to run simulations. Other function arguments required by the algorithm have default values and are not necessary to be inputted unless the user wishes to alter set parameters.

In **Fig. 3.3**, all input parameters are known *a priori* except H_i , which is the number of haplotypes found at each iteration of the algorithm, and $R_i = \frac{H_i}{H^*}$, which is the observed fraction of haplotype recovery at iteration i . The equation to compute N^*

$$N^*_{i+1} = N_i + \frac{N_i}{H_i} (H^* - H_i) = \frac{N_i H^*}{H_i} = \frac{N_i}{R_i} \quad (3.1)$$

is quite intuitive since as H_i approaches H^* , $H^* - H_i$ approaches zero, $R_i = \frac{H_i}{H^*}$ approaches one, and consequently, N_i approaches N^* . In the first part of the above equation, the quantity $\frac{N_i}{H_i} (H^* - H_i)$ is the amount by which the haplotype accumulation curve is extrapolated, which incorporates random error and uncertainty regarding the true value of θ in the search space being explored. Nonparametric estimates formed from the above iterative method produce a convergent monotonically-increasing sequence, which becomes

closer and closer to N^* as the number of iterations increase; that is,

$$N_1^* \leq N_2^* \leq \dots \leq N_i^* \leq N_{i+1}^* \rightarrow N^* \quad (3.2)$$

which is clearly a desirable property. Since haplotype accumulation curves are bounded below by one and bounded above by H^* , then the above sequence has a lower bound equal to the initial guess for specimen sampling sufficiency (N) and an upper bound of N^* .

Along with the iterated haplotype accumulation curves and haplotype frequency barplots, simulation output consists of the five initially proposed “measures of sampling closeness”, the estimate of θ (N^*) based on Phillips *et al.*’s [118] sampling model, in addition to the number of additional samples needed to recover all estimated total haplotype variation for a given species ($N^* - N$; **Fig. 3.4**) (**Table 3.1**).

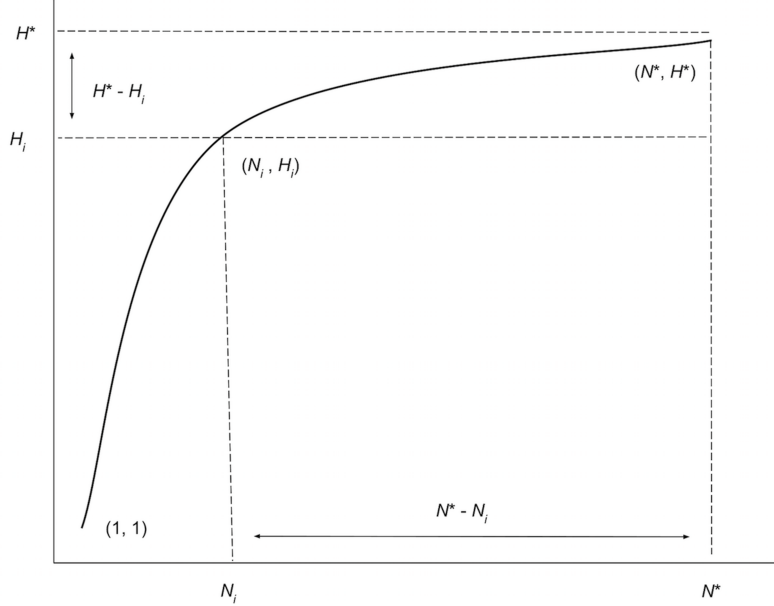


Figure 3.4: Graphical depiction of the iterative extrapolation sampling model as described in detail herein. The figure is modified from Phillips *et al.* [116]. The x -axis is meant to depict the number of specimens sampled, whereas the y -axis is meant to convey the cumulative number of unique haplotypes uncovered for every additional individual that is randomly sampled. N_i and H_i refer respectively to specimen and haplotype numbers that are observed at each iteration (i) of HACSIm for a given species. N^* is the total sample size that is needed to capture all H^* haplotypes that exist for a species.

These five quantities are given as follows: (1) Mean number of haplotypes sampled: H_i , (2) Mean number of haplotypes not sampled: $H^* - H_i$, (3) Proportion of haplotypes sampled: $\frac{H_i}{H^*}$, (4) Proportion of haplotypes not sampled: $\frac{H^* - H_i}{H^*}$, (5) Mean number of individuals not sampled: $N^* - N_i = \frac{N_i}{H_i} (H^* - H_i)$ and are analogous to absolute and relative approximation error metrics seen in numerical analysis. It should be noted that the mean number of haplotypes captured at each iteration, H_i , will not necessarily be increasing, even though estimates of the cumulative mean value of N^* are. It is easily seen above that H_i approaches H^* with increasing number of iterations. Similarly, as the simulation

progresses, $H^* - H_i$, $\frac{H^* - H_i}{H^*}$ and $N^* - N_i = \frac{N_i}{H_i} (H^* - H_i)$ all approach zero, while $\frac{H_i}{H^*}$ approaches one. The rate at which curves approach H^* depends on inputs to both `HAC.sim()` and `HAC.simrep()`. Once the algorithm has converged to the desired level of haplotype recovery, a summary of findings is outputted consisting of (1) the initial guess (N) for sampling sufficiency; (2) the total number of iterations until convergence and simulation runtime (in seconds); (3) the final estimate (N^*) of sampling sufficiency, along with an approximate $(1 - \alpha)100\%$ confidence interval (see next paragraph); and, (4) the number of additional specimens required to be sampled ($N^* - N$) from the initial starting value. Iterations are automatically separated by a progress meter for easy visualization.

An approximate symmetric $(1 - \alpha)100\%$ CI for θ is derived using the (first order) Delta Method [22]. This approach relies on the asymptotic normality result of the CLT and employs a first-order Taylor series expansion around θ to arrive at an approximation of the variance (and corresponding standard error) of N^* . Such an approach is convenient since the sampling distribution of N^* would likely be difficult to compute exactly due to specimen sample sizes being highly taxon-dependent. An approximate (large sample) $(1 - \alpha)100\%$ CI for θ is given by

$$N^* \pm z_{1-\frac{\alpha}{2}} \left(\frac{\hat{\sigma}_H}{H} \sqrt{N^*} \right) \quad (3.3)$$

where $z_{1-\frac{\alpha}{2}}$ denotes the appropriate critical value from the standard Normal distribution and $\hat{\sigma}_H$ is the estimated standard deviation of the mean number of haplotypes recovered at

N^* . The interval produced by this approach is quite tight, shrinking as H_i tends to H^* . By default, `HACSim` computes 95% confidence intervals for the abovementioned quantities.

It is important to consider how a confidence interval for θ should be interpreted. For instance, a 95% CI for θ of (L, U) , where L and U are the lower and upper endpoints of the confidence interval respectively, does *not* mean that the true sampling sufficiency lies between (L, U) with 95% probability. Instead, resulting confidence intervals for θ are themselves random and should be interpreted in the following way: with repeated sampling, one can be $(1 - \alpha)100\%$ confident that the true sampling sufficiency for $p\%$ haplotype recovery for a given species lies in the range (L, U) $(1 - \alpha)100\%$ of the time. That is, on average, $(1 - \alpha)100\%$ of constructed confidence intervals will contain θ $(1 - \alpha)100\%$ of the time. It should be noted however that as given computed confidence intervals are only approximate in the limit, desired nominal probability coverage may not be achieved. In other words, the proportion of times calculated $(1 - \alpha)100\%$ intervals actually contain θ may not be met.

`HACSim` has been implemented as an object-oriented framework to improve modularity and overall user-friendliness. Scenarios of hypothetical and real species are contained within helper functions which comprise all information necessary to run simulations successfully without having to specify certain function arguments beforehand. To carry out simulations of sampling haplotypes from hypothetical species, the function `HACHypothetical()` must first be called. Similarly, haplotype sampling for real

species is handled by the function `HACReal()`. In addition to all input parameters required by `HAC.sim()` and `HAC.simrep()` outlined in **Table 3.1**, both `HACHypothetical()` and `HACReal()` take further arguments. Both functions take the optional argument `filename` which is used to save results outputted to the R console to a CSV file. When either `HACHypothetical()` or `HACReal()` is invoked (*i.e.*, assigned to a variable), an object herein called `HACSOBJ` is created containing the 13 arguments employed by `HACSim` in running simulations. Note the generated object can have any name the user desires. Further, all simulation variables are contained in an environment called ‘`envr`’ that is hidden from the user.

3.3 Results

Here, we outline some simple examples that highlight the overall functionality of `HACSim`. When the code below is run, outputted results will likely differ from those depicted here since our method is inherently stochastic. Hence, it should be stressed that there is not one single solution for the problem at hand, but rather multiple solutions [131]. This is in contrast to a completely deterministic model, where a given input always leads to the same unique output. To ensure reproducibility, the user can set a random seed value using the base R function `set.seed()` prior to running `HAC.simrep()`. It is important that a user set a working directory in R prior to running `HACSim`, which will ensure all created files (‘`seqs.fas`’ and ‘`output.csv`’) are stored in a single location for easy access and reference at a later time. In all scenarios, default parameters were unchanged (`perms =`

$10000, p = 0.95$).

3.3.1 Application of HACSim to Hypothetical Species Equal Haplotype Frequencies

Fig. 3.5 shows sample graphical output of the proposed haplotype accumulation curve simulation algorithm for a hypothetical species with $N = 100$ and $H^* = 10$. All haplotypes are assumed to occur with equal frequency (*i.e.*, `probs = 0.10`). Algorithm output is shown below.

```
## Set parameters for hypothetical species ##
> N <- 100 # total number of sampled individuals
> Hstar <- 10 # total number of haplotypes
> probs <- rep(1/Hstar, Hstar) # equal haplotype frequency

#### Run simulations ####
> HACSOBJ <- HACHypothetical(N = N, Hstar = Hstar, probs = probs) # call helper function
# set seed here if desired, e.g., set.seed(12345)
> HAC.simrep(HACSOBJ)
Simulating haplotype accumulation...
|=====| 100%

--- Measures of Sampling Closeness ---
Mean number of haplotypes sampled: 10
Mean number of haplotypes not sampled: 0
Proportion of haplotypes sampled: 1
Proportion of haplotypes not sampled: 0

Mean value of N*: 100
Mean number of specimens not sampled: 0

Desired level of haplotype recovery has been reached

----- Finished. -----
The initial guess for sampling sufficiency was N = 100 individuals
The algorithm converged after 1 iterations and took 3.637 s
The estimate of sampling sufficiency for p = 95% haplotype recovery is N* = 100
individuals ( 95% CI: 100-100 )
The number of additional specimens required to be sampled for p = 95% haplotype recovery
is N* - N = 0 individuals
```

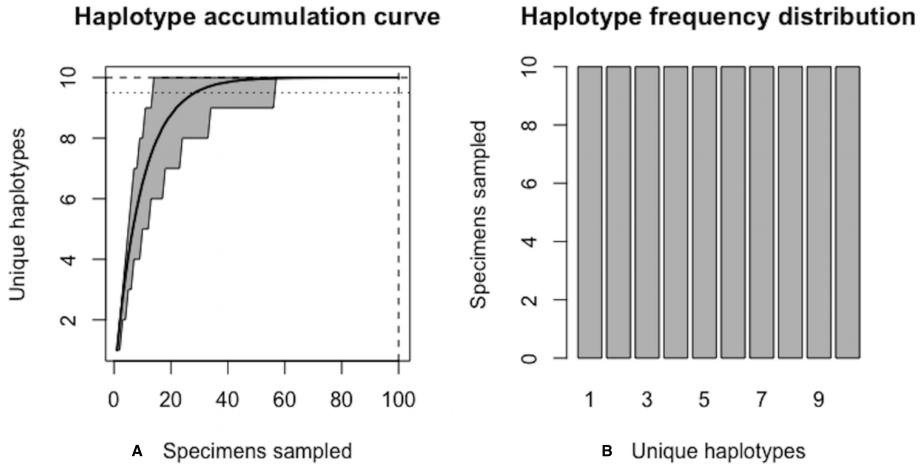


Figure 3.5: Graphical output of `HAC.sim()` for a hypothetical species with equal haplotype frequencies. **A:** Iterated haplotype accumulation curve. **B:** Corresponding haplotype frequency barplot. For the generated haplotype accumulation curve, the 95% confidence interval for the number of unique haplotypes accumulated is depicted by gray error bars. Dashed lines depict the observed number of haplotypes (*i.e.*, RH^*) and corresponding number of individuals sampled found at each iteration of the algorithm. The dotted line depicts the expected number of haplotypes for a given haplotype recovery level (here, $p = 95\%$) (*i.e.*, pH^*). In this example, $R = 100\%$ of the $H^* = 10$ estimated haplotypes have been recovered for this species based on a sample size of only $N = 100$ specimens.

Algorithm output shows that $R = 100\%$ of the $H^* = 10$ haplotypes are recovered from the random sampling of $N = 100$ individuals, with lower and upper 95% confidence limits of 100-100. No additional specimens need to be collected ($N^* - N = 0$). Simulation results, consisting of the six “measures of sampling closeness” computed at each iteration, can be optionally saved in a comma-separated value (CSV) file called ‘output.csv’ (or another filename of the user’s choosing). **Fig. 3.5** shows that when haplotypes are equally frequent in species populations, corresponding haplotype accumulation curves reach an asymptote very quickly. As sampling effort is increased, the confidence interval becomes narrower,

thereby reflecting one's increased confidence in having likely sampled the majority of haplotype variation existing for a given species. Expected counts of the number of specimens possessing a given haplotype can be found from running

`max(envrdspecs) * envr$probs` in the R console once a simulation has converged. However, real data suggest that haplotype frequencies are not equal.

Unequal Haplotype Frequencies

Fig. 3.6 and **Fig. 3.7** show sample graphical output of the proposed haplotype accumulation curve simulation algorithm for a hypothetical species with $N = 100$ and $H^* = 10$. All haplotypes occur with unequal frequency. Haplotypes 1-3 each have a frequency of 30%, while the remaining seven haplotypes each occur with a frequency of c . 1.4%.

```
## Set parameters for hypothetical species ##
> N <- 100
> Hstar <- 10
> probs <- c(rep(0.30, 3), rep(0.10/7, 7)) # three dominant haplotypes each with 30%
frequency

#### Run simulations ####
> HACSOBJ <- HACHypothetical(N = N, Hstar = Hstar, probs = probs)
> HAC.simrep(HACSOBJ)
Simulating haplotype accumulation...
|=====| 100%
--- Measures of Sampling Closeness ---
Mean number of haplotypes sampled: 8.3291
Mean number of haplotypes not sampled: 1.6709
Proportion of haplotypes sampled: 0.83291
Proportion of haplotypes not sampled: 0.16709

Mean value of N*: 120.061
Mean number of specimens not sampled: 20.06099

Desired level of haplotype recovery has not yet been reached
|=====| 100%
--- Measures of Sampling Closeness ---
```

```

Mean number of haplotypes sampled: 9.2999
Mean number of haplotypes not sampled: 0.7001
Proportion of haplotypes sampled: 0.92999
Proportion of haplotypes not sampled: 0.07001

Mean value of N*: 179.5718
Mean number of specimens not sampled: 12.57182

Desired level of haplotype recovery has not yet been reached
|=====
|===== 100%

--- Measures of Sampling Closeness ---

Mean number of haplotypes sampled: 9.5358
Mean number of haplotypes not sampled: 0.4642
Proportion of haplotypes sampled: 0.95358
Proportion of haplotypes not sampled: 0.04642

Mean value of N*: 188.7623
Mean number of specimens not sampled: 8.762348

Desired level of haplotype recovery has been reached

----- Finished. -----
The initial guess for sampling sufficiency was N = 100 individuals
The algorithm converged after 6 iterations and took 33.215 s
The estimate of sampling sufficiency for p = 95% haplotype recovery is N* = 180
individuals ( 95% CI: 178.278-181.722)

The number of additional specimens required to be sampled for p = 95% haplotype recovery
is N* - N = 80 individuals

```

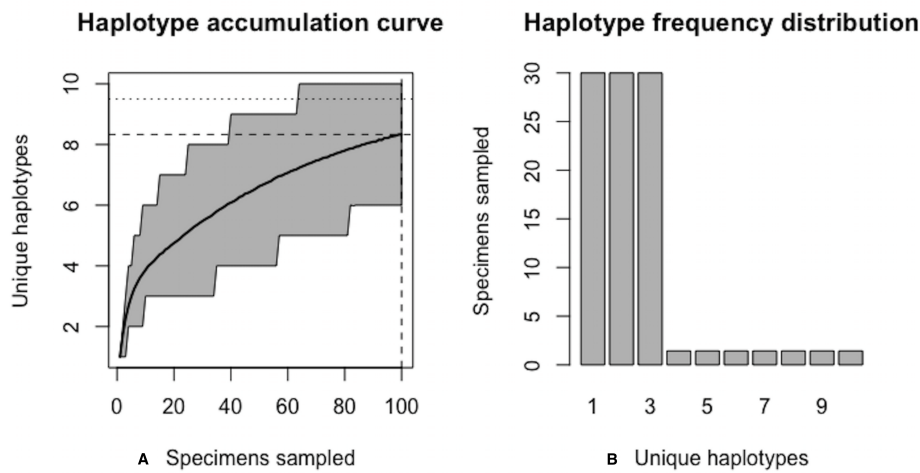


Figure 3.6: Initial graphical output of `HAC.sim()` for a hypothetical species having three dominant haplotypes. In this example, initially, only $R = 83.3\%$ of the $H^* = 10$ estimated haplotypes have been recovered for this species based on a sample size of $N = 100$ specimens.

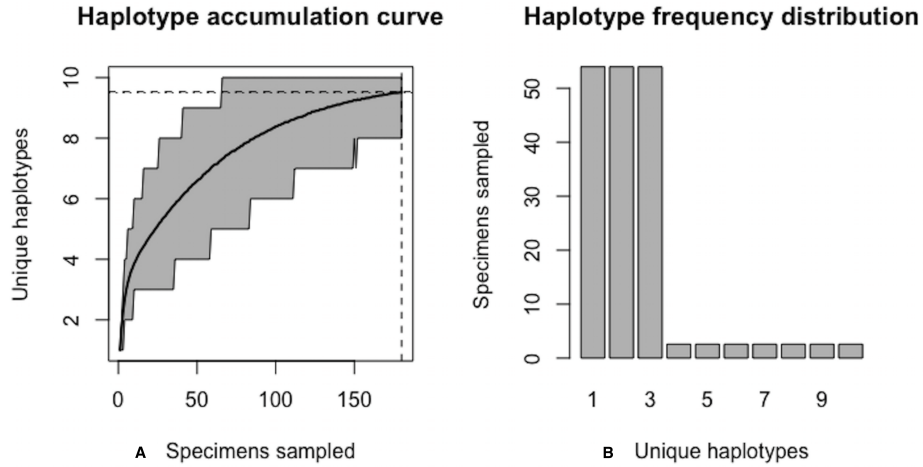


Figure 3.7: Final graphical output of `HAC.sim()` for a hypothetical species having three dominant haplotypes. In this example, upon convergence, $R = 95.4\%$ of the $H^* = 10$ estimated haplotypes have been recovered for this species based on a sample size of $N = 180$ specimens.

Note that not all iterations are displayed above for the sake of brevity; only the first and last two iterations are given. With an initial guess of $N = 100$, only $R = 83.3\%$ of all $H^* = 10$ observed haplotypes are recovered. The value of $N^* = 121$ in the first iteration above serves as an improved initial guess of the true sampling sufficiency, which is an unknown quantity that is being estimated. This value is then fed back into the algorithm and the process is repeated until convergence is reached.

Using Equation (1), the improved sample size was calculated as

$N^* = 100 + \frac{100}{8.3291} (10 - 8.3291) = 120.061$. After one iteration, the curve has been extrapolated by an additional $N^* - N_i = 20.06099$ individuals. Upon convergence, $R = 95.4\%$ of all observed haplotypes are captured with a sample size of $N^* = 180$ specimens,

with a 95% CI of 178.278-181.722. Given that $N = 100$ individuals have already been sampled, the number of additional specimens required is $N^* - N = 80$ individuals. The user can verify that sample sizes close to that found by HACSim are needed to capture 95% of existing haplotype variation. Simply set $N = N^* = 180$ and rerun the algorithm. The last iteration serves as a check to verify that the desired level of haplotype recovery has been achieved. The value of $N^* = 188.7623$ that is outputted at this step can be used as a good starting guess to extrapolate the curve to higher levels of haplotype recovery to save on the number of iterations required to reach convergence. To do this, one simply runs `HACHypothetical()` with $N = 189$.

3.3.2 Application of HACSim to Real Species

Because the proposed iterative haplotype accumulation curve simulation algorithm simply treats haplotypes as numeric labels, it is easily generalized to any biological taxa and genetic loci for which a large number of high-quality DNA sequence data records is available in public databases such as BOLD. In the following examples, HACSim is employed to examine levels of standing genetic variation within animal species using 5'-COI.

Lake Whitefish (*Coregonus clupeaformis*)

An interesting case study on which to focus is that of Lake whitefish (*Coregonus clupeaformis*). Lake whitefish are a commercially, culturally, ecologically and

economically important group of salmonid fishes found throughout the Laurentian Great Lakes in Canada and the United States, particularly to the Saugeen Ojibway First Nation (SON) of Bruce Peninsula in Ontario, Canada, as well as non-indigenous fisheries [128].

The colonization of refugia during Pleistocene glaciation is thought to have resulted in high levels of cryptic species diversity in North American freshwater fishes [3, 4, 5, 74]. [107] wished to investigate this hypothesis in larval Lake Huron lake whitefish. Despite limited levels of gene flow and likely formation of novel divergent haplotypes in this species, surprisingly, no evidence of deep evolutionary lineages was observed across the three major basins of Lake Huron despite marked differences in larval phenotype and adult fish spawning behaviour [107]. This may be the result of limited sampling of intraspecific genetic variation, in addition to presumed panmixia [107]. While lake whitefish represent one of the most well-studied fishes within BOLD, sampling effort for this species has nevertheless remained relatively static over the past few years. Thus, lake whitefish represent an ideal species for further exploration using HACSim.

In applying the developed algorithm to real species, sequence data preparation methodology followed that which is outlined in Phillips *et al.* [118]. Curation included the exclusion of specimens linked to GenBank entries, since those records without the BARCODE keyword designation lack appropriate metadata central to reference sequence library construction and management [58]. Our approach here was solely to assess comprehensiveness of single genomic sequence databases rather than incorporating

sequence data from multiple repositories; thus, all DNA barcode sequences either originating from, or submitted to GenBank were not considered further. As well, the presence of base ambiguities and gaps/indels within sequence alignments can lead to bias in estimate haplotype diversity for a given species.

Currently (as of November 28, 2018), BOLD contains public (both barcode and non-barcode) records for 262 *C. clupeaformis* specimens collected from Lake Huron in northern parts of Ontario, Canada and Michigan, USA. Of the barcode sequences, $N = 235$ are of high quality (full-length (652 bp) and comprise no missing and/or ambiguous nucleotide bases). Haplotype analysis reveals that this species currently comprises $H^* = 15$ unique COI haplotypes. Further, this species shows a highly-skewed haplotype frequency distribution, with a single dominant haplotype accounting for c. 91.5% (215/235) of all individuals (**Fig. 3.8**).

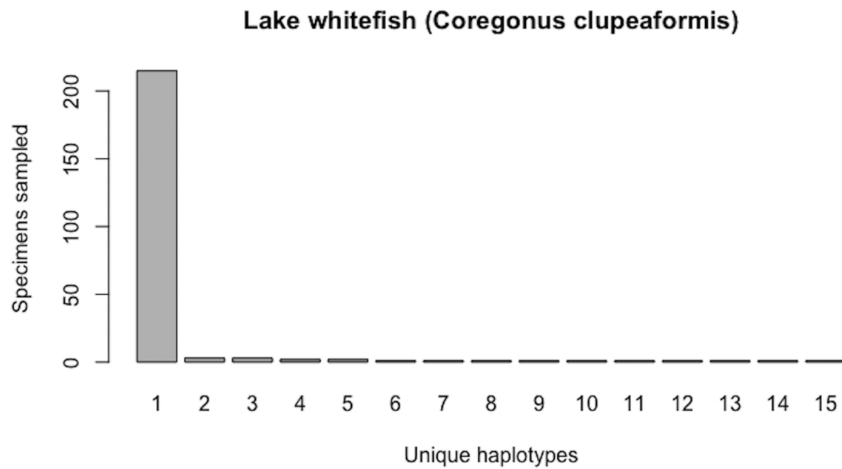


Figure 3.8: Initial haplotype frequency distribution for $N = 235$ high-quality lake whitefish (*Coregonus clupeaformis*) COI barcode sequences obtained from BOLD. This species displays a highly-skewed pattern of observed haplotype variation, with Haplotype 1 accounting for c. 91.5% (215/235) of all sampled records.

The output of HACSim is displayed below.

```
### Run simulations ###
> HACSObj <- HACReal()
> HAC.simrep(HACSObj)
Simulating haplotype accumulation...
|=====
--- Measures of Sampling Closeness ---
Mean number of haplotypes sampled: 11.0705
Mean number of haplotypes not sampled: 3.9295
Proportion of haplotypes sampled: 0.7380333
Proportion of haplotypes not sampled: 0.2619667

Mean value of N*: 318.4138
Mean number of specimens not sampled: 83.4138

Desired level of haplotype recovery has not yet been reached
|=====
--- Measures of Sampling Closeness ---
Mean number of haplotypes sampled: 13.8705
Mean number of haplotypes not sampled: 1.1295
Proportion of haplotypes sampled: 0.9247
Proportion of haplotypes not sampled: 0.0753

Mean value of N*: 603.439
Mean number of specimens not sampled: 45.43895

Desired level of haplotype recovery has not yet been reached
|=====
```

--- Measures of Sampling Closeness ---

Mean number of haplotypes sampled: 14.3708
 Mean number of haplotypes not sampled: 0.6292
 Proportion of haplotypes sampled: 0.9580533
 Proportion of haplotypes not sampled: 0.04194667

Mean value of N^* : 630.4451
 Mean number of specimens not sampled: 26.44507

Desired level of haplotype recovery has been reached

----- Finished. -----

The initial guess for sampling sufficiency was $N = 235$ individuals
 The algorithm converged after 8 iterations and took 241.235 s
 The estimate of sampling sufficiency for $p = 95\%$ haplotype recovery is $N^* = 604$
 individuals (95% CI: 601.504-606.496)

The number of additional specimens required to be sampled for $p = 95\%$ haplotype recovery

is $N^* - N = 369$ individuals

From the above output, it is clear that current specimen sample sizes found within BOLD for *C. clupeaformis* are probably not sufficient to capture the majority of within-species COI haplotype variation. An initial sample size of $N = 235$ specimens corresponds to recovering only 73.8% of all $H^* = 15$ unique haplotypes for this species (**Fig. 3.9**).

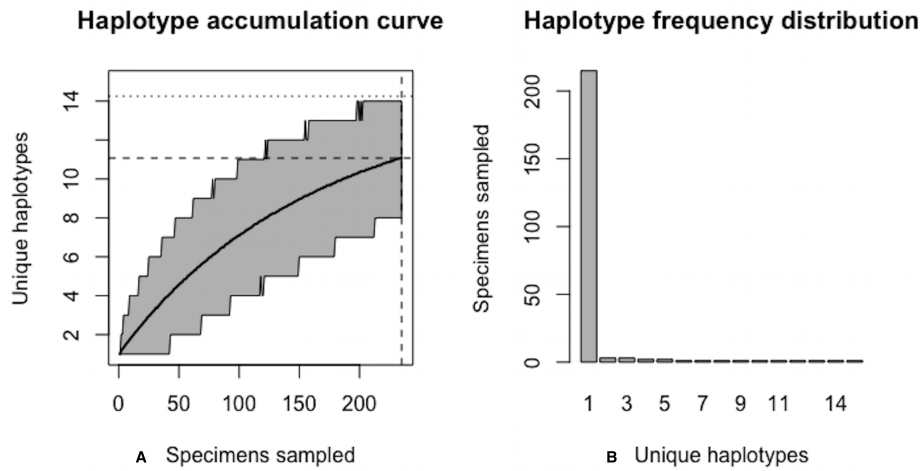


Figure 3.9: Initial graphical output of `HAC.sim()` for a real species (Lake whitefish, *C. clupeaformis*) having a single dominant haplotype. In this example, initially, only $R = 73.8\%$ of the $H^* = 15$ estimated haplotypes for this species have been recovered based on a sample size of $N = 235$ specimens. The haplotype frequency barplot is identical to that of **Fig. 3.8**.

A sample size of $N^* = 604$ individuals (95% CI: 601.504-606.496) would likely be needed to observe 95% of all existing genetic diversity for lake whitefish (**Fig. 3.10**).

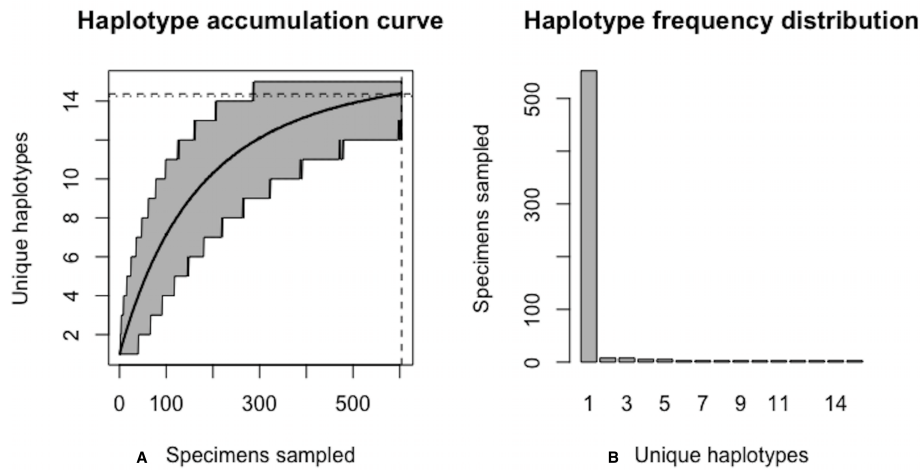


Figure 3.10: Final graphical output of `HAC.sim()` for Lake whitefish (*C. clupeaformis*) having a single dominant haplotype. Upon convergence, $R = 95.8\%$ of the $H^* = 15$ estimated haplotypes for this species have been uncovered with a sample size of $N = 604$ specimens.

Since $N = 235$ individuals have been sampled previously, only $N^* - N = 369$ specimens remain to be collected.

Deer tick (*Ixodes scapularis*)

Ticks, particularly the hard-bodied ticks (Arachnida: Acari: Ixodida: Ixodidae), are well-known as vectors of various zoonotic diseases including Lyme disease [105]. Apart from this defining characteristic, the morphological identification of ticks at any lifestage, by even expert taxonomists, is notoriously difficult or sometimes even impossible [106]. Further, the presence of likely high cryptic species diversity in this group means that turning to molecular techniques such as DNA barcoding is often the only feasible option for reliable species diagnosis. Lyme-competent specimens can be accurately detected through

employing a sensitive quantitative PCR (qPCR) procedure [106]. However, for such a workflow to be successful, wide coverage of within-species haplotype variation from across broad geographic ranges is paramount to better aid design of primer and probe sets for rapid species discrimination. Furthermore, the availability of large specimen sample sizes for tick species of medical and epidemiological relevance is necessary for accurately assessing the presence of the barcode gap.

Notably, the deer tick (*Ixodes scapularis*), native to Canada and the United States, is the primary carrier of *Borrelia burgdorferi*, the bacterium responsible for causing Lyme disease in humans in these regions. Because of this, *I. scapularis* has been the subject of intensive taxonomic study in recent years. For instance, in a recent DNA barcoding study of medically-relevant Canadian ticks, [106] found that out of eight specimens assessed for the presence of *B. burgdorferi*, 50% tested positive. However, as only exoskeletons and a single leg were examined for systemic infection, the reported infection rate may be a lower bound due to the fact that examined specimens may still harbour *B. burgdorferi* in their gut. As such, this species is well-represented within BOLD and thus warrants further examination within the present study.

As of August 27, 2019, 531 5'-COI DNA barcode sequences are accessible from BOLD's Public Data Portal for this species. Of these, $N = 349$ met criteria for high quality outlined in Phillips *et al.* [118]. A 658 bp MUSCLE alignment comprised $H^* = 83$ unique haplotypes. Haplotype analysis revealed that Haplotypes 1-8 were represented by more

than 10 specimens (range: 12-46; **Fig. 3.11**).

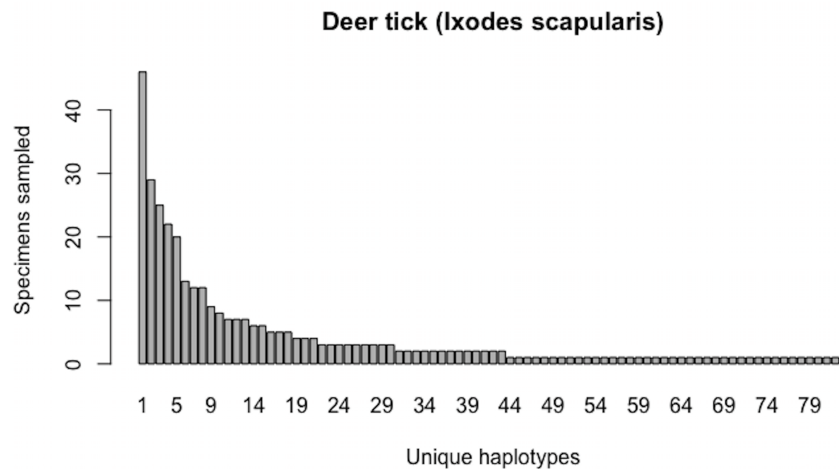


Figure 3.11: Initial haplotype frequency distribution for $N = 349$ high-quality deer tick (*Ixodes scapularis*) COI barcode sequences obtained from BOLD. In this species, Haplotypes 1-8 account for c. 51.3% (179/349) of all sampled records.

Simulation output of HACSIm is depicted below.

```
### Run simulations ###
> HACSOBJ <- HACReal()
> HAC.simrep(HACSOBJ)
Simulating haplotype accumulation...
|=====| 100%
--- Measures of Sampling Closeness ---
Mean number of haplotypes sampled: 65.3514
Mean number of haplotypes not sampled: 17.6486
Proportion of haplotypes sampled: 0.7873663
Proportion of haplotypes not sampled: 0.2126337
Mean value of N*: 443.2499
Mean number of specimens not sampled: 94.24988

Desired level of haplotype recovery has not yet been reached
|=====| 100%
--- Measures of Sampling Closeness ---
Mean number of haplotypes sampled: 78.3713
Mean number of haplotypes not sampled: 4.6287
Proportion of haplotypes sampled: 0.9442325
Proportion of haplotypes not sampled: 0.05576747
Mean value of N*: 802.7684
Mean number of specimens not sampled: 44.76836

Desired level of haplotype recovery has not yet been reached
```

```
| ====== 100%
```

```
--- Measures of Sampling Closeness ---
```

```
Mean number of haplotypes sampled: 79.2147  
Mean number of haplotypes not sampled: 3.7853  
Proportion of haplotypes sampled: 0.954394  
Proportion of haplotypes not sampled: 0.04560602
```

```
Mean value of N*: 841.3716  
Mean number of specimens not sampled: 38.37161
```

```
Desired level of haplotype recovery has been reached
```

```
----- Finished. -----
```

```
The initial guess for sampling sufficiency was N = 349 individuals  
The algorithm converged after 8 iterations and took 1116.468 s  
The estimate of sampling sufficiency for p = 95% haplotype recovery is N* = 803  
individuals ( 95% CI: 801.551-804.449 )
```

The number of additional specimens required to be sampled for p = 95% haplotype recovery
is N* - N = 454 individuals

The above results clearly demonstrate the need for increased specimen sample sizes in deer ticks. With an initial sample size of $N = 349$ individuals, only 78.7% of all observed haplotypes are recovered for this species (**Fig. 3.12**).

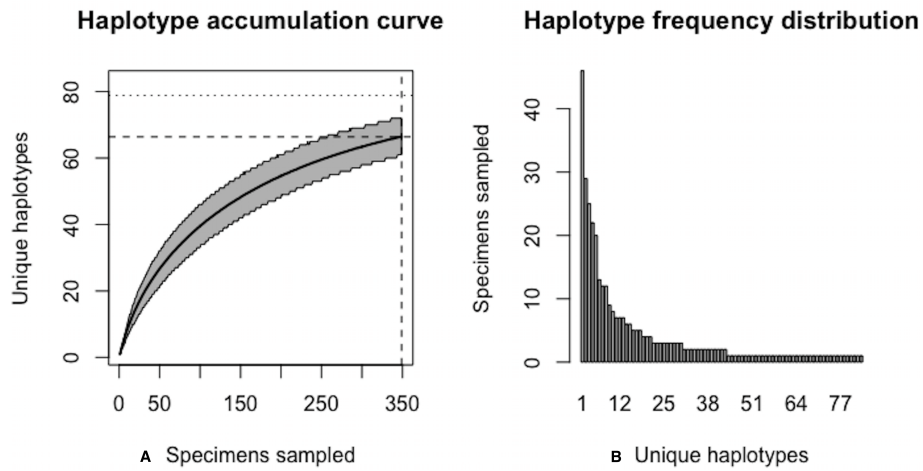


Figure 3.12: Initial graphical output of `HAC.sim()` for a real species (Deer tick, *I. scapularis*) having eight dominant haplotypes. In this example, initially, only $R = 78.7\%$ of the $H^* = 83$ estimated haplotypes for this species have been recovered based on a sample size of $N = 349$ specimens. The haplotype frequency barplot is identical to that of **Fig. 3.11**.

$N^* = 803$ specimens (95% CI: 801.551-804.449) is necessary to capture at least 95% of standing haplotype variation for *I. scapularis* (**Fig. 3.13**).

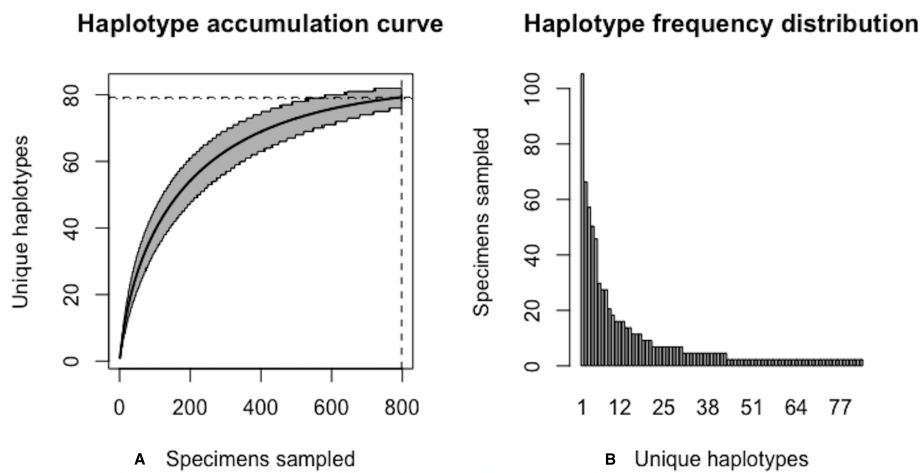


Figure 3.13: Final graphical output of `HAC.sim()` for deer tick (*I. scapularis*) having eight dominant haplotypes. Upon convergence, $R = 95.4\%$ of the $H^* = 83$ estimated haplotypes for this species have been uncovered with a sample size of $N = 803$ specimens.

Thus, a further $N^* - N = 454$ specimens are required to be collected.

Scalloped hammerhead (*Sphyrna lewini*)

Sharks (Chondrichthyes: Elasmobranchii: Selachimorpha) represent one of the most ancient extant lineages of fishes. Despite this, many shark species face immediate extinction as a result of overexploitation, together with a unique life history (e.g., K-selected, predominant viviparity, long gestation period, lengthy time to maturation) and migration behaviour [61]. A large part of the problem stems from the increasing consumer demand for, and illegal trade of, shark fins, meat and bycatch on the Asian market. The widespread, albeit lucrative practice of “finning”, whereby live sharks are definned and immediately released, has led to the rapid decline of once stable populations [133]. As a result, numerous shark species are currently listed by the International Union for the Conservation of Nature (IUCN) and the Convention on International Trade in Endangered Species of Wild Fauna and Flora (CITES). Interest in the molecular identification of sharks through DNA barcoding is multifold. The COI reference sequence library for this group remains largely incomplete. Further, many shark species exhibit high intraspecific distances within their barcodes, suggesting the possibility of cryptic species diversity. Instances of hybridization between sympatric species has also been documented. As establishing species-level matches to partial specimens through morphology alone is difficult, and such a task becomes impossible once fins are processed and sold for consumption or use in traditional medicine, DNA barcoding has paved a clear path forward

for unequivocal diagnosis in most cases.

The endangered hammerheads (Family: Sphyrnidae) represent one of the most well-sampled groups of sharks within BOLD to date. Fins of the scalloped hammerhead (*Sphyraena lewini*) are especially highly prized within IUU (Illegal, Unregulated, Unreported) fisheries due to their inclusion as the main ingredient in shark fin soup.

As of August 27, 2019, 327 *S. lewini* specimens (sequenced at both barcode and non-barcode markers), collected from several Food and Agriculture Organization (FAO) regions, including the United States, are available through BOLD's Public Data Portal. Of these, all high-quality records ($N = 171$) were selected for alignment in MEGA7 and assessment via HACSim. The final alignment was found to comprise $H^* = 12$ unique haplotypes, of which three were represented by 20 or more specimens (range: 28-70; **Fig. 3.14**).

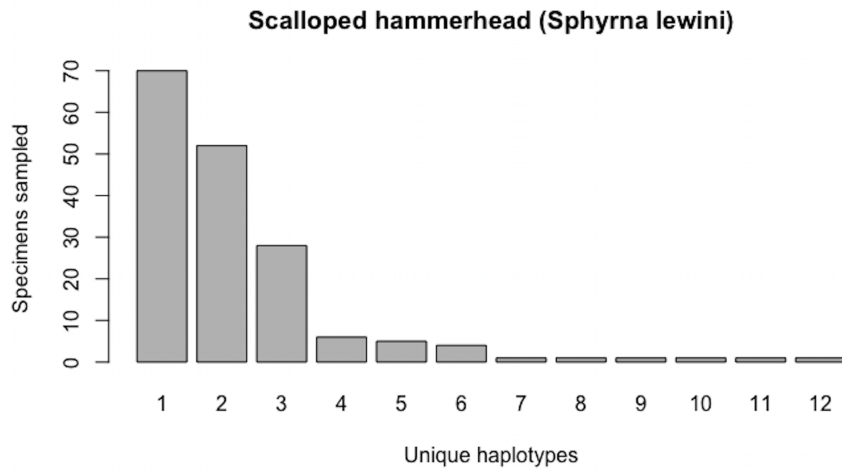


Figure 3.14: Initial haplotype frequency distribution for $N = 171$ high-quality scalloped hammerhead (*Sphyra lewini*) COI barcode sequences obtained from BOLD. In this species, Haplotypes 1-3 account for c. 87.7% (150/171) of all sampled records.

HACSim results are displayed below.

```
### Run simulations ###
> HACSOBJ <- HACReal()
> HAC.simrep(HACSOBJ)
Simulating haplotype accumulation...
|=====
--- Measures of Sampling Closeness ---
Mean number of haplotypes sampled: 9.9099
Mean number of haplotypes not sampled: 2.0901
Proportion of haplotypes sampled: 0.825825
Proportion of haplotypes not sampled: 0.174175

Mean value of N*: 207.0657
Mean number of specimens not sampled: 36.06566

Desired level of haplotype recovery has not yet been reached
|=====| 100%

--- Measures of Sampling Closeness ---
Mean number of haplotypes sampled: 11.3231
Mean number of haplotypes not sampled: 0.6769
Proportion of haplotypes sampled: 0.9435917
Proportion of haplotypes not sampled: 0.05640833

Mean value of N*: 413.3144
Mean number of specimens not sampled: 23.31438

Desired level of haplotype recovery has not yet been reached
|=====| 100%
```

```

--- Measures of Sampling Closeness ---
Mean number of haplotypes sampled: 11.4769
Mean number of haplotypes not sampled: 0.5231
Proportion of haplotypes sampled: 0.9564083
Proportion of haplotypes not sampled: 0.04359167

Mean value of N*: 432.8695
Mean number of specimens not sampled: 18.8695

Desired level of haplotype recovery has been reached

----- Finished. -----
The initial guess for sampling sufficiency was N = 171 individuals
The algorithm converged after 9 iterations and took 174.215 s
The estimate of sampling sufficiency for p = 95% haplotype recovery is N* = 414
individuals ( 95% CI: 411.937-416.063 )

The number of additional specimens required to be sampled for p = 95% haplotype recovery
is N* - N = 243 individuals

```

Simulation output suggests that only 82.6% of all unique haplotypes for the scalloped hammerhead have likely been recovered (**Fig. 15**) with a sample size of $N = 171$.

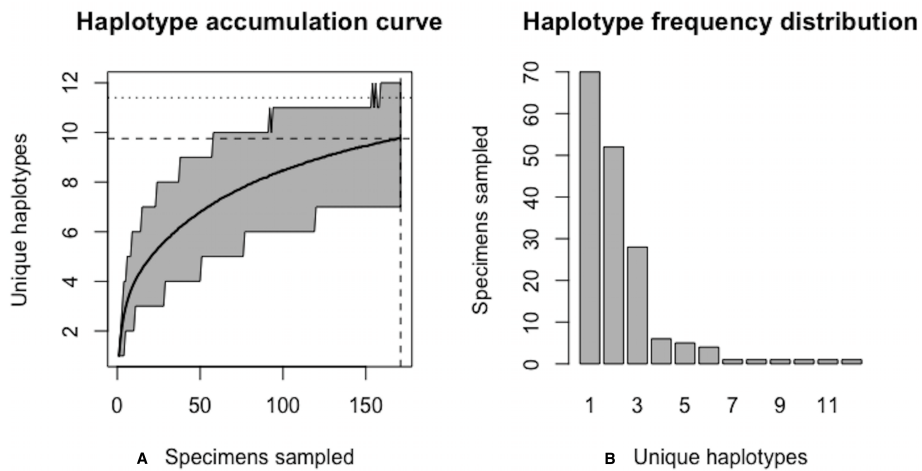


Figure 3.15: Initial graphical output of `HAC.sim()` for a real species (Scalloped hammerhead, *S. lewini*) having three dominant haplotypes. In this example, initially, only $R = 82.6\%$ of the $H^* = 12$ estimated haplotypes for this species have been recovered based on a sample size of $N = 171$ specimens. The haplotype frequency barplot is identical to that of **Fig. 3.14**.

Further, `HACsim` predicts that $N^* = 414$ individuals (95% CI: 411.937-416.063) probably

need to be randomly sampled to capture the majority of intraspecific genetic diversity within 5'-COI (**Fig. 3.16**).

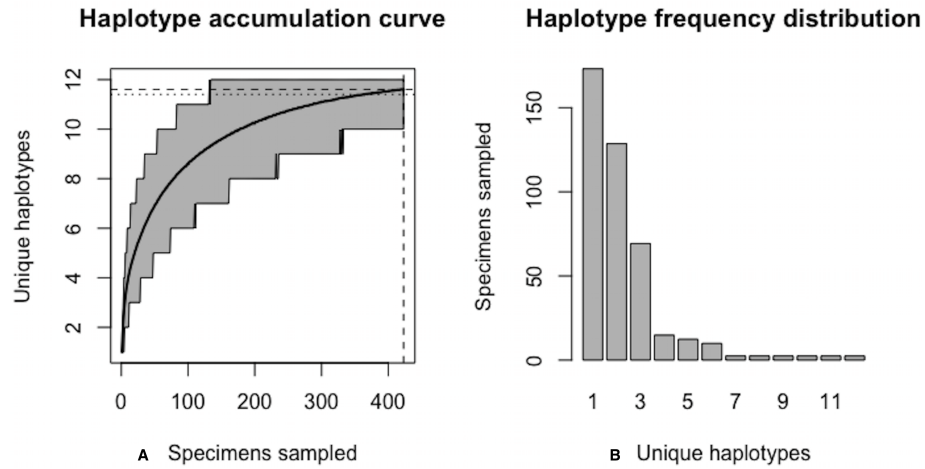


Figure 3.16: Final graphical output of `HAC.sim()` for scalloped hammerhead (*S. lewini*) having three dominant haplotypes. Upon convergence, $R = 95.6\%$ of the $H^* = 12$ estimated haplotypes for this species have been uncovered with a sample size of $N = 414$ specimens.

Since 171 specimens have already been collected, this leaves an additional $N^* - N = 243$ individuals which await sampling.

3.4 Discussion

3.4.1 Initializing HACSim and Overall Algorithm Behaviour

The overall stochastic behaviour of HACSim is highly dependent on the number of permutations used upon algorithm initialization. Provided that the value assigned to the `perms` argument is set high enough, numerical results ouputted by HACSim will be found to be quite consistent between consecutive runs whenever all remaining parameter values remain unchanged. It is crucial that `perms` not be set to too low a value to prevent the

algorithm from getting stuck at local maxima and returning suboptimal solutions. This is a common situation with popular optimization algorithms such as hill-climbing. Attention therefore must be paid to avoid making generalizations based on algorithm performance and obtained simulation results [131].

In applying the present method to simulated species data, it is important that selected simulation parameters are adequately reflective of those observed for real species. Thus, initial sample sizes should be chosen to cover a wide range of values based on those currently observed within BOLD. Such information can be gauged through examining species lists associated with BOLD records, which are readily accessible through Linnean search queries within the Taxonomy browser.

As with any iterative numerical algorithm, selecting good starting guesses for initialization is key. While `HACSim` is globally convergent (*i.e.*, convergence is guaranteed for any value of $N \geq H^*$), a good strategy when simulating hypothetical species is to start the algorithm by setting $N = H^*$. In this way, the observed fraction of haplotypes found, R , will not exceed the desired level of haplotype recovery p , and therefore lead to overestimation of likely required specimen sample sizes. Setting N high enough will almost surely result in R exceeding p . Thus, arbitrarily large values of N may not be biologically meaningful or practical. However, in the case of hypothetical species simulation, should initial sample sizes be set too high, such that $R > p$, a straightforward workaround is to observe where the dashed horizontal line intersects the final haplotype

accumulation curve (*i.e.*, not the line the touches the curve endpoint). The resulting value of N at this point will correspond with p quite closely. This can be seen in **Fig. 5**, where an eyeball guess just over $N^* = 20$ individuals is necessary to recover $p = 95\%$ haplotype variation. A more reliable estimate can be obtained through examining the dataframe “d” outputted once the algorithm has halted (via `envr$d`). In this situation, simply look in the row corresponding to $pH^* \geq 0.95(10) \geq 9.5$. The required sample size is the value given in the first column (`specs`). This is accomplished via the R code

```
envr$d[which(envr$d$means >= envr$p * envr$Hstar), ] [1, 1].
```

The novelty of `HACSim` is that it offers a systematic means of estimating likely specimen sample sizes required to assess intraspecific haplotype diversity for taxa within large-scale genomic databases like GenBank and BOLD. Estimates of sufficient sampling suggested by our algorithm can be employed to assess barcode coverage within existing reference sequence libraries and campaign projects found in BOLD. While comparison of our method to already-established ones is not yet possible, we anticipate that `HACSim` will nevertheless provide regulatory applications with an unprecedented view and greater understanding of the state of standing genetic diversity (or lack thereof) within species.

3.4.2 Additional Capabilities and Extending Functionality of `HACSim`

In this paper, we illustrate the application of haplotype accumulation curves to the broad assessment of species-level genetic variation. However, `HACSim` is quite flexible in that one can easily explore likely required sample sizes at higher taxonomic levels (*e.g.*

order, family, genus) or specific geographic regions (*e.g.*, salmonids of the Great Lakes) with ease. Such applicability will undoubtedly be of interest at larger scales (*i.e.*. entire genomic sequence libraries). For instance, due to evidence of sampling bias in otherwise densely-sampled taxa housed in BOLD (*e.g.*, Lepidoptera), D’Ercole *et al.* (J. D’Ercole, 2019, unpublished data) wished to assess whether or not intraspecific haplotype variation within butterfly species remains unsampled. To test this, the authors employed HACSim to examine sampling comprehensiveness for species comprising a large barcode reference library for North American butterflies spanning 814 species and 14623 specimens.

We foresee use of HACSim being widespread within the DNA barcoding community. As such, improvements to existing code in terms of further optimization and algorithm runtime, as well as implementation of new methods by experienced R programmers in the space of DNA-based taxonomic identification, seems bright.

Potential extensions of our algorithm include support for the exploration of genetic variation at the Barcode Index Number (BIN) level [124], as well as high-throughput sequencing (HTS) data for metabarcoding and environmental DNA (eDNA) applications. Such capabilities are likely to be challenging to implement at this stage until robust operational taxonomic unit (OTU) clustering algorithms are developed (preferably in R). One promising tool in this regard for barcoding of bulk samples of real species and mock communities of known species composition is JAMP (**J**ust **A**ny **M**etabarcoding **P**ipeline) devised for use in R by Elbrecht and colleagues [45]. JAMP includes a sequence

read denoising tool that can be used to obtain haplotype numbers and frequency information (H^* and `probs`). However, because JAMP relies on third-party software (particularly USEARCH [43] and VSEARCH [125]), it cannot be integrated within HACSim itself and will thus have to be used externally. In extending HACSim to next-generation space, two issues arise. First, it is not immediately clear how the argument N , is to be handled since multiple reads could be associated with single individuals. That is, unlike in traditional Sanger-based sequencing, there is not a one-to-one correspondence between specimen and sequence [1, 145]. Second, obtaining reliable haplotype information from noisy HTS datasets is challenging without first having strict quality filtering criteria in place to minimize the occurrence of rare, low-copy sequence variants which may reflect artifacts stemming from the Polymerase Chain Reaction (PCR) amplification step or sequencing process [16, 45, 142]. Turning to molecular population genetics theory might be the answer [1]. Wares and Pappalardo [145] suggest three different approaches to estimating the number of specimens of a species that may have contributed to a metabarcoding sample: (1) use of prior estimates of haplotype diversity, together with observed number of haplotypes; (2) usage of Ewens' sampling formula [46] along with estimates of Watterson's θ (not to be confused with the θ denoting true sampling sufficiency herein) [146], as well as total number of sampled haplotypes; and (3) employment of an estimate of θ and the number of observed variable sites (S) within a multiple sequence alignment. A direct solution we propose might be to use sequencing coverage/depth (*i.e.*, the number of sequence reads) as a proxy for number of individuals. The outcome of this would be an estimate of the

mean/total number of sequence reads required for maximal haplotype recovery. However, the use of read count as a stand-in for number of specimens sampled would require the unrealistic assumption that all individuals (*i.e.*, both alive and dead) shed DNA into their environment at equal rates. The obvious issue with extending HACSim to handle HTS data is computing power, as such data typically consists of millions of reads spanning multiple gigabytes of computer memory.

3.4.3 Summary

Here, we introduced a new statistical approach to assess specimen sampling depth within species based on existing gene marker variation found in public sequence databanks such as BOLD and GenBank. HACSim is both computationally efficient and easy to use. We show utility of our proposed algorithm through both hypothetical and real species genomic sequence data. For real species (here, lake whitefish, deer tick and scalloped hammerhead), results from HACSim suggest that comprehensive sampling for species comprising large barcode libraries within BOLD, such as Actinopterygii, Arachnida and Elasmobranchii is far from complete. With the availability of HACSim, appropriate sampling guidelines based on the amount of potential error one is willing to tolerate can now be established. For the purpose of addressing basic questions in biodiversity science, the employment of small taxon sample sizes may be adequate; however, this is not the case for regulatory applications, where greater than 95% coverage of intraspecific haplotype variation is needed to provide high confidence in sequence matches defensible in a court of

law.

Of immediate interest is the application of our method to other ray-finned fishes, as well as other species from deeply inventoried taxonomic groups such as Elasmobranchii (*e.g.* sharks), Insecta (*e.g.* Lepidoptera, Culicidae (mosquitoes)), Arachnida (*e.g.*, ticks) and Chiroptera (bats) that are of high conservation, medical and/or socioeconomic importance. Although we explicitly demonstrate the use of HACSim through employing COI, it would be interesting to extend usage to other barcode markers such as the ribulose-1,5-bisphosphate carboxylase/oxygenase large subunit (rbcL) and maturase K (matK) chloroplast genes for land plants, as well as the nuclear internal transcribed spacer (ITS) marker regions for fungi. The application of our method to non-barcode genes routinely employed in specimen identification like mitochondrial cytochrome *b* (cyt*b*) in birds for instance [9, 82], nuclear rhodopsin (rho) for marine fishes [60] or the phosphoenolpyruvate carboxykinase (PEPCK) nuclear gene for bumblebees [150] is also likely to yield interesting results since sequencing numerous individuals at several different genomic markers can often reveal evolutionary patterns not otherwise seen from employing a single-gene approach (*e.g.*, resolution of cryptic species or confirmation/revision of established taxonomic placements) [150].

While it is reasonable that HACSim can be applied to genomic regions besides 5'-COI, careful consideration of varying rates of molecular evolution within rapidly-evolving gene markers and the effect on downstream inferences is paramount, as is sequence quality.

Previous work in plants (Genus: *Taxus*) by Liu *et al.* [87] has found evidence of a correlation between mutation rate and required specimen sampling depth: genes evolving at faster rates will likely require larger sample sizes to estimate haplotype diversity compared to slowly-evolving genomic loci. We simply focused on 5'-COI because it is by far the most widely sequenced mitochondrial locus for specimen identification, owing to its desirable biological properties as a DNA barcode for animal taxa and because it has an associated data standard to help filter out poor-quality data. [116]. However, it should be noted that species diagnosis using COI and other barcode markers is not without its challenges. While COI accumulates variation at an appreciable rate, certain taxonomic groups are not readily distinguished on the basis of their DNA barcodes (*e.g.*, the so-called “problem children”, such as Cnidaria, which tend to lack adequate sequence divergence [18]). Other taxa, like Mollusca, are known to harbour indel mutations [83]. Introns within Fungi greatly complicate sequence alignment [94]. Thus, users of HACSim must exercise caution in interpreting end results with other markers, particularly those which are not protein-coding.

It is necessary to consider the importance of sampling sufficiency as it pertains to the myriad regulatory applications of specimen identification established using DNA barcoding (*e.g.*, combatting food fraud) in recent years. It since has become apparent that the success of such endeavours is complicated by the ever-evolving state of public reference sequence libraries such as those found within BOLD, in addition to the inclusion of questionable sequences and lack of sufficient metadata for validation purposes in other genomic databases like GenBank (*e.g.*, [62]). Dynamic DNA-based identification

systems may produce multiple conflicting hits to otherwise corresponding submissions over time. This unwanted behaviour has led to a number of regulatory agencies creating their own *static* repositories populated with expertly-identified sequence records tied to known voucher specimens deemed fit-for-purpose for molecular species diagnosis and forensic compliance (*e.g.* the United States Food and Drug Administration (USFDA)'s Reference Standard Sequence Library (RSSL) employed to identify unknown seafood samples from species of high socioeconomic value). While such a move has partially solved the problem of dynamism inherent in global sequence databases, there still remains the issue of low sample sizes that can greatly inflate the perception of barcode gaps between species. Obtaining adequate representation of standing genetic variation, both within and between species, is therefore essential to mitigating false assignments using DNA barcodes. To this end, we propose the use of HACSim to assess the degree of saturation of haplotype accumulation curves to aid regulatory scientists in rapidly and reliably projecting likely sufficient specimen sample sizes required for accurate matching of unknown queries to known Linnean names.

A defining characteristic of HACSim is its convergence behaviour: the method converges to the desired level of haplotype recovery p for any initial guess N specified by the user. Based on examples explored herein, it appears likely that already-sampled species within repositories like BOLD are far from being fully characterized on the basis of existing haplotype variation. In addition to this, it is important to consider the current limitations of our algorithm. We can think of only one: it must be stressed that appropriate sample

size trajectories are not possible for species with only single representatives within public DNA sequence databases because haplotype accumulation is unachievable with only one DNA sequence and/or a single sampled haplotype. Hence, HACSim can only be applied to species with at least two sampled specimens. Thus, application of our method to assess necessary sample sizes for full capture of extant haplotype variation in exceedingly rare or highly elusive taxa is not feasible. Despite this, we feel that HACSim can greatly aid in accurate and rapid barcode library construction necessary to thoroughly appreciate the diversity of life on Earth.

3.5 Conclusions

Herein, a new, easy-to-use R package was presented that can be employed to estimate intraspecific sample sizes for studies of genetic diversity assessment, with a particular focus on animal DNA barcoding using the COI gene. HACSim employs a novel nonparametric stochastic iterative extrapolation algorithm with good convergence properties to generate haplotype accumulation curves. Because our approach treats species' haplotypes as numeric labels, any genomic locus can be targeted to probe levels of standing genetic variation within multicellular taxa. However, we stress that users must exercise care when dealing with sequence data from non-coding regions of the genome, since these are likely to comprise sequence artifacts such as indels and introns, which can both hinder successful sequence alignment and lead to overestimation of existing haplotype variation within species. The application of our method to assess likely required sample sizes for both

hypothetical and real species produced promising results. We argue the use of HACSim will be of broad interest in both academic and industry settings, most notably, regulatory agencies such as the Canadian Food Inspection Agency (CFIA), Agriculture and Agri-Food Canada (AAFC), United States Department of Agriculture (USDA), Public Health Agency of Canada (PHAC) and the USFDA. While HACSim is an ideal tool for the analysis of Sanger sequencing reads, an obvious next step is to extend usability to Next-Generation Sequencing (NGS), especially HTS applications. With these elements in place, even the full integration of HACSim to assess comprehensiveness of taxon sampling within large sequence databases such as BOLD seems like a reality in the near future.

Acknowledgments

We wish to greatly acknowledge the efforts of Rodger Gwiazdowski in providing valuable edits to this manuscript. In addition, comments by Sarah (Sally) Adamowicz improved overall readability and flow of the manuscript considerably.

This work was supported by a University of Guelph College of Physical and Engineering Science (CPES) Graduate Excellence Entrance Scholarship awarded to JDP.

The Dish With One Spoon Covenant speaks to our collective responsibility to steward and sustain the land and environment in which we live and work, so that all peoples, present and future, may benefit from the sustenance it provides. As we continue to strive to strengthen our relationships with and continue to learn from our Indigenous neighbours, we recognize the partnerships and knowledge that have guided the research conducted in our labs. We acknowledge that the University of Guelph resides in the ancestral and treaty lands of several Indigenous peoples, including the Attawandaron people and the Mississaugas of the Credit, and we recognize and honour our Anishinaabe, Haudenosaunee, and Métis neighbours. We acknowledge that the work presented here has occurred on their traditional lands so that we might work to build lasting partnerships that respect, honour, and value the culture, traditions, and wisdom of those who have lived here since time immemorial.

Author Contributions

JDP conducted the literature review and wrote the manuscript. DJG acted as an advisor in statistics. RHH acted as an advisor in DNA barcoding. All authors contributed to the revision of this manuscript and approved the final version.

Conflict of Interest

None declared.

Chapter 4

Solving the genetic specimen sample size problem for DNA barcoding with a local search optimization algorithm

Jarrett D. Phillips^{1*}, Scarlett E. Bootsma¹, Daniel J. Gillis¹, Robert H. Hanner^{2,3}

¹*School of Computer Science, University of Guelph, Guelph, ON., Canada, N1G2W1*

²*Biodiversity Institute of Ontario, University of Guelph, Guelph, ON., Canada, N1G2W1*

³*Department of Integrative Biology, University of Guelph, Guelph, ON., Canada, N1G2W1*

ABSTRACT

Biodiversity manifests itself in many ways. One way is through the lens of species genetic diversity. DNA barcoding offers a systematic means of documenting such diversity in the face of global species extinction. One question of interest among DNA “barcoders” is: How many specimens of a given species do we need to sample before we can stop? That is, what sample size is needed to capture a given level of a species’ genetic diversity? This is not an easy question to answer! At a practical level, specimen sample sizes typically range from 1-10 individuals per species. However, a number of studies have demonstrated through both empirical investigations and statistical simulations that such small, largely arbitrary sample sizes are far from enough. In fact, some studies even suggest that hundreds to thousands of individuals may be necessary to be sampled before sampling can safely be stopped.

Here, a detailed statistical simulation study is carried out to test the overall performance of HACSim, short for **Haplotype Accumulation Curve Simulator**, a new R package developed to greatly facilitate the process of estimating likely required specimen sample sizes for recovery of species genetic variation based on saturation observed in haplotype accumulation curves. The approach underlying HACSim is fundamentally different from what has been attempted before. What separates HACSim from previously proposed methods is that it is a nonparametric approach that combines two clever statistical ideas to systematically propose plausible specimen sample sizes necessary to adequately

recover a given level of haplotype diversity for a species of interest. These are: (1) stochasticity (*i.e.*, randomness) and (2) iteration. These two characteristics together represent a step forward in thinking critically about how genetic variation manifests itself in contemporary patterns of biological diversification and how well current sampling efforts contribute to our understanding of these patterns and the underlying evolutionary processes that generate and maintain them. Throughout the present work, both hypothetical and real-world examples are employed to demonstrate the general utility of `HACSim` in relation to assessing both the comprehensiveness of specimen sampling as well as the downstream construction and curation of species barcode reference sequence libraries.

4.1 Introduction

4.1.1 Background

A central problem surrounding most biodiversity assessment studies concerns the robust estimation of required specimen sample sizes necessary to address a given research question of interest in ecology and evolutionary biology. Unfortunately, the specimen sample size problem is fraught with myriad challenges due in part to the inherent difficulty of adequate specimen collection in light of factors such as lack of project funding, as well as species rarity. This problem has largely persisted unabated throughout the years. One area where the issue of sample size determination has been sorely felt is in the discipline of DNA-based species diagnosis, especially DNA barcoding.

DNA barcoding [65] employs short, universal regions of genomic DNA, such as the *c.* 648 bp fragment taken from the 5' end of the cytochrome *c.* oxidase subunit I (COI) gene for animals [67], to readily identify unknown specimens to known species by matching queries to reference sequences housed in barcode libraries such as those found in the Barcode of Life Data Systems (BOLD; [123]; <http://www.boldsystems.org>) and GenBank. Early on, when DNA barcoding was first proposed, estimates of sufficient sample sizes needed to recover levels of standing genetic variation within species of interest were often quite low and rather arbitrary, typically 20 or fewer specimens per species [116, 117, 118]. Even some early studies have expressed the need for more comprehensive sampling efforts [159], but until now, a systematic approach was not available to provide optimal

specimen sample sizes to adequately capture intraspecific DNA sequence variation. Such a tool is promising since required specimen sample sizes will vary considerably based on evolutionary history and life history of the species under consideration. For instance, different genomic marker loci evolve at different rates; thus, more rapidly evolving genes will likely require larger sample sizes compared to more slowly-evolving molecular loci [116].

Before proceeding any further, a brief explanation of the genetic specimen sample size problem (hereafter referred to as the GSSSP) as it pertains to DNA barcoding in animals is needed. Suppose that N individuals of a given species of interest have been sampled at random from the field. Mitochondrial DNA from said individuals is then isolated and the COI gene amplified and sequenced. The result is a set of N DNA sequences of which some are identical across individuals and others distinct. Such unique sequences are termed *haplotypes*. The GSSSP asks the following question: Has all species' haplotype variation likely been found from sampling only N specimens? If not, then what sample size N^* is needed to be sufficiently confident that the majority of haplotype diversity (H^*) has been captured?

The majority of molecular biodiversity researchers of studies devoted wholly or in part to the GSSSP generally proceed in one of two ways when assessing haplotype sampling completeness for species of interest: (1) through simply plotting haplotype accumulation curves, and based on visual inspection as to the degree of saturation of the resulting curve,

making an uninformed decision as to whether or not greater sampling effort is needed; and/or, (2) through naïvely assuming that available data used to construct such curves strongly conform to specific parametric statistical models. Unfortunately, both of these paths are inherently flawed. Firstly, decisions surrounding taxon sampling depth must be supported with quantitative evidence in the form of statistical hypothesis testing procedures or simulation studies because specimen sampling is both a costly and laborious endeavour [20, 132]. Recognizing this, in addition to plotting haplotype accumulation curves for a wide variety of ray-finned fishes (Chordata: Actinopterygii), [118] employed simple linear regression on the endpoints of accumulation curves to test the hypothesis that there was no evidence of additional haplotypes remaining to be sampled for a species. This was accomplished through testing that terminal curve slopes are equal to zero. Phillips *et al.* [118] then calibrated their findings with a crude deterministic base model of likely required specimen sampling levels necessary to recover all estimated total haplotypes that might exist for a given species, grounded on the unrealistic assumption that species' haplotypes are sampled uniformly across known ecologic and geographic ranges. Estimates of sampling sufficiency produced by Phillips *et al.*'s [118] model are likely to be heavily biased due to the restrictive assumption of uniformity of species' haplotypes. Moreover, because specimen sampling is an inherently stochastic process, a move away from a purely deterministic model and toward a more realistic one is needed to better inform the GSSSP.

4.1.2 Phillips *et al.*'s (2020) Haplotype Sampling Model

With these considerations in mind and knowledge in hand, [117] devised a nonparametric stochastic, population-based local optimization framework within the R Statistical Environment [122], called `HACSim` (**Haplotype Accumulation Curve Simulator**), to estimate likely required sample sizes based on existing DNA barcode sequence data. Their approach employs an initial guess of sampling sufficiency (N) to iteratively propose improving estimates of sample size necessary to capture a predefined minimum cutoff (p), typically 95%, of observed haplotype diversity for both hypothetical and real species based on a species' haplotype frequency distribution (`probs`), representing the probability of occurrence of each haplotype in a randomly-collected specimen sample. A user need only additionally supply the number of permutations (`perms`) to be employed in the search, which acts to control both the *numerical* accuracy and precision of computed sample size estimates by increasing or decreasing the smoothness of the generated accumulation curve. Note here that improving the *statistical* accuracy/precision of said estimates would require more specimens to be sampled. Each randomly generated permutation represents a plausible assignment of species haplotypes to every sampled specimen. In simulating hypothetical species, H^* must be less than or equal to N (this constraint is always satisfied for real species). The case of $N = H^*$ corresponds to encountering a new, previously unseen species' haplotype for every additional specimen that is collected. For real species, N , H^* and `probs` are calculated automatically from an imported FASTA file of aligned and trimmed single-marker DNA sequences.

Two important assumptions arise in considering the overall utility of HACSim for assessing standing levels of genetic variation within species [117]:

1. that haplotypic variation observed in a randomly collected sample of specimens is representative of the true species' population (which is unknown *a priori*); and,
2. that unsampled haplotypes are rare in a species' population (*i.e.*, haplotypes occur at low frequency, potentially found in only 1-2 individuals – otherwise they would have already been sampled).

Assumption 1 is a common one adopted in many statistical resampling procedures such as nonparametric bootstrapping and is equivalent to treating a randomly drawn sample as if it were in fact the population of interest. Implicit in the present haplotype sampling model is the fact a randomly drawn sample of individuals makes up only a small fraction of the total species' population size. Assumption 2 is a strong, yet unrealistic one that is necessary within the framework of the underlying model. Whereas the total number of expected haplotypes that might exist for a given species' is readily estimated from observed data (such as through the Chao1 abundance estimator [24]), the probabilities associated with unseen haplotypes cannot be known with absolute certainty [117]. Therefore, the number of observed unique haplotypes for a species serves as a reasonable proxy for the total number of haplotypes that might exist for said species. In the context of the GSSSP investigated herein, Assumptions 1 and 2 together amount to assuming that all genetic diversity observed in reference sequence databases such as BOLD and related repositories

arise from a single *infinitely-large* panmictic (*i.e.*, randomly-mating) species' population of constant size from which individuals are randomly sampled without replacement [118]. That is, the current model underlying HACSim disregards both the contribution of genetic drift which acts to alter haplotype frequencies in small species populations, as well as spatial effects which arise as a result of population substructuring via gene flow [116]. It is recognized that the abovementioned assumptions will likely not be met for most real species. Violations of stated assumptions can only be mitigated through more thorough specimen sampling, and therefore further sampling of standing intraspecific haplotype variation. Extensions to HACSim's underlying sampling algorithm to better reflect true evolutionary dynamics at both the population and species levels have yet to be fully investigated.

Here, we employ the definition of sampling sufficiency intially proposed by [118]: the sample size at which sampling accuracy is maximized and above which no new information is likely to be gained. The authors of the current study note that this definition is slightly misleading as extensive sampling effort may result in only small gains in accuracy. A better term in this case to replace “maximized” in the above definition would be *converged*. When running simulations of real taxa obtained from reference sequence databases, the number of DNA sequences in a final single-species multiple sequence alignment, the corresponding number of observed unique species' haplotypes, and the species' haplotype frequency distribution are all used for algorithm initialization.

Specifically, the iteration scheme used by `HACSim` is

$$N_{i+1}^* = \frac{N_i H^*}{H_i} \quad (4.1)$$

where H_i is the cumulative mean number of observed unique species' haplotypes found from randomly sampling N_i individuals at iteration i .

Drawing on the field of evolutionary computation, which is loosely based on Darwinian theory, H_i can be likened to a fitness function that is to be maximized across all sampled specimens. Specifically, the “fitness” function being optimized above is expressed mathematically as

$$H_i = \frac{1}{\text{perms}} \sum_j x_{jN} \quad (4.2)$$

where x_{jN} is a `perms` \times N array and $j \in \{1, \dots, \text{perms}\}$ denotes array rows. The array generated internally by `HACSim` consists of positive integers in the range $[1, H^*]$ that are drawn randomly according to `probs`, a sorted vector of decreasing values between 0 and 1, whose elements must sum to 1. The filled population array forms the representation of solutions encoding the algorithm's search space (see below for a detailed discussion). Elements within each row of the filled array are sampled according to `probs`. That is, if, say, there are $N = 100$ individuals and Haplotype 1 occurs at 90% frequency, then approximately 90 individuals would be randomly assigned a label of 1. This scheme then continues for all remaining haplotypes. Accumulation of unique species' haplotypes is

then carried out through randomly sampling individual specimens (columns) of said array across all permutations (array rows). Cumulative means of the number of haplotypes recovered for each specimen, as per Equation 2, are then computed across all sampled permutations. The last array column corresponds to sampling N individuals for a given species in Equation 2. Equation 1 produces a monotonically-increasing and convergent sequence of estimates for sampling sufficiency even though the average number of species' haplotypes found at each iteration of HACSim may fluctuate randomly; eventually, H_i will approach H^* and therefore N_i approaches N^* . HACSim terminates when the observed proportion of haplotypes retrieved ($R = \frac{H_i}{H^*}$) is at least p . The rate of convergence of outputted haplotype accumulation curves to an asymptote depends highly on the value of `perms`. When `perms` is set high enough, the endpoint of the resulting curve, generated at each iteration of the algorithm, will be close in magnitude to the maximum value of the cumulative mean calculated across all columns of the constructed array. This behaviour provides a clear rationale for selection of the objective function being optimized herein. Further, the inclusion of a larger number of permutations acts to incorporate more diverse solutions into the search, while at the same time permitting HACSim's iterative search to "hone in" on promising solutions through exploitation/intensification of the problem space. Such behaviour is in sharp contrast to setting `perms` to a small value, where HACSim is reduced to searching the space of potential solutions randomly, while simultaneously performing a much broader search through exploration/diversification. Striking a careful balance between exploration/diversification and exploitation/intensification is key to

avoiding premature algorithmic convergence and search efficiency issues.

Algorithm estimates provided by HACSim correspond to the point on the x -axis of haplotype accumulation curves where saturation of species genetic variation is likely to occur. Since one is interested in devising an optimal stopping rule for specimen sampling, it becomes necessary to closely monitor the endpoint of haplotype accumulation curves generated at each iteration of HACSim's run. A single run of HACSim entails successively generating `perms` accumulation curves internally and outputting a mean curve at each iteration. Each successive iteration within a single run of HACSim is an extrapolation of the curve generated in the preceding iteration. The x -value corresponding to the point where the curve endpoint touches the imaginary horizontal line formed by the prespecified threshold for haplotype recovery is our best estimate of the sample size needed to fully characterize haplotype variation within a species, given current genomic data. Further details on the internal workings of HACSim can be found in [117].

4.1.3 Assessing the Computational and Statistical Performance of HACSim Background

To fully assess the variability of any stochastic optimization algorithm, it is essential to carry out many independent runs under identical starting conditions. Repeated generation of random pseudodata drawn from known probability distributions under carefully designed experiments is the hallmark of statistical simulation studies [19, 96]. When it

comes to designing any simulation study to test the performance of new statistical methods, one actually knows (or at least pretends to know) the ground truth underlying a given data-generating process. Within the present study, comparing estimates of sample size proposed by HACSim (N^*) to the “true” sampling sufficiency (θ) is not possible because the actual number of specimens of a particular species needed to be sampled to retrieve a given level of genetic diversity, while assumed to be fixed, is not known in advance. If this were indeed the case, and specimen collection was feasible, then all specimens could reasonably be sampled without too much effort. Instead, the goal here lies in maximizing the degree of “closeness” of the estimated fraction of a species’ haplotype diversity recovered (R) to the desired level of haplotype diversity to be captured (p). The hypothetical species examples and real species case studies employed by [117] were meant to illustrate proof-of-concept of the method, and therefore only one cycle of HACSim was performed for each case. In the context of the present study, a single realization representing an estimate for specimen sampling sufficiency is unlikely to be useful on its own. Running a non-deterministic algorithm in succession often reveals multiple valid local optima for a search problem of interest, each which must be carefully weighed [131]. As such, this necessitates a brief discussion around HACSim’s *search space*.

Theory

A search space encompasses the domain over which a function is to be optimized (*i.e.*, either minimized or maximized) and includes all plausible solutions to said search

problem. The search space explored by stochastic optimization algorithms can be best framed in the context of a person attempting to ascend to the top of hill or mountain. Said hill (or mountain) contains numerous peaks, plateaus and valleys, each with varying levels of steepness that together form a fitness landscape. The hill’s (or mountain’s) terrain is analogous to local optima encountered in an algorithmic search problem. In general, solving the GSSSP through pure brute force (*i.e.*, exhaustive search) or random search is difficult owing to the size of the search space that must be explored: both specimen- and haplotype-level information need to be taken into account. Here, a (partial) solution to the GSSSP corresponds to the generation of a permutation. In the present work, the notion of a “permutation” is distinct from the traditional mathematical meaning of the term. Within the field of combinatorics, a permutation is any (re)ordering of elements contained in a set. Herein, a random permutation appearing in the array generated by HACSim according to some underlying probability distribution may comprise elements which are different from those appearing in any other permutation. For instance, one permutation of five specimens drawn from a uniform distribution over observed species’ haplotypes labels may be given by the tuple (2, 1, 1, 5, 2), while another may be (5, 1, 3, 4, 4). “Permutation” is used here to simply emulate terminology used in similar R packages that construct haplotype (and species) accumulation curves such as `spider` [17] and `vegan` [39]. Since HACSim can be considered a population-based metaheuristic, the state space size explored would be

[28]

$$|S| = (H^*)^N. \quad (4.3)$$

Equation 3 above denotes the number of ways of assigning H^* haplotypes to N individuals *with* replacement (*i.e.*, repetition is permitted), and where the order in which haplotypes are allocated to specimens is important. Thus, the probability of reaching the global optimum once across the entire fitness landscape under random search (that is, selecting a candidate solution uniformly at random) is approximately given by

$$P(G) = \frac{1}{(H^*)^N} \quad (4.4)$$

where G is defined as the event “reaching the global optimum”. Even for a “reasonable” number of specimens and observed species’ haplotypes typical of many taxon-focused DNA barcoding studies, the search space can become prohibitively large due to fundamental biological processes and mechanisms underpinning the evolution of species (*e.g.*, mutation). Therefore, in the case of the GSSSP, the fitness landscape is not guaranteed to be defined by a strictly unimodal hill/mountain. Typically, in most optimization problems, several different potential solutions are tried in a systematic way, making a given future observation more likely to be the global optimum compared to earlier ones. For instance, via Equation 3 and Equation 4, the search space characterizing a species represented by $N = 100$ individuals and $H^* = 10$ unique haplotypes would contain $|S| = 10^{100}$ potential solutions where the probability of finding the globally optimal

solution is only $P(G) = 10^{-100}$. Moreover, as with many other stochastic optimization algorithms, the size of the search space actually explored in a given run of HACSim is exceedingly small.

It is important to realize that sample size estimates provided by HACSim are strongly affected by parameters specific to algorithm tuning, particularly `perms`. That is, it should be stressed that while HACSim does indeed provide a convergence guarantee, it provides no guarantee of global optimality; the tool merely computes a “good enough” (*i.e.*, locally optimal) solution in a finite amount of computation time. Thus, solution quality is entirely dependent on the number of permutations a user deems appropriate for their species of interest and is willing to employ given computational power constraints, as well as tests of researchers’ patience and sanity. Within HACSim, `perms` must be at least two to allow calculation of confidence interval (CI) estimates for generated curves; however, such a permutation size is not sufficient. In general, it is advised that `perms` be set to a “large” value to minimize the effects of Monte Carlo sampling error through reducing the variance in resulting haplotype accumulation curves and their associated “measures of sampling closeness”, as well as ensuring the search does not become trapped in local optima. When too few permutations are employed, HACSim will tend to return estimates (N^*) equal to, or too close to, the initial guess (N) for sampling sufficiency. To avoid such behaviour, typically `perms` is set to 10000 or higher, but this strongly affects algorithm runtime since more candidate solutions in the search space need to be enumerated [117].

While there are $|S| = (H^*)^N$ possible orderings (or resamples) of all observed species' haplotypes to each collected specimen, a number of such orderings are equivalent, and thus redundant, under the exchangeability property of random variables [26]. That is, given two sequences of random variables having the exact same elements in common, their joint probability distribution is unchanged whenever elements in either sequence are reordered. Hence, here, ordering of haplotypes to individual specimens is irrelevant, and, without proof (though easily proved with either a combinatorial proof or mathematical induction), the search space is considerably reduced to a size of

$$|S| = \binom{N + H^* - 1}{N} = \binom{N + H^* - 1}{H^* - 1} = \frac{(N + H^* - 1)!}{N!(H^* - 1)!} \quad (4.5)$$

where $n! = \prod_{i=1}^n i$ ($n!$ read as “ n factorial”) expresses the number of permutations of n distinct objects, and $\binom{n}{k} = \frac{n!}{k!(n-k)!}$ is the binomial coefficient, denoting the number of ways to select k unique objects from a total of n *without* replacement, neglecting the order in which objects are sampled. Equation 5 above expresses the total number of ways to assign N indistinguishable specimens to H^* distinguishable haplotypes *with* replacement when the order in which haplotypes are drawn is unimportant. Such a scheme closely mirrors a classic urn sampling process seen in population genetics (specifically, Coalescent theory [80]) whereby distinctly-coloured marbles (or another similar entity such as balls) representing individual alleles are picked at random one at a time from one or several identical urns. The probability of attaining the global optimum within the reduced space is

now

$$P(G) = \frac{1}{\binom{N+H^*-1}{N}} = \frac{1}{\binom{N+H^*-1}{H^*-1}} = \frac{N!(H^*-1)!}{(N+H^*-1)!} \quad (4.6)$$

Here, employing the same example discussed previously, the search space now comprises only $|S| = \binom{100+10-1}{100} = \binom{100+10-1}{10-1} = 4.26 \times 10^{12}$ possible solutions, and thus the probability of locating the global optimum is significantly higher at $P(G) = 2.35 \times 10^{-13}$. Yet, for most real species, the reduced search space is still far too large to blindly explore; that is, random specimen sampling is no longer a feasible option.

4.1.4 Outline of the Current Study

Here, we develop and present details of an extensive statistical simulation study of the overall computational performance of HACSim from the perspective of key stochastic optimization algorithm properties such as unbiasedness and robustness of suggested sampling sufficiency estimates. To do this, focus is placed specifically on the simulation of various haplotype composition scenarios in hypothetical species. In addition, we test HACSim's ability to capture haplotype variation in real species of traditional, regulatory, forensic and human health importance.

The brief explanation outlined here on the sheer size of HACSim's search space strongly motivates the remainder of the present study. In particular, the need to repeat simulations a large number of times to properly assess both algorithm variability, as well as the need to

examine the plausibility of various local optima for specimen sampling sufficiency found by HACSim given current sampling intensities, is stressed throughout.

4.2 Methods

To better understand HACSim's overall suitability as a general tool for assessing specimen sampling completeness on the basis of standing levels of intraspecific haplotype variation, a small statistical simulation study was conducted examining both equal and unequal haplotype frequency distributions. Hypothetical and real species scenarios were each run 100 times with the default number of permutations (`perms = 10000`) at three different levels of haplotype recovery: $p = 0.80$, $p = 0.90$ and $p = 0.95$. A total of 100 runs was chosen due to the computational expense of HACSim. All simulations (HACSim plus the simulation study) were carried out on a standard laptop running Ubuntu 20.04 64 bit, along with a 8 GB RAM Intel Core i5-7200U CPU @ 2.50GHz 4 256GB SSD processor. Statistical analysis was performed in R version 3.6.3 via RStudio on a MacBook Pro running macOS High Sierra with a 2.7 GHz Intel Core i5 processor with 8 GB 1867 MHz DDR3 of RAM.

4.2.1 Hypothetical Species

Four different scenarios were tested on hypothetical species through running HACSim. In all cases, an initial sample size of $N = 100$ individuals was assumed where $H^* = 10$ COI haplotypes were observed. One hundred specimens and ten haplotypes were selected here

since these order of magnitudes is common within many sampled species found in BOLD.

Scenarios altered observed haplotype distributions as follows:

- Scenario I (all species' haplotypes equally frequent according to a uniform distribution): Haplotypes 1-10 each have a frequency of 10%
- Scenario II (1 dominant haplotype): Haplotype 1 occurs at a frequency of 90%; haplotypes 2-10 each occur with 1.111% frequency
- Scenario III (2 dominant haplotypes): Haplotypes 1 and 2 each occur at 45% frequency; haplotypes 3-10 with a frequency of 1.250%
- Scenario IV (3 dominant haplotypes): Haplotypes 1-3 each occur with 30% frequency; haplotypes 4-10 at a frequency of 1.429%.

The above scenarios are in no way meant to exactly mimic haplotype frequencies present in real species populations; rather, Scenarios I-IV reflect a tradeoff between “interestingness” and algorithm runtime. Further, while there are numerous parameters that can be tweaked within `HACSim` itself, a careful parameter sensitivity analysis is not the goal of the present study. This is not to say that altering either the number of permutations or the proportion of observed haplotype diversity to recover will produce unpredictable results. Clearly, increasing (decreasing) `perms` results in increased (decreased) numerical accuracy/precision of model estimates and smoother (noisier) haplotype accumulation curves, while leading to slow (fast) computation. Similarly, increasing (decreasing) `p`

leads to higher (lower) estimates of sampling sufficiency (N^*), since more (fewer) species' haplotypes (*i.e.*, higher (lower) H_i) need to be captured. Additionally, since specimen sample sizes are presumed to be strongly taxon-specific, due to differences in evolutionary origins and life history traits among species, and because HACSim is meant to be a general modelling framework, it is highly unlikely that a single combination of `perms` and `p` can be found that works for the majority of taxa.

4.2.2 Real Species

To better place HACSim on more solid biological ground, the algorithm was tested on a variety of real species of socioeconomic, medical/veterinary and agricultural importance mined from BOLD. In addition to the three species analyzed by [117] (Lake whitefish (*Coregonus clupeaformis*) ($N = 235$, $H^* = 15$), Deer tick (*Ixodes scapularis*) ($N = 349$, $H^* = 83$) and Scalloped hammerhead shark (*Sphyrna lewini*) ($N = 171$, $H^* = 12$)), barcode data from Pea aphid (*Acyrtosiphon pisum*), Common mosquito (*Culex pipiens*) and Gypsy moth (*Lymantria dispar*) were also assessed. The reasoning for selecting these three additional species in particular is due to their negative anthropogenic impacts, in addition to both their taxonomic diversity (occurring across three separate genera) and having wide representativeness in BOLD. Despite this, much existing haplotype variation remains to be fully characterized. Deeper sampling coverage of these and other species will enable accurate identifications through contributing to the construction of barcode reference libraries found in publicly-available genomic sequence databases. Geographic variation of

collected samples is necessary for the rapid development of robust primer and probe sets for use in quantitative Polymerase Chain Reaction (qPCR) assays to aid species diagnosis, as well as gaining a better understanding of the phylogeography of relevant species. Brief aspects of the biology concerning the three additional abovementioned species is given in the below subsections. Information on species examined by Phillips *et al.* [117] can be found in that publication.

DNA barcode sequences for these three species were downloaded from BOLD's Public Data Portal on January 24, 2021. Sequence preprocessing in MEGA7 [81] was identical to that outlined in [117]. In particular, records originating from GenBank, as well as sequences comprising missing data (external gaps), IUPAC ambiguity codes, or insertions/deletions (indels) were excluded due to quality concerns [58] and likely overestimation of standing intraspecific haplotype variation [118, 116, 117]. All species' multiple sequence alignments new to this study were trimmed to a final length of 658 bp.

Pea aphid (*Acyrtosiphon pisum*)

In addition to being highly detrimental to the agriculture sector, aphids (Hemiptera: Aphidoidea) present an interesting focal case study for DNA barcoding due to their complex life cycles across diverse morphological forms, coupled with their unique modes of reproduction [49].

As one of the most recognizable plant pest species, the pea aphid (*Acyrtosiphon pisum*)

exhibits remarkable levels of phenotypic plasticity, often switching between winged and non-winged forms, as well as adopting both sexual and asexual (*i.e.*, parthenogenetic) mating strategies in response to changing environmental conditions and seasonality.

A total of 653 public sequence records for *A. pisum* were mined from BOLD. Of these, $N = 356$ meet stringent criteria outlined above and by [117]. The obtained DNA alignment revealed a total of $H^* = 12$ unique haplotypes, with Haplotype 1 occurring at a frequency of 96.6% (**Figure 1**).

Common mosquito (*Culex pipiens*)

Mosquitoes (Diptera: Culicidae) are noted as both nuisance pests and vectors of zoonotic pathogens such as West Nile virus, Dengue virus, malaria-causing *Plasmodium* virus and Zika virus, which together cause millions of deaths worldwide annually. Further, the small size of most species often precludes successful identification on the basis of morphology by even expert taxonomists. Thus, the importance of rapid identification of potentially infected specimens through genomic solutions like DNA barcoding can greatly propel the development of effective control measures imperative in avoiding further illness and deaths [11].

The common mosquito (*Culex pipiens*) is a geographically-widespread species of great interest to practitioners within parasitology and medical entomology fields across the globe. In addition to their complex ecology and their ability to adapt to a wide range of

environments, *C. pipiens* also forms a species complex with other closely-related species due to shared biological characteristics; hence, instances of potential cryptic diversity have been well documented.

A total of 1280 DNA sequences from *C. pipiens* were retrieved from BOLD. After processing, the number of useable 5'-COI sequences dropped to only $N = 217$. The final sequence alignment consisted of $H^* = 25$ species' haplotypes, with a single dominant haplotype (Haplotype 1) at 84.3% (**Figure 2**).

Gypsy Moth (*Lymantria dispar*)

As a group, Lepidoptera (comprising butterflies and moths) has long been a prime target to assess the efficacy of DNA barcoding due to the geographically-widespread distribution and the morphological diversity of its member species, so much so that they presently make up more than 1.2 million specimen records found on BOLD.

In what can only be perceived a “genetic paradox of invasion” [40], invasive alien species (IAS) have both fascinated and frustrated biologists for decades due to their highly successful colonization potential in spite of multiple introductions originating from small founder populations and experiencing genetic bottlenecks that act to promote inbreeding. Notwithstanding, invasive insects introduced to North America from elsewhere (*e.g.*, Europe) have caused over 30 billion dollars in damage to forest ecosystems [158].

Taxa of the Tussock moth group (Lymantriinae) are well-known as notorious plant

pests. The gypsy moth (*Lymantria dispar*) is a highly-invasive lepidopteran responsible for mass destruction of, and billions of dollars in damage to, forests worldwide, especially in North America. Within Canada, this species is highly regulated by the Canadian Food Inspection Agency (CFIA). To facilitate timely eradication of this and other unwanted pest species, recent research efforts have focused on developing molecular methods to better track their introduction, establishment and subsequent spread (*e.g.*, salt traps; [93, 157]). DNA barcoding in particular has been shown to be a highly valuable tool in rapidly identifying *Lymantria* specimens of biosecurity concern [35].

Due to the great interest in *L. dispar*, a number of specimen records have been deposited on BOLD over the years. As of this writing, over 3300 specimens have been submitted, albeit the majority coming from GenBank. For the present study, 3362 sequence records were obtained. However, only $N = 365$ were of high quality. The resulting alignment comprised $H^* = 58$ haplotypes. Several dominant haplotypes were found for this species. Haplotypes 1-5 ranged from 3.56%-23.3% in frequency (**Figure 3**).

4.2.3 Simulation Study

A custom R script (**Supplemental Information**) was developed to carry out the simulation study through testing whether values of N^* reported by HACS_{im} actually correspond to capturing at least p% of observed haplotype diversity for each examined species scenario through random sampling alone. To accomplish this, three different artificial populations of sizes 1000, 10000 and 100000 were initially explored for both

hypothetical and real species scenarios. Population sizes for most real species are difficult to ascertain with certainty. Thus, selected population sizes are not meant to reflect ground truth; rather, said values were chosen merely to test the limits of HACSim. Since it can be argued that the abovestated population sizes are not likely reflective of biological reality, particularly for invertebrate taxa, a fourth, much larger population size of 10000000 was also tested to introduce more biological realism into the simulations. For each population, subsets of N^* individuals corresponding to those found from running HACSim were randomly sampled without replacement and the proportion of observed haplotypes recovered was calculated according to the underlying haplotype frequency distribution for all hypothetical and real species scenarios. This scheme was repeated 50 times for each unique value of N^* , after which an average was taken. Averages were displayed along with 95% CIs computed using the Central Limit Theorem (CLT) with the R package `ggplot2` [147].

Local optima were characterized for all hypothetical and real species through enumerating the total number of solutions found, reporting the range of said solutions, locating the highest mode(s) in the fitness landscape, computing the standard deviation of all plausible optima, and indicating the number of times the highest mode(s) occurred.

For each value of N^* found by the simulation study, coverage probabilities of constructed large-sample confidence intervals (based on the CLT) for the fraction of observed haplotypes recovered were compared with the nominal interval coverage of 95%

(along with 80% and 90%) to assess whether or not said confidence intervals actually capture at least 95% (similarly, 80% and 90%) of observed species' haplotype variation. In practice, coverage probabilities rarely match nominal values, unless observations are normally distributed or sample sizes are sufficiently large. Given that coverages were computed on the basis of detected local optima, exact 95% binomial (Clopper-Pearson) confidence intervals were also calculated (via `binom.test()` in R) to better assess estimate uncertainty. Observed coverage probabilities were deemed as conservative if they were found to be greater than the stated nominal coverage of 95% (in addition to 80% and 90%), permissive if they were less than the prespecified coverage, or exact if both estimated and true coverages were equal to these values.

4.2.4 Statistical Analysis

The Kruskal Wallis (KW) test was employed to assess whether or not simulation results differed significantly across population sizes. The KW test is the nonparametric equivalent of a one-way analysis of variance (ANOVA) for independent samples and is appropriate whenever observations are suspected to deviate from those coming from normally-distributed populations. All tests were carried out using the base R `kruskal.test()` function at the 5% level of significance with a two-sided alternative hypothesis.

The KW test extends the Mann-Whitney U test (also known as the Wilcoxon Rank Sum test) to more than two groups. The U test is the nonparametric version of the

two-independent-samples t test. Performing successive pairwise t -tests on three or more groups is problematic. See the following paragraphs for more information.

Regarding hypothetical taxa, p -values could only be calculated for Scenarios II-IV given that Scenario I (equal haplotype frequencies) resulted in only a single mode (*i.e.*, the same value of N^* was found across all 100 repetitions of HACSim). In cases where the KW test could be conducted for both hypothetical and real species, a total of six different combinations of population size were assessed. Haplotype frequency distributions were compared for each the following population size pairings: (1) 1000 *vs.* 10000, (2) 1000 *vs.* 100000, (3) 1000 *vs.* 10000000, (4) 10000 *vs.* 100000, (5) 10000 *vs.* 10000000 and (6) 1000000 *vs.* 10000000.

A brief discussion here of the problem of testing multiple statistical inferences simultaneously is necessary. The issue at hand is that such a procedure will tend to inflate the Family-wise Error Rate (FWER). The FWER corresponds the Type I error rate, that is, the probability of rejecting the null hypothesis of no significant difference between groups when one in fact exists, given the null hypothesis is true, can be quite high. Because one of the present goals of this study is to assess significance at the 5% level ($\alpha = 0.05$, 95% confidence) for $n = 6$ distinct pairwise comparisons, the probability of committing a Type I error is $\text{FWER} = 1 - (1 - \alpha)^n = 1 - (1 - 0.05)^6 \approx 0.265$. The FWER increases with larger values of α (smaller confidence levels). Fortunately, various methods have been proposed for controlling the FWER.

Herein, the Bonferroni correction is employed to minimize the risk of falsely rejecting a true null hypothesis. While conservative, Bonferroni's procedure is still quite popular due to its inherent simplicity when addressing the multiple comparisons problem. The procedure works by rejecting all hypotheses with p -values less than or equal to $\frac{\alpha}{n}$. Thus, for $\alpha = 0.05$ with six comparisons, the null would be rejected whenever $p \leq \frac{0.05}{6} \approx 0.0083$. Employing a p -value cutoff of 0.83% leads to a reduction in the Type I error rate of approximately 4.9%.

Following the KW test, Dunn's post-hoc test with the Bonferroni correction was implemented using the function `dunn.test()` [37] from the R package `dunn.test` to assess which population sizes differed significantly from each another.

4.3 Results and Discussion

Results presented herein pertain primarily to $p = 0.95$ at a population size of 10000. Specific findings for $p = 0.80$, $p = 0.90$ and remaining population sizes for $p = 0.95$ can be found within **Supplemental Information**.

4.3.1 Effect of Population Size

Several plausible local optima for specimen sampling sufficiency were found by HACSim in all hypothetical species (**Figures 4-6** and **Table 5**) and real species scenarios (**Figures 7-12** and **Table 6**) except Scenario I (results not shown), where only a single

optimum was obtained. Many of the detected optima across all hypothetical and real species scenarios were tied in frequency of occurrence, suggesting that the fitness landscape is not unimodal. The fact that the solution landscape comprises many small peaks, plateaus and deep valleys suggests that it is quite rugose in shape. Both Scenario IV (**Figure 6**) and *L. dispar* (**Figure 11**) showed multiple separate highest mode optima: two and three respectively. Two real species, *A. pisum* (**Figure 7**) and *L. dispar* displayed two overlapping sets of local optima for differing population sizes: one for a population size of 1000 and another for population sizes of 10000, 100000 and 1000000 (**Table 6**). Local optima located for a population size of 1000 comprised a subset of those optima found with population sizes of 10000, 100000 and 1000000. HACSim was successful in avoiding getting trapped in local basins of attraction too near to the initial estimates set for sampling sufficiency (*i.e.*, the initial number of observed specimens, N) owing to a large number of permutations being employed within simulation runs. Several of these optima were found multiple times across the 100 runs of HACSim: between 1-100 times for hypothetical species scenarios (**Figures 4-6**) and 1-6 times in the case of real species (**Figures 7-12**). A general trend seen for hypothetical species, but not real taxa, was the reduction in both number of local optima and the spread (range and standard deviation) of said optima as the number of dominant haplotypes increased (equivalently, as the number of rare haplotypes decreased) with the exception of Scenario I (**Table 5**). The tandem reduction in the standard deviation of feasible solutions and the number of observed local optima for hypothetical species seems to indicate that high permutation sizes promotes efficient exploitation of the

problem search space; however, such a pattern likely cannot be said of real species in light of the scope of current experiments performed herein. Rather, results for real taxa appear to suggest that optimal specimen sampling is easier for some species but not others. It is expected that the diversity of various modes within the fitness landscape found using the current algorithm is likely to decrease as more permutations are employed when initializing HACS_{im}; conversely, increasing the number of independent runs of HACS_{im} will result in local optima being found with greater frequency. Yet, many located optima should be shared among differing combinations of permutations and simulation runs.

On average, HACS_{im} was found to recover desired level of standing haplotype diversity for both hypothetical and real species at all assessed population sizes in most cases (**Figures 16-21, Tables 1 and 2, Supplemental Information**). Further, the variability of the observed proportion of species' haplotypes captured was found to decrease with increasing values of N^* , indicating that, on average, larger specimen sample sizes are better able to retrieve desired levels of haplotype diversity compared to smaller ones. Interestingly, for Scenario III (population size 1000), Deer tick (population size 1000), Gypsy moth (population size 1000) and Scalloped hammerhead shark (population sizes 100000 and 10000000), the mean fraction of recovered observed haplotypes fell below the desired 95% haplotype recovery cutoff (**Figure 21, Supplemental Information**). Given that proportions were often less than 95% at a population size of 1000 for real species, it remains unclear whether such a trend is due to employing a small number of replications (here, 50), too few runs or is the result of evolutionary processes governing intraspecific genetic

variation. The latter could be easily tested through examining more closely-related taxa (*e.g.*, those within the same genus) or perhaps species occupying the same geographic region or ecological niche. Low values observed at population sizes of 100000 and 10000000 are likely due to chance alone. In any case, whenever feasible, researchers should aim to use as many replications and HACSim runs as possible, particularly when the desired level of haplotype recovery is high.

In general, based on results obtained from simulation study output, population size was found to have little effect on the ability of HACSim to successfully capture sufficient levels of observed species' haplotype diversity, for both hypothetical and real species, despite having only utilized 50 replications and 100 independent runs of HACSim (**Tables 3 and 4, Supplemental Information**). The estimated proportion of haplotype diversity found across all hypothetical and real species examples did not fall below 90%; in fact, many estimates were consistently above the desired 95% threshold. This result is not all that surprising since the default number of permutations (`perms` = 10000) was employed within HACSim. Thus, increasing the number of replications employed in the simulation study is unlikely to be of any real benefit, as it will only act to increase runtime substantially.

Assessment of confidence interval coverage for both hypothetical and real species was revealing. Most computed probabilities were quite conservative (**Tables 7 and 8, Supplemental Information**). The Clopper-Pearson binomial confidence interval is asymmetric and is often found to be very conservative in practice. As a result, estimated

CI coverages across all scenarios explored herein were found to be well above the required 95% level, with few exceptions. In the latter case, such a finding is likely due to the fact that only 100 repetitions of HACSim were employed in the simulation study due to computation time constraints (see next section below for further discussion). Among problematic scenarios, coverage probabilities were lowest for a population size of 1000. Only in one instance, *L. dispar*, was coverage found to be zero. In this case, CI endpoints lied slightly to the left of the desired nominal coverage. Better (higher) interval coverage probabilities should be observed with an increasing number of algorithm runs.

For both hypothetical and real species scenarios examined within the present study, differences in proportions of observed unique haplotypes captured were found to be statistically significant at the 5% level based on the KW test (results not shown). Post-hoc analysis via Dunn's test seems to point to statistical differences only when comparing small vs. large population sizes (e.g., 1000 vs. 10000000). Any deviation from this trend is likely attributed to random chance alone (given that HACSim is stochastic in nature and that only 50 replications were employed within the simulation study) rather than being due to any true effect. This suggests that population size plays little to no role in affecting the overall performance of HACSim. This assertion appears to be supported by results found in

Tables 1 and 2, as well as **Supplemental Information**.

4.3.2 Algorithm Runtimes

Completion time for Scenario I was around the five minute mark, whereas simulation of Scenarios II-IV took around one hour each. Runtimes for real species were considerably longer, ranging from approximately 4 hours in the case of the scalloped hammerhead shark ($N = 171$, $H^* = 12$) to 30 hours for deer tick ($N = 349$, $H^* = 83$). Interestingly, the most data-heavy species in terms of number of DNA sequences (Gypsy moth: $N = 365$, $H = 58$) took only *c.* 28 hours to finish. Such an observation might be explained by differences among operating systems and underlying compilers used in running `HACSim`, as well as overall cleanliness of the underlying algorithm R and C++ code. While for the most part algorithm runtimes appear to scale proportionally with the size and characteristics of the generated population array (*i.e.*, depending on N , H^* and `perms`) for a given value of p , due to the variation in species' haplotype frequency distributions (`probs`) and the stochastic nature of `HACSim`, obtaining exact algebraic expressions for average- and worst-case algorithm time complexities is not straightforward. However, generally speaking, algorithm runtimes were shortest for a haplotype recovery of $p = 0.80$ and longest for $p = 0.95$. Computation times for $p = 0.80$ spanned about five minutes (Scenarios I and III) to *c.* six hours (Deer tick), while those for $p = 0.90$ ranged from *c.* five minutes (Scenario I) to *c.* 10.5 hours (Gypsy moth).

4.4 Conclusion

In the present work, a detailed simulation study was carried out to test the performance of HACSim, a local optimization algorithm developed in R to assess specimen sampling completeness for DNA barcoding on the basis of saturation levels observed in plotted species' haplotype accumulation curves. The goal was to explore the potential use of HACSim in proposing adequate sample sizes in the context of the Genetic Specimen Sample Size Problem (GSSSP). Haplotype sampling carried out within HACSim is meant to closely approximate real sampling of species' genetic variation in the field, albeit in a much more systematic and monetarily-cheap fashion. Analysis was conducted on a wide variety of hypothetical and real species scenarios across various levels of haplotype recovery. Selection of hypothetical species scenarios reflected a tradeoff between "interestingness" and algorithm runtime. Real species scenarios largely comprised taxa of socioeconomic and regulatory/forensic importance, in particular invasive species and those of cultural and medical significance.

Herein, HACSim identified many local optima that could conceivably capture differing levels of standing haplotype variation for both hypothetical and real species. While the highest modal value of N^* was employed as an estimate of the "true" sampling sufficiency for a species (θ), the mode may not tell the whole story. Unlike in the context of other population-based metaheuristics like genetic algorithms, where the notion of a "best" solution is often readily evident from a given evalution of the objective function, such is

not the case with HACSim. In actuality, realizations of N^* form a *distribution*. Given that specimen sampling is dictated strongly by availability of time and resources, reporting other summary statistics, particularly the minimum and maximum alongside the mode will allow researchers to better weigh benefits and costs of collection in the field and therefore make an informed decision on how “best” ought to be defined for taxa under study. This is especially important when it comes to assessing genetic diversity for species at risk for example.

A central theme stressed throughout this work is the importance of algorithm replication due to the stochastic nature of HACSim. Simulation study results obtained herein seem to point to the overall utility of HACSim as a general and flexible tool to estimate likely required specimen sample sizes for DNA barcoding. Despite this, for HACSim to be made a routine part of the DNA barcoder’s toolkit, much work still remains to be accomplished.

Because researchers will most likely be more interested in simulating haplotype accumulation curves for real species based on existing barcode data retrieved from databases like BOLD, as opposed to hypothetical species, it becomes essential to further automate HACSim for this task. Due to its iterative nature, parallelization *within* a given run of HACSim is likely to be challenging without switching entirely to a more powerful or efficient programming language like C++ or Julia; however, speeding up computations *among* runs is a trivial fix. This becomes especially critical if and when sample size estimation is needed for species with very large numbers of representatives. For instance,

within BOLD, humans (*Homo sapiens*) comprise over 48000 barcode sequence records as of March 24, 2021, despite the majority originating from GenBank.

A key assumption of HACSim is that it requires a good representation of within-species haplotype variation. As a result, HACSim works best for already well-sampled species lineages. Any attempt to employ HACSim on species with small numbers of specimens would likely lead to biases in outputted estimates of sample size and the proportion of recovered standing haplotype diversity. It remains to be seen how the present algorithm performs for taxa with only tens, say, of collected individuals. This is clearly a necessary step since most DNA sequence data within BOLD originate from only a handful of specimens.

One element not explored in detail here is the potential effect of `perms` on outputted results of HACSim. Since computation time grows directly with permutation size, for large taxon datasets, that would otherwise take several hours to run, users can simply reduce `perms` to a lower number, with the added caveat that obtained estimates will be much more variable (and hence, not as trusting) across runs. As a result, noisiness apparent in algorithm estimates and the generated species' haplotype accumulation curves can thus be attributed to ineffective traversal of the solution search space.

Another area worth exploring further is relaxing the assumption of panmixia within species. Most models in population genetics necessarily assume *a priori* that species are panmictic across their entire geologic/ecologic range. This is obviously not an ideal

scenario since in many cases, this assumption will not hold for many taxa. For example, genetic diversity within North American freshwater fishes, in contrast to marine species which tend to exhibit large dispersal abilities, exists in small localized patches consistent with glacial recession during the Pleistocene. As a result, subsequent colonization of refugia ensued, leading to high levels of cryptic speciation. Initially, [116] envisaged a haplotype sampling model that would be able to accomodate elements of population structuring that are more apparent in real species. However, incorporation of such phenomena would be challenging to implement within the current local optimization framework for two reasons. First, accurate estimation of population genetic parameters such as deme number and migration rates that are central to well-known models like Wright's island model [153] and Kimura's stepping stone model [79] would prove difficult for most taxa without reliance on external software outside of R. The authors of HACSim and its associated publication [117] wished to develop a stand-alone R package that would make users' lives as stress-free as possible. This was partially achieved through HACSim's reliance on just one tuning parameter — `perms`, something that is rare in most other stochastic methods like evolutionary algorithms. Given that so much more is still to be investigated regarding HACSim, introducing new functionality is easier said than done. Additionally, such capability would require further code optimization to ensure reasonable runtimes. Many stochastic optimization algorithms applied to large problems are notoriously slow due to the size of the search space that needs to be explored. Due to the nature of the genetic specimen sample size problem, any proposed approach for estimating

sample sizes needs to be fast and reliable. HACSim seems to fit this requirement, at least for reasonably large values of N and H^* .

A noteworthy extension of HACSim involves the simulation of DNA sequences according to various models of nucleotide substitution. Such a function would allow users to provide the number of DNA sequences to simulate, the number of unique species' haplotypes, the basepair alignment length, the haplotype frequency distribution, the nucleotide frequency distribution, the appropriate codon table to utilize, the desired DNA substitution model and the overall mutation rates. Such a capability would add an additional layer of biological realism on top of existing features offered by HACSim.

Despite much more work to be realized, results obtained within the present study suggest that HACSim is a reasonable tool for estimating likely required specimen sample sizes for species of interest based on genetic variation observed within COI barcodes. Next steps should be devoted to employing HACSim on non-barcode genes such those for plants (rbcL/matK) and fungi (ITS), provided existing reference sequence are mature enough.

Supplemental Information

Figures associated with running `HACSim` with $p = 0.80$ and $p = 0.90$ for both hypothetical and real species can be found on the primary author's GitHub repository available at: <https://github.com/jphill01/PhD-Thesis-Appendix>.

Conflict of Interest

None declared.

Acknowledgements

We wish to thank Robert (Rob) Young for helpful discussions throughout this work.

We acknowledge that the University of Guelph resides on the ancestral lands of the Attawandaron people and the treaty lands and territory of the Mississaugas of the Credit. We recognize the significance of the Dish with One Spoon Covenant to this land and offer our respect to our Anishinaabe, Haudenosaunee and Métis neighbours as we strive to strengthen our relationships with them.

Author Contributions

JDP wrote the manuscript, approved all developed code as well as analyzed and interpreted all experimental results. SEB wrote required code and performed all

experiments. DJG acted as an advisor in statistics. RHH acted as an advisor in DNA barcoding. All authors contributed to the revision of this manuscript and approved the final version.

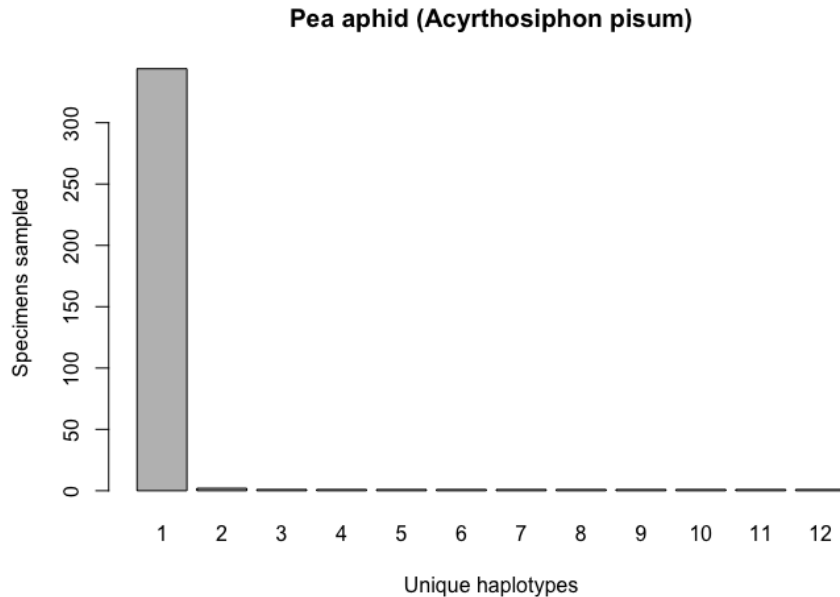


Figure 4.1: Initial haplotype frequency distribution for $N = 356$ high-quality Pea aphid (*Acyrthosiphon pisum*) COI barcode sequences obtained from BOLD. This species displays a highly-skewed pattern of observed haplotype variation, Haplotype 1 accounts for c. 96.6% (344/356) of all sampled records.

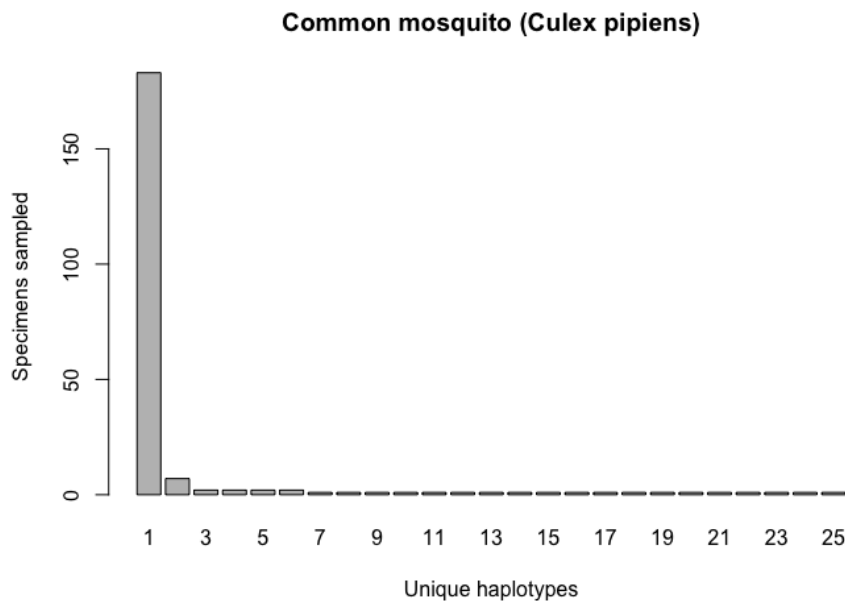


Figure 4.2: Initial haplotype frequency distribution for $N = 217$ high-quality Common mosquito (*Culex pipiens*) COI barcode sequences obtained from BOLD. In this species, Haplotype 1 accounts for c. 84.3% (183/217) of all sampled records.

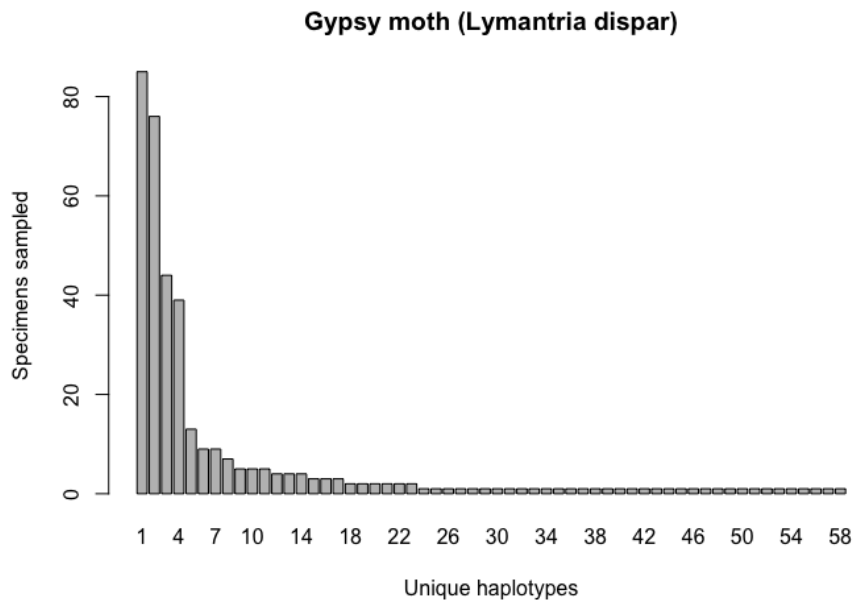


Figure 4.3: Initial haplotype frequency distribution for $N = 365$ high-quality Gypsy moth (*Lymantria dispar*) COI barcode sequences obtained from BOLD. In this species, Haplotypes 1-5 account for c. 70.4% (257/365) of all sampled records.

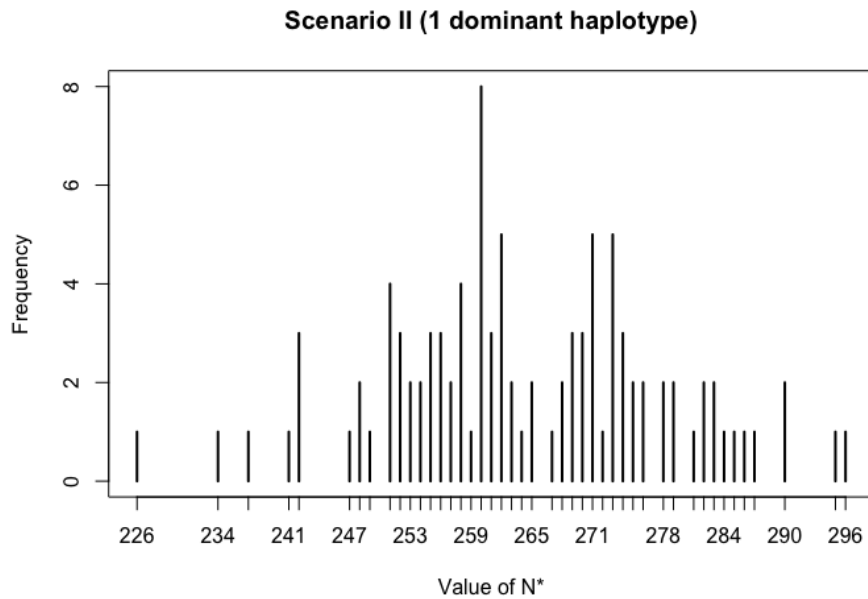


Figure 4.4: Frequency plot showing all located local optima and the number of times each was found by HACSIm for Scenario II (1 dominant haplotype).

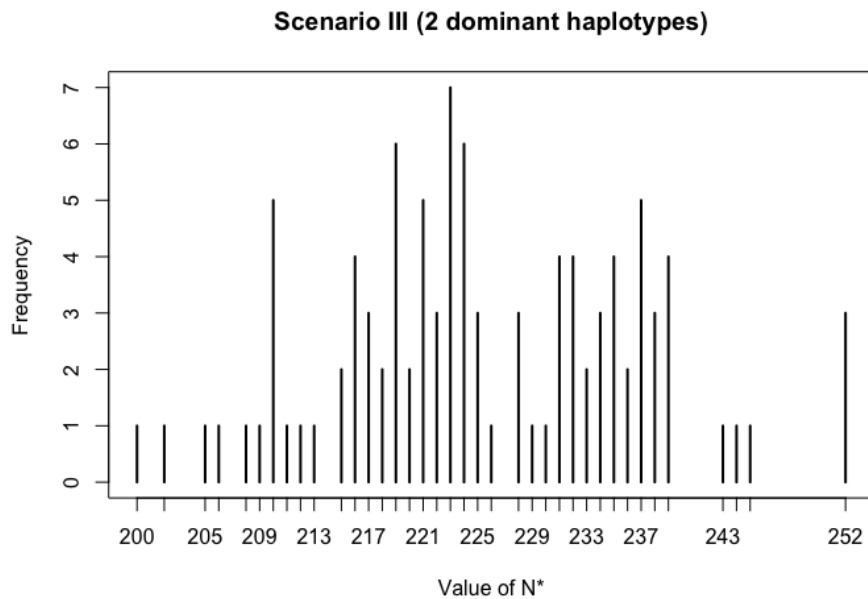


Figure 4.5: Frequency plot showing all located local optima and the number of times each was found by HACSIm for Scenario III (2 dominant haplotypes).

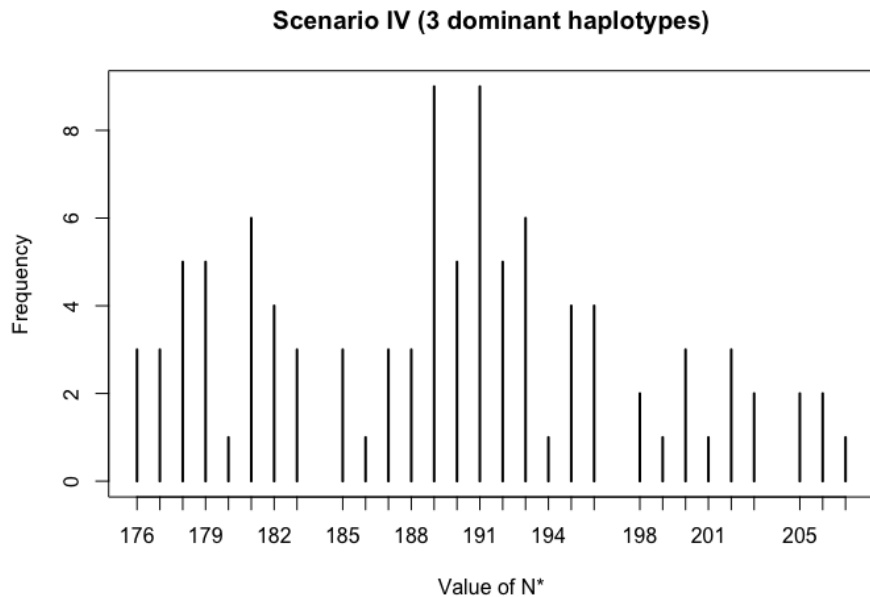


Figure 4.6: Frequency plot showing all located local optima and the number of times each was found by HACSIm for Scenario IV (3 dominant haplotypes).

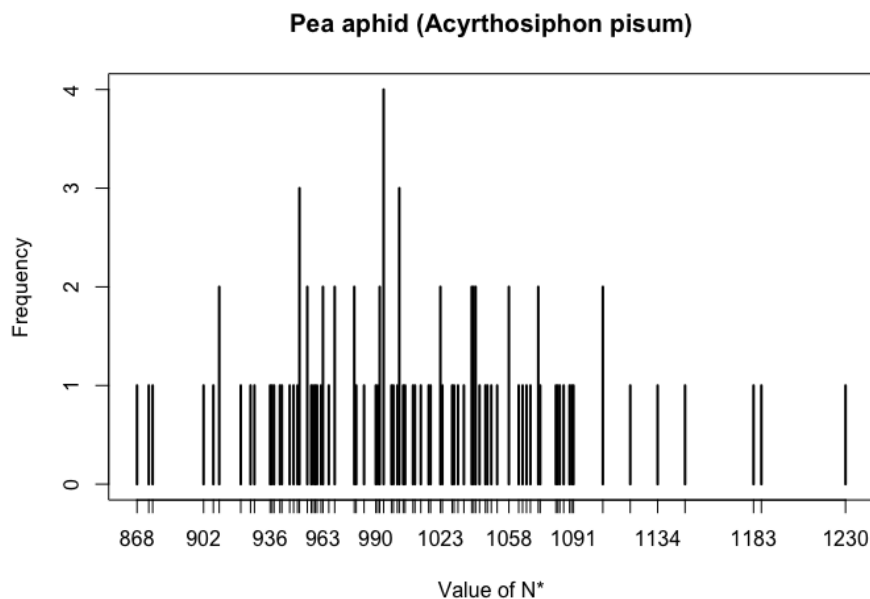


Figure 4.7: Frequency plot showing all located local optima and the number of times each was found by HACSIm for Pea aphid (*Acyrthosiphon pisum*).

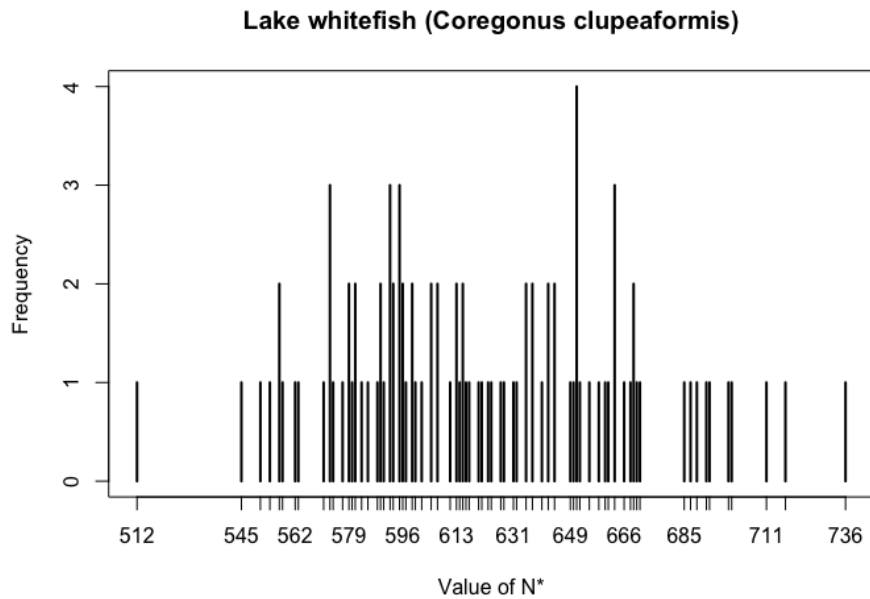


Figure 4.8: Frequency plot showing all located local optima and the number of times each was found by HACSIm for Lake whitefish (*Coregonus clupeaformis*).

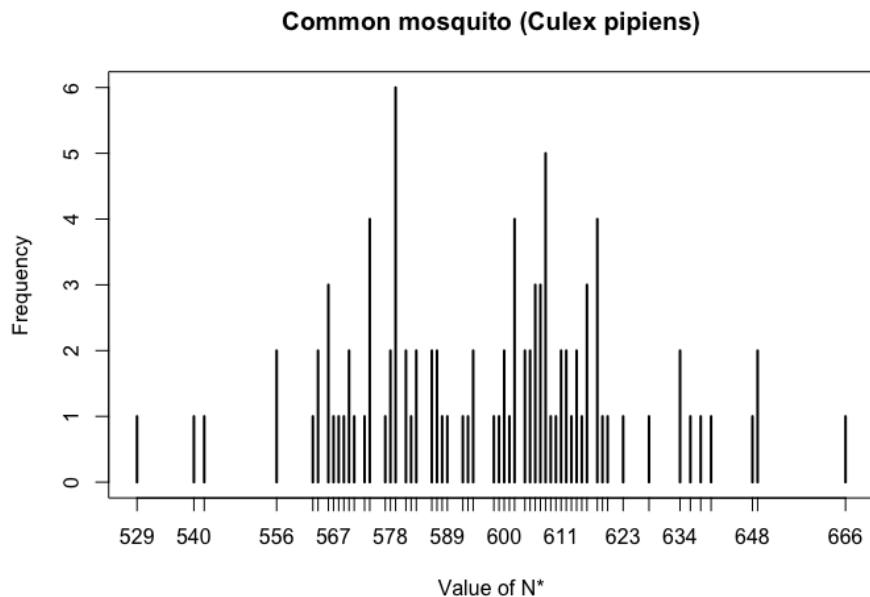


Figure 4.9: Frequency plot showing all located local optima and the number of times each was found by HACSIm for Common mosquito (*Culex pipiens*).

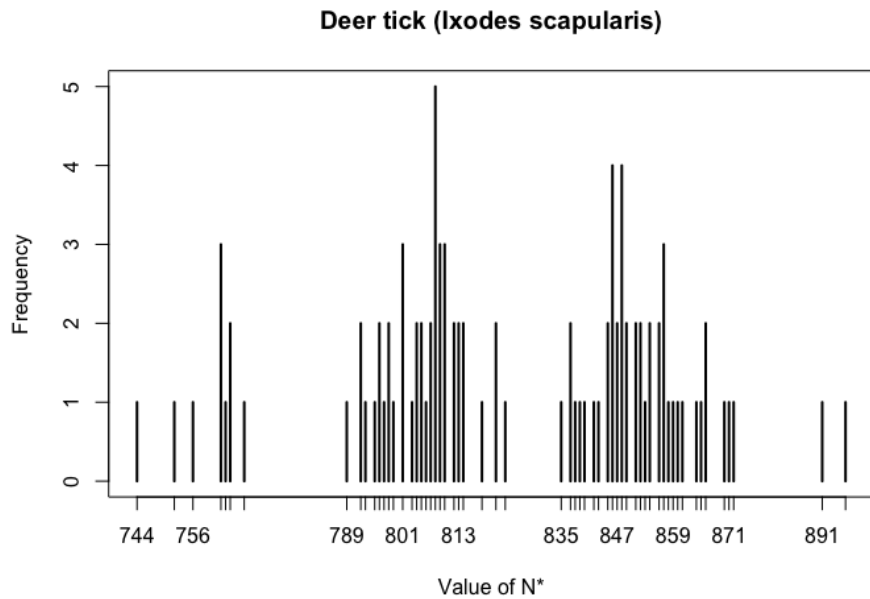


Figure 4.10: Frequency plot showing all located local optima and the number of times each was found by HACSim for Deer tick (*Ixodes scapularis*).

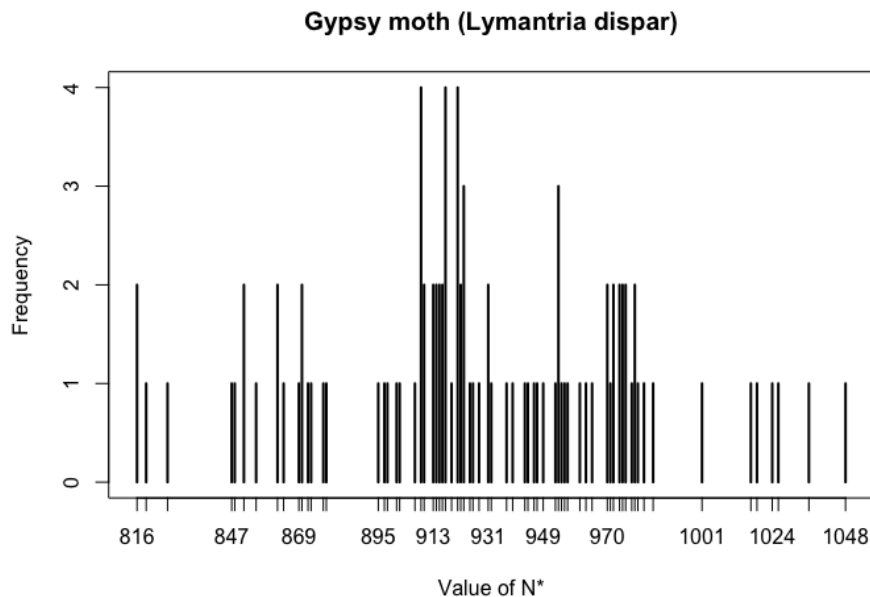


Figure 4.11: Frequency plot showing all located local optima and the number of times each was found by HACSim for Gypsy moth (*Lymantria dispar*).

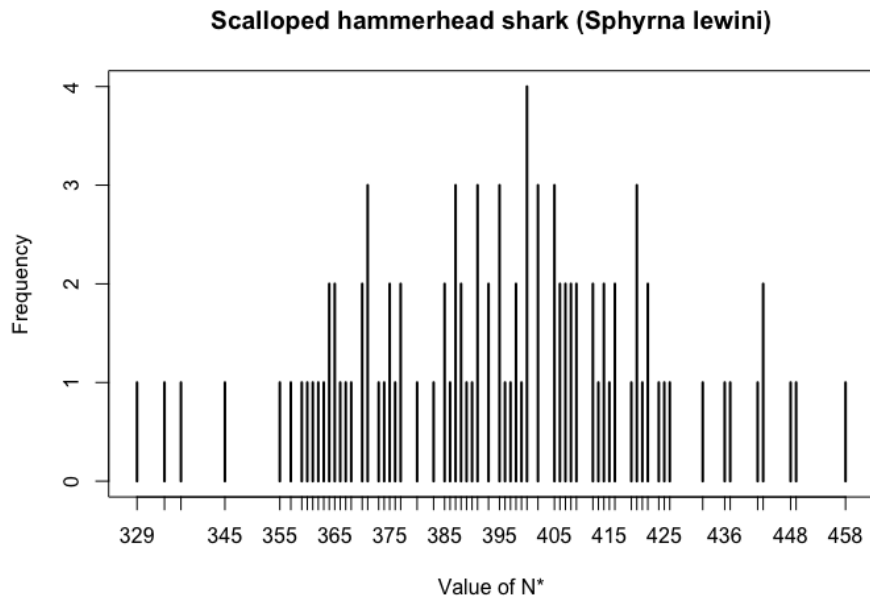


Figure 4.12: Frequency plot showing all located local optima and the number of times each was found by HACSim for Scalloped hammerhead shark (*Sphyrna lewini*).

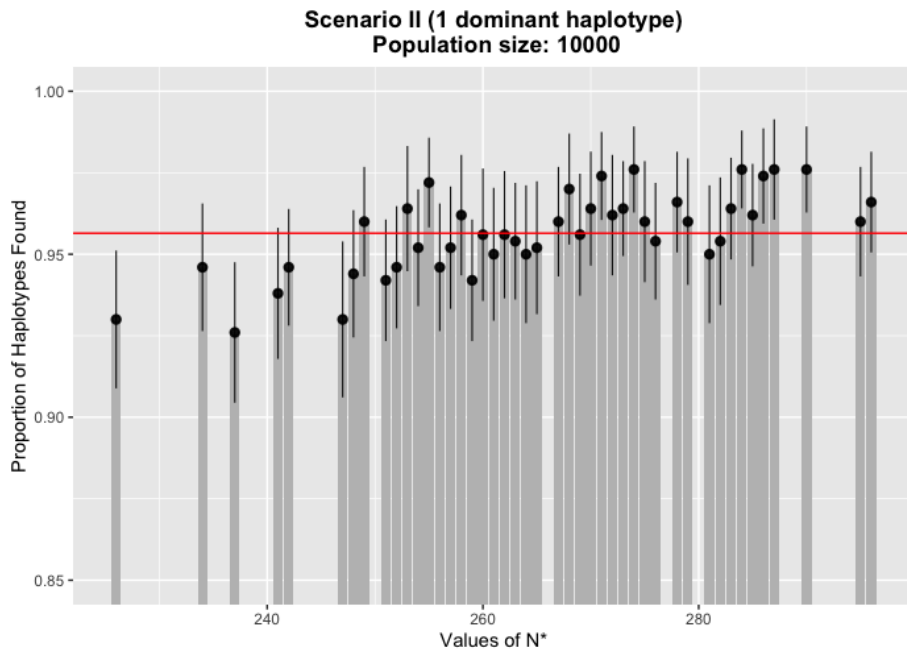


Figure 4.13: Plot showing all located local optima and the proportion of observed haplotypes captured for Scenario II (1 dominant haplotype) with 95% confidence intervals for a population size of 10000. The mean proportion across 50 replications is depicted as a black dot. The mean proportion across all located local optima is displayed as a solid red horizontal line. The thickness of displayed grey error bars is a construct of `ggplot2` based on the number of local optima and holds no additional meaning in the context of this study.

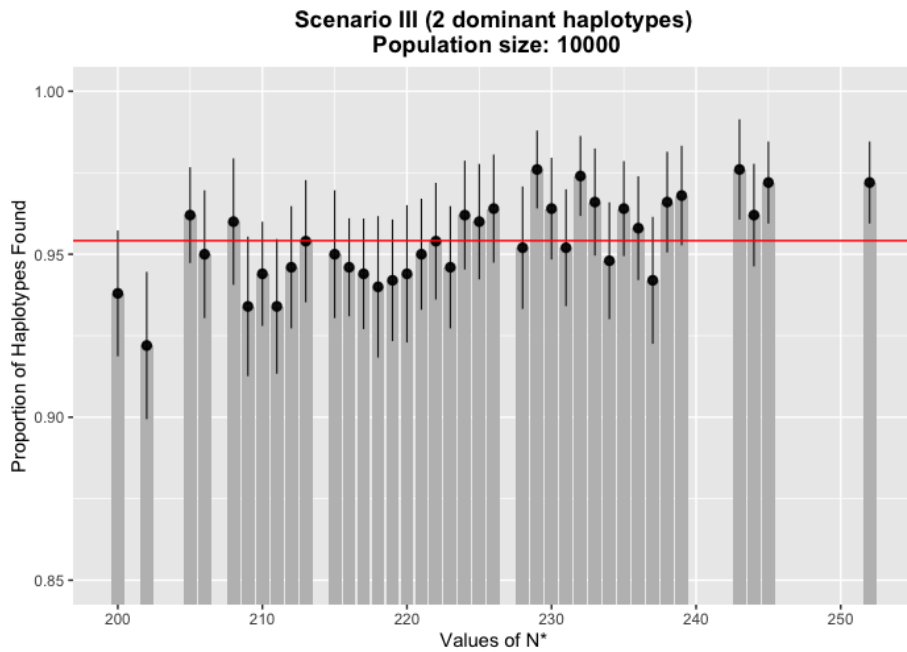


Figure 4.14: Plot showing all located local optima and the proportion of observed haplotypes captured for Scenario III (2 dominant haplotypes) with 95% confidence intervals for a population size of 10000. The mean proportion across 50 replications is depicted as a black dot. The mean proportion across all located local optima is displayed as a solid red horizontal line. The thickness of displayed grey error bars is a construct of `ggplot2` based on the number of local optima and holds no additional meaning in the context of this study.

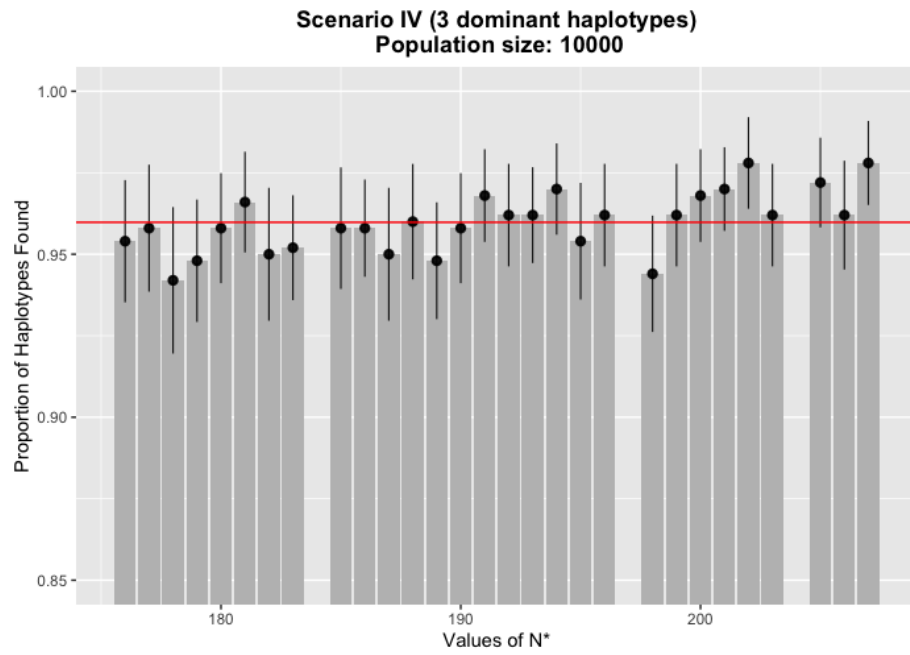


Figure 4.15: Plot showing all located local optima and the proportion of observed haplotypes captured for Scenario IV (3 dominant haplotypes) with 95% confidence intervals for a population size of 10000. The mean proportion across 50 replications is depicted as a black dot. The mean proportion across all located local optima is displayed as a solid red horizontal line. The thickness of displayed grey error bars is a construct of `ggplot2` based on the number of local optima and holds no additional meaning in the context of this study.

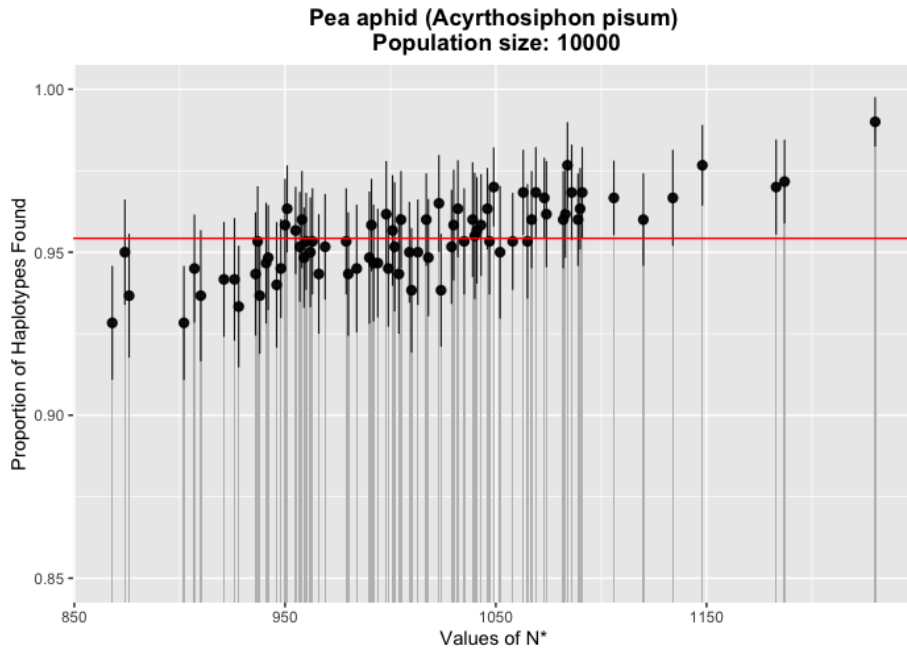


Figure 4.16: Plot showing all located local optima and the proportion of observed haplotypes captured for Pea aphid (*A. pisum*) with 95% confidence intervals for a population size of 10000. The mean proportion across 50 replications is depicted as a black dot. The mean proportion across all located local optima is displayed as a solid red horizontal line. The thickness of displayed grey error bars is a construct of `ggplot2` based on the number of local optima and holds no additional meaning in the context of this study.

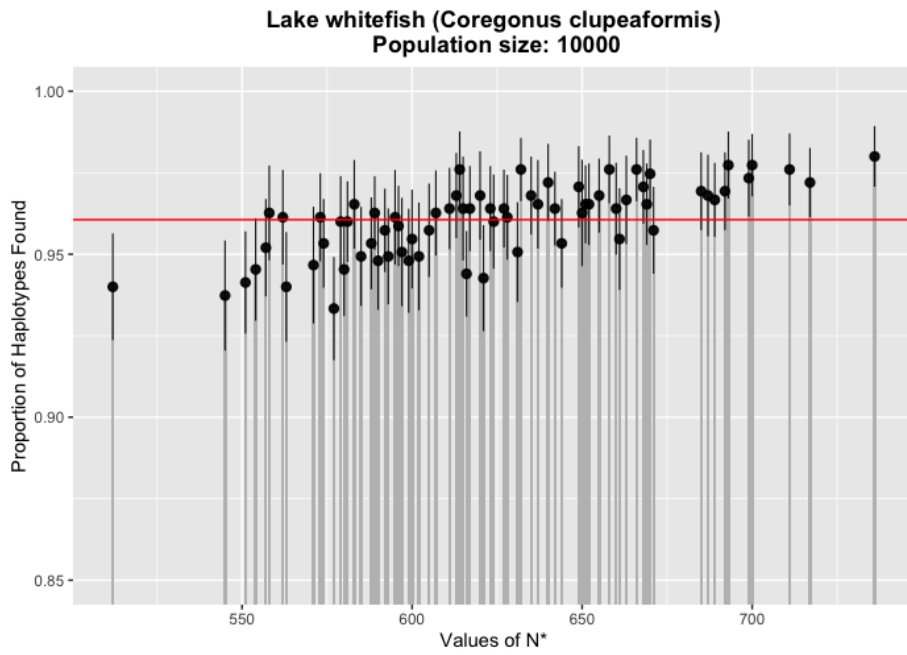


Figure 4.17: Plot showing all located local optima and the proportion of observed haplotypes captured for Lake whitefish (*C. clupeaformis*) with 95% confidence intervals for a population size of 10000. The mean proportion across 50 replications is depicted as a black dot. The mean proportion across all located local optima is displayed as a solid red horizontal line. The thickness of displayed grey error bars is a construct of `ggplot2` based on the number of local optima and holds no additional meaning in the context of this study.

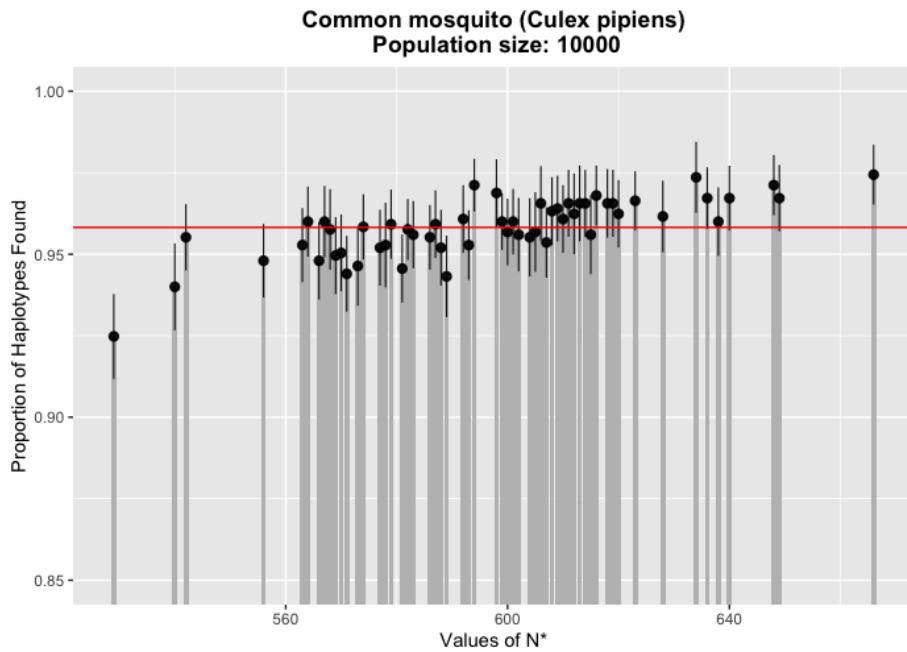


Figure 4.18: Plot showing all located local optima and the proportion of observed haplotypes captured for Common mosquito (*C. pipiens*) with 95% confidence intervals for a population size of 10000. The mean proportion across 50 replications is depicted as a black dot. The mean proportion across all located local optima is displayed as a solid red horizontal line. The thickness of displayed grey error bars is a construct of `ggplot2` based on the number of local optima and holds no additional meaning in the context of this study.

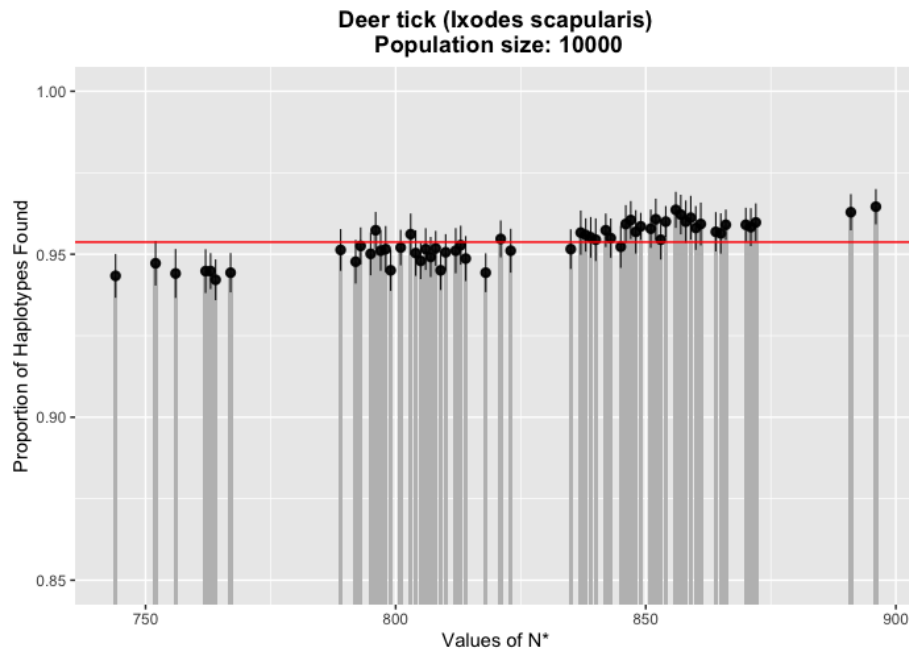


Figure 4.19: Plot showing all located local optima and the proportion of observed haplotypes captured for Deer tick (*I. scapularis*) with 95% confidence intervals for a population size of 10000. The mean proportion across 50 replications is depicted as a black dot. The mean proportion across all located local optima is displayed as a solid red horizontal line. The thickness of displayed grey error bars is a construct of `ggplot2` based on the number of local optima and holds no additional meaning in the context of this study.

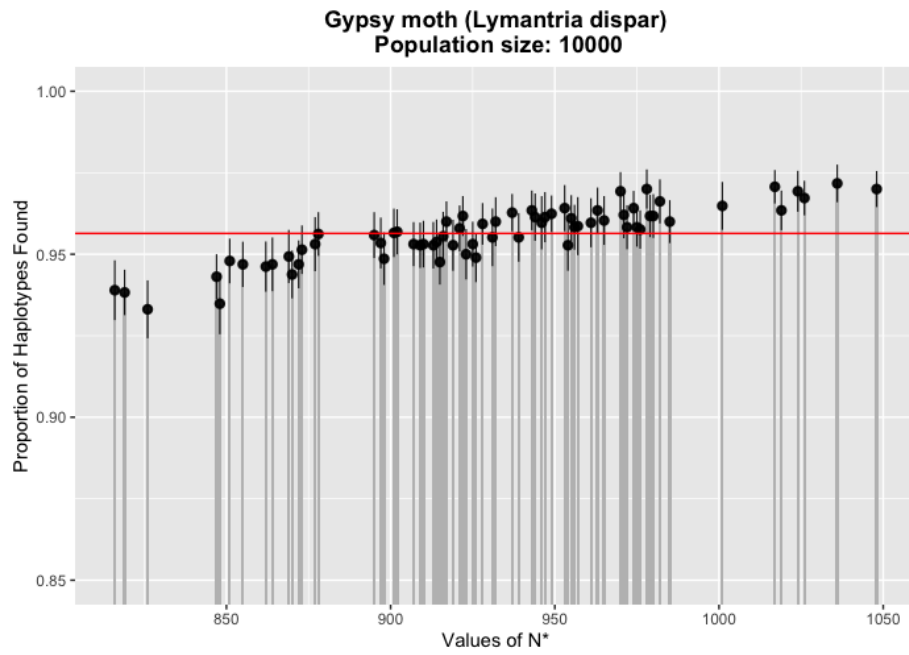


Figure 4.20: Plot showing all located local optima and the proportion of observed haplotypes captured for Gypsy moth (*L. dispar*) with 95% confidence intervals for a population size of 10000. The mean proportion across 50 replications is depicted as a black dot. The mean proportion across all located local optima is displayed as a solid red horizontal line. The thickness of displayed grey error bars is a construct of ggplot2 and thus holds no additional meaning in the context of this study.

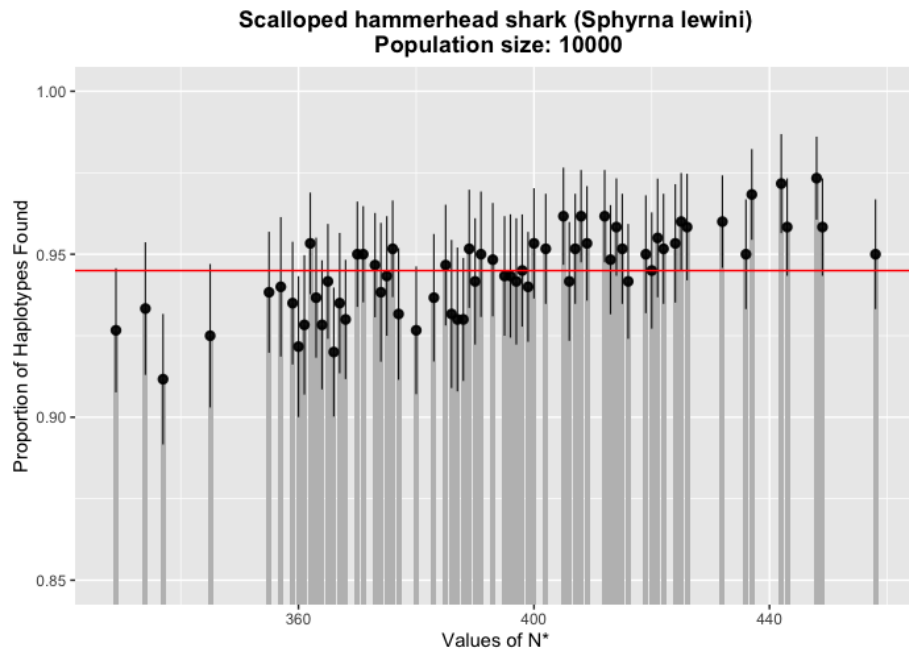


Figure 4.21: Plot showing all located local optima and the proportion of observed haplotypes captured for Scalloped hammerhead shark (*S. lewini*) with 95% confidence intervals for a population size of 10000. The mean proportion across 50 replications is depicted as a black dot. The mean proportion across all located local optima is displayed as a solid red horizontal line. The thickness of displayed grey error bars is a construct of `ggplot2` and thus holds no additional meaning in the context of this study.

Table 4.1: Mean proportion of observed unique haplotypes found over 50 replications of the simulation study for hypothetical species. In all cases, HACSim was run 100 times. Estimates correspond to the solid red horizontal lines depicted in confidence interval plots found within **Figures 15-23** and Supplemental Information accompanying the present article.

Scenario	Pop. size	R Mean	R Range	R Std. dev.
II	1000	0.9623111	0.936-0.980	0.009999596
II	10000	0.9564444	0.926-0.976	0.01262673
II	100000	0.9530222	0.914-0.978	0.01527697
II	10000000	0.9540444	0.918-0.978	0.0125081
III	1000	0.9345789	0.886-0.970	0.01479158
III	10000	0.9541579	0.922-0.976	0.012973
III	100000	0.9508421	0.924-0.978	0.01369657
III	10000000	0.9548421	0.93-0.97	0.01019413
IV	1000	0.9649655	0.940-0.988	0.01165726
IV	10000	0.9597931	0.942-0.978	0.00926352
IV	100000	0.9542069	0.930-0.978	0.01166613
IV	10000000	0.9544138	0.936-0.980	0.01276579

Table 4.2: Mean proportion of observed unique haplotypes found over 50 replications of the simulation study for real species. In all cases, HACSim was run 100 times. Estimates correspond to the solid red horizontal lines depicted in confidence interval plots found within the Supplemental Information accompanying the present article.

Species	Pop. size	R Mean	R Range	R Std. dev.
Pea aphid (<i>Acyrtosiphon pisum</i>)	1000	0.99875	0.991667-1	0.002122249
Pea aphid (<i>Acyrtosiphon pisum</i>)	10000	0.95425	0.9283333-0.99	0.01141193
Pea aphid (<i>Acyrtosiphon pisum</i>)	100000	0.9553333	0.92-0.98	0.01178631
Pea aphid (<i>Acyrtosiphon pisum</i>)	1000000	0.951375	0.92-0.9766667	0.01300431
Lake whitefish (<i>Coregonus clupeaformis</i>)	1000	0.9627397	0.932-0.9826667	0.01185695
Lake whitefish (<i>Coregonus clupeaformis</i>)	10000	0.9606027	0.9333333-0.98	0.01096356
Lake whitefish (<i>Coregonus clupeaformis</i>)	100000	0.9523288	0.908-0.976	0.01333848
Lake whitefish (<i>Coregonus clupeaformis</i>)	1000000	0.9515251	0.9213333-0.9786667	0.0115071
Common mosquito (<i>Culex pipiens</i>)	1000	0.9560281	0.9264-0.9736	0.00912637
Common mosquito (<i>Culex pipiens</i>)	10000	0.9582316	0.9248-0.9744	0.009031674
Common mosquito (<i>Culex pipiens</i>)	100000	0.9506386	0.9336-0.9720	0.007803245
Common mosquito (<i>Culex pipiens</i>)	1000000	0.9516211	0.9312-0.9680	0.008240812
Deer tick (<i>Ixodes scapularis</i>)	1000	0.9399839	0.9262651-0.9530120	0.00622469
Deer tick (<i>Ixodes scapularis</i>)	10000	0.9537108	0.9421687-0.9645783	0.005785297
Deer tick (<i>Ixodes scapularis</i>)	100000	0.9543695	0.9363855-0.9650602	0.006198889
Deer tick (<i>Ixodes scapularis</i>)	1000000	0.95351	0.9375904-0.9669880	0.005953658
Gypsy moth (<i>Lymantria dispar</i>)	1000	0.9372304	0.9179310-0.9472414	0.006580922
Gypsy moth (<i>Lymantria dispar</i>)	10000	0.9563842	0.9331034-0.9717241	0.0084383
Gypsy moth (<i>Lymantria dispar</i>)	100000	0.9516601	0.9344828-0.9682759	0.007620042
Gypsy moth (<i>Lymantria dispar</i>)	1000000	0.952	0.9317241-0.9658621	0.008136763
Scalloped hammerhead shark (<i>Sphyraena lewini</i>)	1000	0.9647692	0.9383333-0.9883333	0.009811051
Scalloped hammerhead shark (<i>Sphyraena lewini</i>)	10000	0.9449744	0.9116667-0.9733333	0.01280357
Scalloped hammerhead shark (<i>Sphyraena lewini</i>)	100000	0.9494103	0.9166667-0.975	0.01483249
Scalloped hammerhead shark (<i>Sphyraena lewini</i>)	1000000	0.9488974	0.9233333-0.9716667	0.01270073

Table 4.3: Bonferroni-corrected Dunn's post-hoc test results at the 0.83% significance level for comparison of population size *versus* haplotype frequency distribution in hypothetical species. **Note:** KW test statistics, *p*-values and statistical significance for Scenario I could not be calculated.

Scenario	Pop. size pairing	Test statistic	<i>p</i> -value	Significant?
II	1000/10000	2.321910	0.0607	No
II	1000/100000	3.270125	0.0032	Yes
II	1000/10000000	3.221498	0.0038	Yes
II	10000/100000	0.948214	1	No
II	10000/10000000	0.899588	1	No
II	100000/10000000	-0.048626	1	No
III	1000/10000	-5.395702	0	Yes
III	1000/100000	-4.306649	0	Yes
III	1000/10000000	-5.698289	0	Yes
III	10000/100000	1.089052	0.8284	No
III	10000/10000000	-0.302587	1	No
III	100000/10000000	-1.391640	0.4921	No
IV	1000/10000	1.666321	0.2869	No
IV	1000/100000	3.358067	0.0024	Yes
IV	1000/10000000	3.158578	0.0048	Yes
IV	10000/1000000	1.691746	0.2721	No
IV	10000/10000000	1.492257	0.4069	No
IV	100000/10000000	-0.199489	1	No

Table 4.4: Bonferroni-corrected Dunn's post-hoc test results at the 0.83% significance level for comparison of population size *versus* haplotype frequency distribution in real species.

Species	Pop. size pairing	Test statistic	p-value	Significant?
<i>A. pisum</i>	1000/10000	8.506172	0	Yes
<i>A. pisum</i>	1000/100000	8.018331	0	Yes
<i>A. pisum</i>	1000/10000000	9.347884	0	Yes
<i>A. pisum</i>	10000/100000	-0.619214	1	No
<i>A. pisum</i>	10000/10000000	1.068381	0.8560	No
<i>A. pisum</i>	100000/10000000	1.687596	0.2745	No
<i>C. clupeaformis</i>	1000/10000	0.943485	1	No
<i>C. clupeaformis</i>	1000/100000	4.763034	0	Yes
<i>C. clupeaformis</i>	1000/10000000	5.407390	0	Yes
<i>C. clupeaformis</i>	10000/100000	3.819548	0.0004	Yes
<i>C. clupeaformis</i>	10000/10000000	4.463904	0	Yes
<i>C. clupeaformis</i>	100000/10000000	0.644355	1	No
<i>C. pipiens</i>	1000/10000	-1.341060	0.5397	No
<i>C. pipiens</i>	1000/100000	3.474823	0.0015	Yes
<i>C. pipiens</i>	1000/10000000	2.841229	0.0135	No
<i>C. pipiens</i>	10000/100000	4.815883	0	Yes
<i>C. pipiens</i>	10000/10000000	4.182289	0.0001	Yes
<i>C. pipiens</i>	100000/10000000	-0.633594	1	No
<i>I. scapularis</i>	1000/10000	-8.203564	0	Yes
<i>I. scapularis</i>	1000/100000	-8.852512	0	Yes
<i>I. scapularis</i>	1000/10000000	-8.049710	0	Yes
<i>I. scapularis</i>	10000/100000	-0.648947	1	No
<i>I. scapularis</i>	10000/10000000	0.153853	1	No
<i>I. scapularis</i>	100000/10000000	0.802801	1	No
<i>L. dispar</i>	1000/10000	-10.41106	0	Yes
<i>L. dispar</i>	1000/100000	-7.583586	0	Yes
<i>L. dispar</i>	1000/10000000	-7.927968	0	Yes
<i>L. dispar</i>	10000/100000	2.904956	0.0110	No
<i>L. dispar</i>	10000/10000000	2.551137	0.0322	No
<i>L. dispar</i>	100000/10000000	-0.353819	1	No
<i>S. lewini</i>	1000/10000	7.901210	0	Yes
<i>S. lewini</i>	1000/100000	5.983095	0	Yes
<i>S. lewini</i>	1000/10000000	6.409083	0	Yes
<i>S. lewini</i>	10000/100000	-1.918115	0.1653	No
<i>S. lewini</i>	10000/10000000	-1.492126	0.4070	No
<i>S. lewini</i>	100000/10000000	0.425988	1	No

Table 4.5: Characteristics of local optima found by HACSim for hypothetical species.

Scenario	No. optima	N* range	N* std. dev.	Highest mode(s)	Highest mode freq.
II	45	226-296	13.46854	260	8
III	38	200-252	11.00911	223	7
IV	29	176-207	8.103522	189/191	9

Table 4.6: Characteristics of local optima found by HACSim for real species. For some species, distinct optima were located for different population sizes. * corresponds to a population size of 1000 and ** to population sizes of 10000, 100000 and 1000000.

Species	No. optima	N* range	N* std. dev.	Highest mode(s)	Highest mode freq.
<i>A. pisum</i>	36*/80**	868-999*/868-1230**	33.67656*/68.38036**	994	4
<i>C. clupeiformis</i>	73	512-736	43.3925	651	4
<i>C. pipiens</i>	57	529-666	25.12822	579	6
<i>I. scapularis</i>	60	744-896	32.93915	808	5
<i>L. dispar</i>	63*/70**	816-985*/816-1048**	42.43375*/48.93845**	909/917/921	4
<i>S. lewini</i>	65	329-458	26.39516	400	4

Table 4.7: Coverage probabilities and 95% Clopper-Pearson confidence intervals for hypothetical species across all assessed population sizes. Calculated probabilities are based on the number of observed local optima found using HACSsim.

Scenario	Pop. size	Coverage prob.	95% Exact binomial CI	Coverage type
II	1000	1	(0.9212949, 1)	conservative
II	10000	0.9777778	(0.8822957, 0.9994375)	conservative
II	100000	0.9555556	(0.8485071, 0.9945715)	conservative
II	1000000	0.9555556	(0.8485071, 0.9945715)	conservative
III	1000	0.6578947	(0.4864732, 0.8036709)	permissive
III	10000	0.9736842	(0.861901, 0.999334)	conservative
III	100000	0.9736842	(0.861901, 0.999334)	conservative
III	1000000	0.9736842	(0.861901, 0.999334)	conservative
IV	1000	1	(0.880551, 1)	conservative
IV	10000	1	(0.880551, 1)	conservative
IV	100000	1	(0.880551, 1)	conservative
IV	1000000	1	(0.880551, 1)	conservative

Table 4.8: Coverage probabilities and 95% Clopper-Pearson confidence intervals for real species across all assessed population sizes. Calculated probabilities are based on the number of observed local optima found using HACSim.

Species	Pop. size	Coverage prob.	95% Exact binomial CI	Coverage type
<i>A. pisum</i>	1000	1	(0.9026062, 1)	
<i>A. pisum</i>	10000	0.975	(0.9125928, 0.9969579)	conservative
<i>A. pisum</i>	100000	0.975	(0.9125928, 0.9969579)	conservative
<i>A. pisum</i>	1000000	0.925	(0.8438721, 0.9719795)	permissive
<i>C. clupeiformis</i>	1000	0.9863014	(0.9260237, 0.9996532)	conservative
<i>C. clupeiformis</i>	10000	0.9863014	(0.9260237, 0.9996532)	conservative
<i>C. clupeiformis</i>	100000	0.890411	(0.7954357, 0.9514836)	permissive
<i>C. clupeiformis</i>	1000000	0.9452055	(0.8656062, 0.9848705)	permissive
<i>C. pipiens</i>	1000	0.9649123	(0.8789293, 0.9957221)	conservative
<i>C. pipiens</i>	10000	0.9824561	(0.9060832, 0.9995559)	conservative
<i>C. pipiens</i>	100000	0.9298246	(0.8299602, 0.9805496)	permissive
<i>C. pipiens</i>	1000000	0.9649123	(0.8789293, 0.9957221)	conservative
<i>I. scapularis</i>	1000	0.15	(0.0709562, 0.2657404)	permissive
<i>I. scapularis</i>	10000	0.9833333	(0.9106009, 0.9995781)	conservative
<i>I. scapularis</i>	100000	0.90	(0.7949423, 0.9624087)	permissive
<i>I. scapularis</i>	1000000	0.95	(0.8607568, 0.9895677)	exact
<i>L. dispar</i>	1000	0	(0, 0.05687235)	permissive
<i>L. dispar</i>	10000	0.9428571	(0.8601058, 0.9842129)	permissive
<i>L. dispar</i>	100000	0.90	(0.8047543, 0.9588403)	permissive
<i>L. dispar</i>	1000000	0.8428571	(0.7362002, 0.9188562)	permissive
<i>S. levini</i>	1000	1	(0.9448284, 1)	conservative
<i>S. levini</i>	10000	0.8461538	(0.7352165, 0.9236784)	permissive
<i>S. levini</i>	100000	0.8769231	(0.7718141, 0.9453369)	permissive
<i>S. levini</i>	1000000	0.9076923	(0.8098342, 0.9653663)	permissive

Chapter 5

Lack of statistical rigor in DNA barcoding likely invalidates the presence of a true species' barcode gap

Jarrett D. Phillips^{1*}, Daniel J. Gillis¹, Robert H. Hanner^{2,3}

¹*School of Computer Science, University of Guelph, Guelph, ON., Canada, N1G2W1*

²*Biodiversity Institute of Ontario, University of Guelph, Guelph, ON., Canada, N1G2W1*

³*Department of Integrative Biology, University of Guelph, Guelph, ON., Canada, N1G2W1*

Chapter 6

Conclusion

6.0.1 Thesis Summary

Within the preceding four chapters, the issue of specimen sample size determination for COI DNA barcoding was investigated in detail. COI is very well represented in existing genomic sequence databases, particularly the Barcode of Life Data Systems (BOLD) and GenBank. The present work clearly points to the increased need to incorporate larger sample sizes into current taxon collection efforts. Crude estimates of adequate sample sizes put forth by various researchers typically range from 5-10 specimens per species. However, it is usually the case that only a single or a few specimens can reasonably be sampled due to species rarity. In fact, there is no “one size fits all” when it comes to taxon sampling because different taxa exhibit distinct evolutionary and life histories. Further, different genes used in assessing sampling completeness at the species level have varying rates of molecular evolution. Simulation studies have demonstrated that much larger sample sizes (on the order of hundreds to thousands) are likely needed to reliably ascertain intraspecific genetic variation. Although it would be ideal to sample individuals of a species across its

entire geographical or ecological range, as well as across a variety of molecular genetic loci, such a scheme is hindered greatly by factors such as project costs. Many of the issues are investigated in Chapter 2 of this thesis.

A much better approach to addressing the question of appropriate sample sizes for DNA barcoding is to instead sample an *optimal* number of specimens of a given species of interest. Chapter 3 presents HACSim a stochastic optimization algorithm for determining necessary specimen sample sizes based on saturation observed in plotted haplotype accumulation curves. The model makes a number of simplifying assumptions that are likely to be violated in real species groups, such as the assumption of panmixia (random mating) across species ranges. Further, *HACSim* assumes that genetic variation observed in barcode sequences is biologically real. The presence of various sequence artifacts such as insertion/deletions (indels) and nuclear-mitochondrial inserts (NUMTs)/pseudogenes, as well as amplification/sequencing errors (*e.g.*, incorrect base calls) within user-curated databases likely means that necessary sample size are actually much larger than currently predicted. A detailed simulation study outlined in Chapter 4 shows (1) that HACSim suggests samples sizes higher than those routinely employed in practice within DNA barcoding studies and (2) that HACSim consistently captures desired levels of within-species haplotype diversity across all wide-ranging sample sizes. Despite this, the assumption of representative sampling of species haplotype diversity is quite unrealistic. Future work should investigate the further relaxing of model assumptions, in particular the introduction of population structuring. While HACSim is currently available as an R

package from CRAN, a stand-alone R Shiny web application has also been developed for those users who either lack confidence in programming within R or those users who are uncertain `HACSim` is ideal for their problem of interest. In both cases, the `HACSim` Shiny app can be employed to run all examples included in [117] plus other custom simulations of a user's choosing. The app can be accessed in two ways: (1) through the Shiny server, or (2) through the `HACSim` R package itself via the `launchApp()` function.

Finally, Chapter 5 makes a case for the lack of statistical rigor in DNA barcoding as it pertains to accurate estimation of the DNA barcode gap. Arguments revolve around three main areas: (1) improper allocation of specimen sampling effort required to adequately probe levels of standing intraspecific genetic variation, (2) improperly visualizing within- and among-species genetic distances and (3) the inconsistent, inappropriate use, or absence of statistical inferential procedures in DNA barcoding gap analyses. In addressing each of these omissions, simple statistical solutions are offered that are readily accessible to the non-statistician.

References

- [1] ADAMS, C., KNAPP, M., GEMMELL, N., JEUNEN, G.-J., BUNCE, M., LAMARE, M., AND TAYLOR, H. Beyond biodiversity: Can environmental DNA (eDNA) cut it as a population genetics tool? *Genes* 10, 192 (2019), 1.
- [2] ADCOCK, C. Sample size determination: A review. *Journal of the Royal Statistical Society: Series D (The Statistician)* 46, 2 (1997), 261–283.
- [3] APRIL, J., HANNER, R. H., DION-CÔTÉ, A.-M., AND BERNATCHEZ, L. Glacial cycles as an allopatric speciation pump in north-eastern American freshwater fishes. *Molecular Ecology* 22, 2 (2013), 409–422.
- [4] APRIL, J., HANNER, R. H., MAYDEN, R. L., AND BERNATCHEZ, L. Metabolic rate and climatic fluctuations shape continental wide pattern of genetic divergence and biodiversity in fishes. *PLOS ONE* 8, 7 (2013), e70296.
- [5] APRIL, J., MAYDEN, R. L., HANNER, R. H., AND BERNATCHEZ, L. Genetic calibration of species diversity among North America's freshwater fishes. *Proceedings of the National Academy of Sciences* 108, 26 (2011), 10602–10607.
- [6] ATHEY, T. Assessing Errors in DNA Barcode Sequence Records. Master's thesis, University of Guelph, 2013.
- [7] AUSTERLITZ, F., DAVID, O., SCHAEFFER, B., BLEAKLEY, K., OLTEANU, M., LEBLOIS, R., VEUILLE, M., AND LAREDO, C. DNA barcode analysis: a comparison of phylogenetic and statistical classification methods. *BMC Bioinformatics* 10, 14 (2009), S10.
- [8] AVISE, J. C., ARNOLD, J., BALL, R. M., BERMINGHAM, E., LAMB, T., NEIGEL, J. E., REEB, C. A., AND SAUNDERS, N. C. Intraspecific phylogeography: the mitochondrial DNA bridge between population genetics and systematics. *Annual Review of Ecology and Systematics* 18, 1 (1987), 489–522.
- [9] BAKER, A., SENDRA TAVARES, E., AND ELOURNE, R. Countering criticisms of single mitochondrial DNA gene barcoding in birds. *Molecular Ecology Resources* (2009), 257–268.

- [10] BECKER, S., HANNER, R., AND STEINKE, D. Five years of FISH-BOL: brief status report. *Mitochondrial DNA* 22, sup1 (2011), 3–9.
- [11] BEEBE, N. DNA barcoding mosquitoes: Advice for potential prospectors. *Parasitology* 145, 5 (2018), 622–633.
- [12] BENGTSSON, B. Genetic variation in organisms with sexual and asexual reproduction. *Journal of Evolutionary Biology* 16 (2003), 189.
- [13] BERGSTEN, J., BILTON, D. T., FUJISAWA, T., ELLIOTT, M., MONAGHAN, M. T., BALKE, M., HENDRICH, L., GEIJER, J., HERRMANN, J., FOSTER, G. N., ET AL. The effect of geographical scale of sampling on DNA barcoding. *Systematic Biology* (2012), sys037.
- [14] BERTOLAZZI, P., FELICI, G., AND WEITSCHER, E. Learning to classify species with barcodes. *BMC Bioinformatics* 10, 14 (2009), S7.
- [15] BEVILACQUA, S., UGLAND, K. I., PLICANTI, A., SCUDERI, D., AND TERLIZZI, A. An approach based on the total-species accumulation curve and higher taxon richness to estimate realistic upper limits in regional species richness. *Ecology and Evolution* 8, 1 (2017), 405–415.
- [16] BRAUKMANN, T., IVANOVA, N., PROSSER, S., ELBRECHT, V., STEINKE, D., RATNASHINGHAM, S., DE WAARD, J., SONES, J., ZAKHAROV, E., AND HEBERT, P. Metabarcoding a diverse arthropod mock community. *Molecular Ecology Resources* (2019), 711–727.
- [17] BROWN, S. D., COLLINS, R. A., BOYER, S., LEFORT, M.-C., MALUMBRES-OLARTE, J., VINK, C. J., AND CRUICKSHANK, R. H. Spider: an R package for the analysis of species identity and evolution, with particular reference to DNA barcoding. *Molecular Ecology Resources* 12, 3 (2012), 562–565.
- [18] BUCKLIN, A., STEINKE, D., AND BLANCO-BERCIAL, L. DNA barcoding of marine metazoa. *Annual Review of Marine Science* 3 (2011), 471–508.
- [19] BURTON, A., ALTMAN, D., ROYSTON, P., AND HOLDER, R. The design of simulation studies in medical statistics. *Statistics in Medicine* 25 (2006), 4279–4292.
- [20] CAMERON, S., RUBINOFF, D., AND WILL, K. Who will actually use DNA barcoding and what will it cost? *Systematic Biology* 55, 5 (2006), 844–847.
- [21] ČANDEK, K., AND KUNTNER, M. DNA barcoding gap: reliable species identification over morphological and geographical scales. *Molecular Ecology Resources* 15, 2 (2015), 268–277.

- [22] CASELLA, G., AND BERGER, R. *Statistical Inference*. Duxbury Thomson Learning, 2002.
- [23] CEBALLOS, G., EHRLICH, P. R., BARNOSKY, A. D., GARCÍA, A., PRINGLE, R. M., AND PALMER, T. M. Accelerated modern human–induced species losses: Entering the sixth mass extinction. *Science Advances* 1, 5 (2015), e1400253.
- [24] CHAO, A. Nonparametric estimation of the number of classes in a population. *Scandinavian Journal of Statistics* 11 (1984), 265–270.
- [25] CHEN, F., COATES, B., HE, K., ET AL. Effects of wolbachia on mitochondrial DNA variation in populations of Athetis lepigone (Lepidoptera: Noctuidae) in China. *Mitochondrial DNA Part A* 28, 6 (1984), 826–834.
- [26] CHERNICK, M., AND LABUDDE, R. *Bootstrap Methods with Applications to R*. Wiley, 2011.
- [27] CHIARUCCI, A., BACARO, G., RICOTTA, C., PALMER, M., AND SCHEINER, S. Spatially constrained rarefaction: incorporating the autocorrelated structure of biological communities into sample-based rarefaction. *Community Ecology* 10 (2009), 209–214.
- [28] CHOPARD, B., AND TOMMASINI, M. Search Space. In *An Introduction to Metaheuristics for Optimization*. Springer, 2018.
- [29] CLARE, E. L., LIM, B. K., FENTON, M. B., AND HEBERT, P. D. Neotropical bats: estimating species diversity with DNA barcodes. *PLOS ONE* 6, 7 (2011), e22648.
- [30] COHEN, J. Things I have learned (so far). *American Psychologist* 45, 12 (1990), 1304.
- [31] COLLINS, R., AND CRUICKSHANK, R. The seven deadly sins of DNA barcoding. *Molecular Ecology Resources* 13, 6 (2013), 969–975.
- [32] DA COSTA, L. S., CORNELEO, N. S., AND STEFENON, V. M. Conservation of Forest Biodiversity: how sample size affects the estimation of genetic parameters. *Anais da Academia Brasileira de Ciências* 87, 2 (2015), 1095–1100.
- [33] DASMAHAPATRA, K. K., ELIAS, M., HILL, R. I., HOFFMAN, J. I., AND MALLET, J. Mitochondrial DNA barcoding detects some species that are real, and some that are not. *Molecular Ecology Resources* 10, 2 (2010), 264–273.
- [34] DENGLER, J. Which function describes the species–area relationship best? a review and empirical evaluation. *Journal of Biogeography* 36, 4 (2009), 728–744.

- [35] DEWAARD, J., MITCHELL, A., KEENA, M., GOPURENKO, D., BOYKIN, L., ARMSTRONG, K., POGUE, M., LIMA, J., FLOYD, R., HANNER, R., AND HUMBLE, L. Towards a global barcode library for *Lymantria* (Lepidoptera: Lymantriinae) tussock moths of biosecurity concern. *PLoS ONE* 5, 12 (2010), e14280.
- [36] DI STEFANO, J. How much power is enough? Against the development of an arbitrary convention for statistical power calculations. *Functional Ecology* 17, 5 (2003), 707–709.
- [37] DINNO, A. *dunn.test: Dunn's Test of Multiple Comparisons Using Rank Sums*, 2017. R package version 1.3.5.
- [38] DIXON, C. J. A means of estimating the completeness of haplotype sampling using the Stirling probability distribution. *Molecular Ecology Notes* 6, 3 (2006), 650–652.
- [39] DIXON, P. Vegan, a package of r functions for community ecology. *Journal of Vegetation Science* 14, 6 (2003), 927–930.
- [40] DLUGOSCH, K., ANDERSON, S., BRAASCH, J., CANG, F., AND GILLETTE, H. The devil is in the details: genetic variation in introduced populations and its contributions to invasion. *Molecular Ecology* 24, 9 (2015), 2095–2111.
- [41] EDDELBUETTEL, D., AND FRANÇOIS, R. Rcpp: Seamless R and C++ integration. *Journal of Statistical Software* 40, 8 (2011), 1–18.
- [42] EDDELBUETTEL, D., AND SANDERSON, C. RcppArmadillo: Accelerating R with high-performance C++ linear algebra. *Computational Statistics and Data Analysis* 71 (2014), 1054–1063.
- [43] EDGAR, R. C. Search and clustering orders of magnitude faster than BLAST. *Bioinformatics* 26, 19 (2010), 2460–2461.
- [44] EFRON, B. Bootstrap methods: Another look at the jackknife. *The Annals of Statistics* (1979), 1–26.
- [45] ELBRECHT, V., VAMOS, E. E., STEINKE, D., AND LEESE, F. Estimating intraspecific genetic diversity from community DNA metabarcoding data. *PeerJ* 6 (2018), e4644.
- [46] EWENS, W. J. The sampling theory of selectively neutral alleles. *Theoretical Population Biology* 3, 1 (1972), 87–112.
- [47] EZARD, T., FUJISAWA, T., AND BARRACLOUGH, T. *splits: SPecies' LImits by Threshold Statistics*, 2017. R package version 1.0-19/r52.

- [48] FELENSTEIN, J. The evolutionary advantage of recombination. *Genetics* 78, 2 (1974), 737–756.
- [49] FOOTTIT, R., MAW, H., VON DOHLEN, D., AND HEBERT, P. Species identification of aphids (Insecta: Hemiptera: Aphididae) through DNA barcodes. *Molecular Ecology Resources* 8 (2008), 1189–1201.
- [50] FUJISAWA, T., AND BARRACLOUGH, T. Delimiting species using single-locus data and the Generalized Mixed Yule Coalescent approach: a revised method and evaluation on simulated data sets. *Systematic Biology* 62, 5 (2013), 707–724.
- [51] FUNK, D. J., AND OMLAND, K. E. Species-level paraphyly and polyphyly: frequency, causes, and consequences, with insights from animal mitochondrial DNA. *Annual Review of Ecology, Evolution, and Systematics* 34, 1 (2003), 397–423.
- [52] GOODALL-COPESTAKE, W., TARLING, G., AND MURPHY, E. On the comparison of population-level estimates of haplotype and nucleotide diversity: a case study using the gene cox1 in animals. *Heredity* 109, 1 (2012), 50–56.
- [53] GOTELLI, N. J., AND COLWELL, R. K. Quantifying biodiversity: procedures and pitfalls in the measurement and comparison of species richness. *Ecology Letters* 4, 4 (2001), 379–391.
- [54] GREWE, P. M., KRUEGER, C. C., AQUADRO, C. F., BIRMINGHAM, E., KINCAID, H. L., AND MAY, B. Mitochondrial DNA variation among lake trout (*Salvelinus namaycush*) strains stocked into Lake Ontario. *Canadian Journal of Fisheries and Aquatic Sciences* 50, 11 (1993), 2397–2403.
- [55] GWIAZDOWSKI, R. A., ELKINTON, J. S., DEWAARD, J. R., AND SREMAC, M. Phylogeographic diversity of the winter moths *Operophtera brumata* and *O. bruceata* (Lepidoptera: Geometridae) in Europe and North America. *Annals of the Entomological Society of America* 106, 2 (2013), 143–151.
- [56] HAJIBABAEI, M., SINGER, G. A., HEBERT, P. D., AND HICKEY, D. A. DNA barcoding: how it complements taxonomy, molecular phylogenetics and population genetics. *TRENDS in Genetics* 23, 4 (2007), 167–172.
- [57] HALE, M. L., BURG, T. M., AND STEEVES, T. E. Sampling for microsatellite-based population genetic studies: 25 to 30 individuals per population is enough to accurately estimate allele frequencies. *PLOS ONE* 7, 9 (2012), e45170.
- [58] HANNER, R. Data standards for BARCODE records in INSDC (BRIs).
- [59] HANNER, R., BECKER, S., IVANOVA, N. V., AND STEINKE, D. FISH-BOL and seafood identification: Geographically dispersed case studies reveal systemic market substitution across Canada. *Mitochondrial DNA* 22, sup1 (2011), 106–122.

- [60] HANNER, R., FLOYD, R., BERNARD, A., COLLETTE, B. B., AND SHIVJI, M. DNA barcoding of billfishes. *Mitochondrial DNA* 22, sup1 (2011), 27–36.
- [61] HANNER, R. H., NAAUM, A. M., AND SHIVJI, M. S. Conclusion: DNA-Based Authentication of Shark Products and Implications for Conservation and Management. In *Seafood Authenticity and Traceability: A DNA-based Perspective*, A. M. Naum and R. H. Hanner, Eds., 1 ed. Academic Press, 2016.
- [62] HARRIS, D. J. Can you bank on GenBank? *Trends in Ecology & Evolution* 18, 7 (2003), 317–319.
- [63] HART, M. W., AND SUNDAY, J. Things fall apart: biological species form unconnected parsimony networks. *Biology Letters* 3, 5 (2007), 509–512.
- [64] HAUSMANN, A., GODFRAY, H. C. J., HUEMER, P., MUTANEN, M., ROUGERIE, R., VAN NIEUKERKEN, E. J., RATNASINGHAM, S., AND HEBERT, P. D. Genetic patterns in European geometrid moths revealed by the Barcode Index Number (BIN) system. *PLOS ONE* 8, 12 (2013), e84518.
- [65] HEBERT, P. D., CYWINSKA, A., BALL, S. L., ET AL. Biological identifications through DNA barcodes. *Proceedings of the Royal Society of London B: Biological Sciences* 270, 1512 (2003), 313–321.
- [66] HEBERT, P. D., PENTON, E., BURNS, J., JANZEN, D., AND HALLWACHS, W. Ten species in one: DNA barcoding reveals cryptic species in the neotropical skipper butterfly *Astraptes fulgerator*. *Proceedings of the National Academy of Sciences* 101, 41 (2004), 14812–14817.
- [67] HEBERT, P. D., RATNASINGHAM, S., AND DE WAARD, J. R. Barcoding animal life: cytochrome c oxidase subunit 1 divergences among closely related species. *Proceedings of the Royal Society of London B: Biological Sciences* 270, Suppl 1 (2003), S96–S99.
- [68] HEBERT, P. D., RATNASINGHAM, S., AND ZAKHAROV, E. Counting animal species with dna barcodes: Canadian insects. *Philosophical Transactions of the Royal Society B* 371 (2016), 20150333.
- [69] HEBERT, P. D., STOECKLE, M. Y., ZEMLAK, T. S., AND FRANCIS, C. M. Identification of birds through DNA barcodes. *PLOS Biology* 2, 10 (2004), e312.
- [70] HICKERSON, M. J., MEYER, C. P., AND MORITZ, C. DNA barcoding will often fail to discover new animal species over broad parameter space. *Systematic Biology* 55, 5 (2006), 729–739.

- [71] HOLT, J. A., STONEBERG HOLT, S. D., AND BUREŠ, P. Experimental design in intraspecific organelle DNA sequence studies III: statistical measures of sampling success. *Taxon* 56, 3 (2007), 847–856.
- [72] HORTAL, J., AND LOBO, J. M. An ED-based protocol for optimal sampling of biodiversity. *Biodiversity and Conservation* 14, 12 (2005), 2913–2947.
- [73] HUBERT, N., AND HANNER, R. DNA Barcoding, species delineation and taxonomy: a historical perspective. *DNA Barcodes* 3, 1 (2015), 44–58.
- [74] HUBERT, N., HANNER, R., HOLM, E., MANDRAK, N. E., TAYLOR, E., BURRIDGE, M., WATKINSON, D., DUMONT, P., CURRY, A., BENTZEN, P., ZHANG, J., APRIL, J., AND BERNATCHEZ, L. Identifying Canadian freshwater fishes through DNA barcodes. *PLOS ONE* 3, 6 (2008), e2490.
- [75] HUEMER, P., MUTANEN, M., SEFC, K. M., AND HEBERT, P. D. Testing DNA barcode performance in 1000 species of European Lepidoptera: Large geographic distances have small genetic impacts. *PLOS ONE* 9, 12 (2014), e115774.
- [76] HUNTER, M., OYLER-MCCANCE, S., DORAZIO, R., ET AL. Environmental DNA (eDNA) Sampling Improves Occurrence and Detection Estimates of Invasive Burmese Pythons. *PLOS ONE* 10, 4 (2015), e0121655.
- [77] JIN, Q., HE, L.-J., AND ZHANG, A.-B. A simple 2D non-parametric resampling statistical approach to assess confidence in species identification in DNA barcoding—an alternative to Likelihood and Bayesian approaches. *PLOS ONE* 7, 12 (2012), e50831.
- [78] JOLY, S., STEVENS, M. I., AND VAN VUUREN, B. J. Haplotype networks can be misleading in the presence of missing data. *Systematic Biology* 56, 5 (2007), 857–862.
- [79] KIMURA, M., AND WEISS, G. The stepping stone model of population structure and the decrease of genetic correlation with distance. *Genetics* 49, 4 (1964), 561–576.
- [80] KINGMAN, J. F. C. The coalescent. *Stochastic Processes and their Applications* 13, 3 (1982), 235–248.
- [81] KUMAR, S., STECHER, G., AND TAMURA, K. MEGA7: Molecular evolutionary genetics analysis version 7.0 for bigger datasets. *Molecular Biology and Evolution* (2016), 1870–1874.
- [82] LAVINIA, P., KERR, K., TUBARO, P., HEBERT, P., AND LIJTMAER, D. Calibrating the molecular clock beyond cytochrome b: assessing the evolutionary rate of COI in birds. *Journal of Avian Biology* 47 (2016), 86–91.

- [83] LAYTON, K., MARTEL, A., AND HEBERT, P. Patterns of DNA barcode variation in Canadian marine molluscs. *PLOS ONE* 9, 4 (2014), e95003.
- [84] LEIGH, J. W., AND BRYANT, D. POPART: full-feature software for haplotype network construction. *Methods in Ecology and Evolution* 6, 9 (2015), 1110–1116.
- [85] LENTH, R. V. Some practical guidelines for effective sample size determination. *The American Statistician* 55, 3 (2001), 187–193.
- [86] LINDBLOM, L. Sample size and haplotype richness in population samples of the lichen-forming ascomycete Xanthoria parietina. *The Lichenologist* 41, 05 (2009), 529–535.
- [87] LIU, J., PROVAN, J., GAO, L.-M., AND LI, D.-Z. Sampling strategy and potential utility of indels for DNA barcoding of closely related plant species: a case study in Taxus. *International Journal of Molecular Sciences* 13, 7 (2012), 8740–8751.
- [88] LOHSE, K. Can mtDNA barcodes be used to delimit species? a response to Pons et al. (2006). *Systematic Biology* 58, 4 (2009), 439–442.
- [89] LOU, M., AND GOLDING, G. B. The effect of sampling from subdivided populations on species identification with DNA barcodes using a Bayesian statistical approach. *Molecular Phylogenetics and Evolution* 65, 2 (2012), 765–773.
- [90] LUO, A., LAN, H., LING, C., ZHANG, A.-B., SHI, L., HO, S. Y., AND ZHU, C. A simulation study of sample size for DNA barcoding. *Ecology and Evolution* 5, 24 (2015), 5869–5879.
- [91] MATZ, M. V., AND NIELSEN, R. A likelihood ratio test for species membership based on DNA sequence data. *Philosophical Transactions of the Royal Society of London B: Biological Sciences* 360, 1462 (2005), 1969–1974.
- [92] MEYER, C. P., AND PAULAY, G. DNA barcoding: error rates based on comprehensive sampling. *PLOS Biology* 3, 12 (2005), e422.
- [93] MILIÁN-GARCÍA, Y., YOUNG, R., MADDEN, M., BULLAS-APPLETON, E., AND HANNER, R. Optimization and validation of a cost-effective protocol for biosurveillance of invasive alien species. *Ecology and Evolution* (2021), 1–16.
- [94] MIN, X., AND HICKEY, D. Assessing the effect of varying sequence length on DNA barcoding of fungi. *Molecular Ecology Notes* 7 (2007), 365–373.
- [95] MONAGHAN, M., WILD, R., ELLIOT, M., ET AL. Accelerated species inventory on madagascar using coalescent-based models of species delineation. *Systematic Biology* 58, 3 (2009), 298–311.

- [96] MORRIS, T., WHITE, I., AND CROWTHER, M. Using simulation studies to evaluate statistical methods. *Statistics in Medicine* 38 (2019), 2074–2102.
- [97] MUIRHEAD, J. R., GRAY, D. K., KELLY, D. W., ELLIS, S. M., HEATH, D. D., AND MACISAAC, H. J. Identifying the source of species invasions: sampling intensity vs. genetic diversity. *Molecular Ecology* 17, 4 (2008), 1020–1035.
- [98] MULLER, H. The relation of recombination to mutational advance. *Mutation Research* 1, 1 (1964), 2–9.
- [99] MUTANEN, M., KIVELÄ, S. M., VOS, R. A., DOORENWEERD, C., RATNASINGHAM, S., HAUSMANN, A., HUEMER, P., DINCĂ, V., VAN NIEUKERKEN, E. J., LOPEZ-VAAMONDE, C., ET AL. Species-level para-and polyphyly in DNA barcode gene trees: strong operational bias in European Lepidoptera. *Systematic Biology* 65, 6 (2016), 1024–1040.
- [100] NAAUM, A. M., ST JAQUES, J., WARNER, K., SANTSCHI, L., IMONDI, R., AND HANNER, R. Standards for conducting a DNA barcoding market survey: Minimum information and best practices. *DNA Barcodes* 3, 1 (2015), 80–84.
- [101] NAZARENO, A. G., BEMMELS, J. B., DICK, C. W., AND LOHMANN, L. G. Minimum sample sizes for population genomics: an empirical study from an Amazonian plant species. *Molecular Ecology Resources* 17, 6 (2017), 1136–1147.
- [102] NEI, M. *Molecular Evolutionary Genetics*. Columbia University Press, 1987.
- [103] NEI, M., AND LI, W.-H. Mathematical model for studying genetic variation in terms of restriction endonucleases. *Proceedings of the National Academy of Sciences* 76, 10 (1979), 5269–5273.
- [104] NIELSEN, R., AND MATZ, M. Statistical approaches for DNA barcoding. *Systematic Biology* 55, 1 (2006), 162–169.
- [105] ONDREJICKA, D. A., LOCKE, S. A., MOREY, K., BORISENKO, A. V., AND HANNER, R. H. Status and prospects of DNA barcoding in medically important parasites and vectors. *Trends in Parasitology* 30, 12 (2014), 582–591.
- [106] ONDREJICKA, D. A., MOREY, K., AND HANNER, R. H. DNA barcodes identify medically important tick species in Canada. *Genome* 60, 1 (2017), 74–84.
- [107] OVERDYK, L. M., BRAID, H. E., CRAWFORD, S. S., AND HANNER, R. H. Extending DNA barcoding coverage for Lake Whitefish (*Coregonus clupeaformis*) across the three major basins of Lake Huron. *DNA Barcodes* 3, 1 (2015), 59–65.

- [108] PANTE, E., PUILLANDRE, N., VIRICEL, A., ARNAUD-HAOND, S., AURELLE, D., CASTELIN, M., CHENUIL, A., DESTOMBE, C., FORCIOLE, D., VALERO, M., ET AL. Species are hypotheses: avoid connectivity assessments based on pillars of sand. *Molecular Ecology* 24, 3 (2015), 525–544.
- [109] PAPADOPOULOU, A., MONAGHAN, M., BARRACLOUGH, T., ET AL. Sampling error does not invalidate the yule-coalescent model for species delimitation. a response to Lohse (2009). *Systematic Biology* 58, 4 (2009), 442–444.
- [110] PARADIS, E. pegas: an R package for population genetics with an integrated-modular approach. *Bioinformatics* 26, 3 (2010), 419–420.
- [111] PARADIS, E., CLAUDE, J., AND STRIMMER, K. APE: analyses of phylogenetics and evolution in R language. *Bioinformatics* 20, 2 (2004), 289–290.
- [112] PARR, C. S., GURALNICK, R., CELLINESE, N., AND PAGE, R. D. Evolutionary informatics: unifying knowledge about the diversity of life. *Trends in Ecology & Evolution* 27, 2 (2012), 94–103.
- [113] PEARSON, K. Contributions to the mathematical theory of evolution. *Philosophical Transactions of the Royal Society of London. A* 185 (1894), 71–110.
- [114] PENTINSAARI, M., HEBERT, P. D., AND MUTANEN, M. Barcoding beetles: a regional survey of 1872 species reveals high identification success and unusually deep interspecific divergences. *PLOS ONE* 9, 9 (2014), e108651.
- [115] PFENNINGER, M., BÁLINT, M., AND PAULS, S. Methodological framework for projecting the potential loss of intraspecific genetic diversity due to global climate change. *BMC Evolutionary Biology* 12, 224 (2012), 1–13.
- [116] PHILLIPS, J. D., GILLIS, D. J., AND HANNER, R. H. Incomplete estimates of genetic diversity within species: Implications for DNA barcoding. *Ecology and Evolution* 9, 5 (2019), 2996–3010.
- [117] PHILLIPS, J. D., GILLIS, D. J., AND HANNER, R. H. HACSim: An R package to estimate intraspecific sample sizes for genetic diversity assessment using haplotype accumulation curves. *PeerJ Computer Science* (2020).
- [118] PHILLIPS, J. D., GWIAZDOWSKI, R. A., ASHLOCK, D., AND HANNER, R. An exploration of sufficient sampling effort to describe intraspecific DNA barcode haplotype diversity: examples from the ray-finned fishes (Chordata: Actinopterygii). *DNA Barcodes* 3, 1 (2015), 66–73.
- [119] PONS, J., BARRACLOUGH, T., GOMEZ-ZURITA, ET AL. Sequence-based species delimitation for the DNA taxonomy of undescribed insects. *Systematic Biology* 55, 4 (2006), 595–609.

- [120] PRUETT, C., AND WINKER, K. The effects of sample size on population genetic diversity estimates in song sparrows *Melospiza melodia*. *Journal of Avian Biology* 39 (2008), 252–256.
- [121] PUILLANDRE, N., LAMBERT, A., AND BROUILLET, S. ABGD, Automatic Barcode Gap Discovery for primary species delimitation. *Molecular Ecology* 21 (2011), 1864–1877.
- [122] R CORE TEAM. *R: A Language and Environment for Statistical Computing*. R Foundation for Statistical Computing, Vienna, Austria, 2018.
- [123] RATNASHINGHAM, S., AND HEBERT, P. D. BOLD: The Barcode of Life Data System (<http://www.barcodinglife.org>). *Molecular Ecology Notes* 7, 3 (2007), 355–364.
- [124] RATNASHINGHAM, S., AND HEBERT, P. D. A DNA-based registry for all animal species: the Barcode Index Number (BIN) system. *PLOS ONE* 8, 7 (2013), e66213.
- [125] ROGNES, T., FLOURI, T., NICHOLS, B., QUINCE, C., AND MAHÉ, F. VSEARCH: a versatile open source tool for metagenomics. *PeerJ* 4 (2016), e2584.
- [126] ROSENBERG, N., AND NORDBORG, M. Genealogical trees, coalescent theory and the analysis of genetic polymorphisms. *Nature Genetics Reviews* 3 (2002), 380–390.
- [127] ROSS, H. A., MURUGAN, S., AND LI, W. L. S. Testing the reliability of genetic methods of species identification via simulation. *Systematic Biology* 57, 2 (2008), 216–230.
- [128] RYAN, K., AND CRAWFORD, S. Distribution and abundance of larval lake whitefish (*Coregonus clupeaformis*) in Stokes Bay, Lake Huron. *Journal of Great Lakes Research* 40 (2014), 755–762.
- [129] SHEHATA, H., NAAUM, A., GARDUNO, R., AND HANNER, R. DNA barcoding as a regulatory tool for seafood authentication in Canada. *Food Control* 92 (2018), 147–153.
- [130] SMITH, M., BERTRAND, C., CROSBY, K., ET AL. Wolbachia and DNA barcoding insects: Patterns, potential and problems. *PLOS ONE* 7, 5 (2012), e36514.
- [131] SPALL, J. C. Stochastic Optimization. In *Handbook of Computational Statistics: Concepts and Methods*, J. E. Gentle, W. K. Härdle, and Y. Mori, Eds., 2 ed. Springer, 2012.
- [132] STEIN, E. D., MARTINEZ, M. C., STILES, S., MILLER, P. E., AND ZAKHAROV, E. V. Is DNA barcoding actually cheaper and faster than traditional morphological methods: Results from a survey of freshwater bioassessment efforts in the United States? *PLOS ONE* 9, 4 (2014), e95525.

- [133] STEINKE, D., BERNARD, A. M., HORN, R. L., HILTON, P., HANNER, R., AND SHIVJI, M. S. DNA analysis of traded shark fins and mobulid gill plates reveals a high proportion of species of conservation concern. *Scientific Reports* 7, 9505 (2017), 1–6.
- [134] STEINKE, D., AND HANNER, R. The FISH-BOL collaborators' protocol. *Mitochondrial DNA* 22, sup1 (2011), 10–14.
- [135] STEINKE, D., ZEMLAK, T. S., BOUTILLIER, J. A., AND HEBERT, P. D. DNA barcoding of Pacific Canada's fishes. *Marine Biology* 156, 12 (2009), 2641–2647.
- [136] STOECKLE, M. Y., AND KERR, K. C. Frequency matrix approach demonstrates high sequence quality in avian BARCODEs and highlights cryptic pseudogenes. *PLOS ONE* 7, 8 (2012), e43992.
- [137] STOECKLE, M. Y., AND THALER, D. S. DNA barcoding works in practice but not in (neutral) theory. *PLOS ONE* 9, 7 (2014), e100755.
- [138] STROHM, J. H., GWIAZDOWSKI, R. A., AND HANNER, R. Mitogenome metadata: current trends and proposed standards. *Mitochondrial DNA Part A* 27, 5 (2016), 3263–3269.
- [139] TEMPLETON, A. R., CRANDALL, K. A., AND SING, C. F. A cladistic analysis of phenotypic associations with haplotypes inferred from restriction endonuclease mapping and DNA sequence data. III. Cladogram estimation. *Genetics* 132, 2 (1992), 619–633.
- [140] TERLIZZI, A., ANDERSON, M. J., BEVILACQUA, S., AND UGLAND, K. I. Species-accumulation curves and taxonomic surrogates: an integrated approach for estimation of regional species richness. *Diversity and Distributions* 20 (2014), 356–368.
- [141] TJØRVE, E. Shapes and functions of species-area curves: a review of possible models. *Journal of Biogeography* 30, 6 (2003), 827–835.
- [142] TURON, X., ANTICH, A., PALACIN, C., PRÆBEL, K., AND WANGERSTEEN, O. From metabarcoding to metaphylogeography: separating the wheat from the chaff. *bioRxiv* (2019).
- [143] WARD, R. D., HANNER, R., AND HEBERT, P. D. The campaign to DNA barcode all fishes, FISH-BOL. *Journal of Fish Biology* 74, 2 (2009), 329–356.
- [144] WARD, R. D., ZEMLAK, T. S., INNES, B. H., LAST, P. R., AND HEBERT, P. D. DNA barcoding Australia's fish species. *Philosophical Transactions of the Royal Society of London B: Biological Sciences* 360, 1462 (2005), 1847–1857.

- [145] WARES, J. P., AND PAPPALARDO, P. Can Theory Improve the Scope of Quantitative Metazoan Metabarcoding? *Diversity* 8, 1 (2015), 1.
- [146] WATTERSON, G. On the number of segregating sites in genetical models without recombination. *Theoretical Population Biology* 7, 2 (1975), 256–276.
- [147] WICKHAM, H. *ggplot2: Elegant Graphics for Data Analysis*. Springer-Verlag New York, 2016.
- [148] WIEMERS, M., AND FIEDLER, K. Does the DNA barcoding gap exist? - a case study in blue butterflies (Lepidoptera: Lycaenidae). *Frontiers in Zoology* 4, 8 (2007).
- [149] WILKINSON, M., SZABO, C., FORD, C., YAROM, Y., CROXFORD, A., CAMP, A., AND GOODING, P. Replacing Sanger with Next Generation Sequencing to improve coverage and quality of reference DNA barcodes for plants. *Scientific Reports* 7 (2017), 46040.
- [150] WILLIAMS, P., BYVALTSEV, A., CEDERBERG, B., BEREZIN, M., ØDEGAARD, F., RASMUSSEN, C., RICHARDSON, L., HUANG, J., SHEFFIELD, C., AND WILLIAMS, S. Genes suggest ancestral colour polymorphisms are shared across morphologically cryptic species in arctic bumblebees. *PLOS ONE* 10, 12 (2015), e0144544.
- [151] WILLIAMS, P. H., HUANG, J., RASMONT, P., AND AN, J. Early-diverging bumblebees from across the roof of the world: the high-mountain subgenus Mendacibombus revised from species gene coalescents and morphology (Hymenoptera, Apidae). *Zootaxa* 4204, 1 (2016), 1–72.
- [152] WONG, E. H.-K., SHIVJI, M. S., AND HANNER, R. H. Identifying sharks with DNA barcodes: assessing the utility of a nucleotide diagnostic approach. *Molecular Ecology Resources* 9, s1 (2009), 243–256.
- [153] WRIGHT, S. The genetical structure of populations. *Annals of Eugenics* 15, 1 (1951), 323–354.
- [154] YAO, PENG-CHENG, G., HAI-YAN, W., YA-NAN, ZHANG, J.-H., CHEN, X.-Y., AND LI, H.-Q. Evaluating sampling strategy for DNA barcoding study of coastal and inland halo-tolerant Poaceae and Chenopodiaceae: A case study for increased sample size. *PLOS ONE* 12, 9 (2017), e0185311.
- [155] YOUNG, M. R., BEHAN-PELLETIER, V. M., AND HEBERT, P. D. Revealing the hyperdiverse mite fauna of subarctic Canada through DNA barcoding. *PLOS ONE* 7, 11 (2012), e48755.

- [156] YOUNG, R., ABOTT, C., THERRIAULT, T., AND ADAMOWICZ, S. Barcode-based species delimitation in the marine realm: a test using Hexanauplia (Multicrustacea: Thecostraca and Copepoda). *Genome* 60, 2 (2017), 169–182.
- [157] YOUNG, R., MILIÁN-GARCÍA, Y., YU, J., BULLAS-APPLETON, E., AND HANNER, R. Biosurveillance for invasive insect pest species using an environmental DNA metabarcoding approach and a high salt trap collection fluid. *Ecology and Evolution* (2020), 1–12.
- [158] YOUNG, R., MITTERBOECK, F., LOEZA-QUINTANA, T., AND ADAMOWICZ, S. Rates of molecular evolution and genetic diversity in European vs. North American populations of invasive insect species. *European Journal of Entomology* 115 (2018), 718–728.
- [159] ZHANG, A.-B., HE, L.-J., CROZIER, R. H., MUSTER, C., AND ZHU, C.-D. Estimating sample sizes for DNA barcoding. *Molecular Phylogenetics and Evolution* 54, 3 (2010), 1035–1039.
- [160] ZHANG, J., KAPLI, P., PAVLIDIS, P., AND STAMATAKIS, P. A general species delimitation method with applications to phylogenetic placements. *Bioinformatics* 29, 22 (2013), 2869–2876.

Appendix A

Additional Information Accompanying Chapter 3

Supplemental information can be found at <https://peerj.com/articles/cs-243/>.

Internal R code for HACSim can be found at <https://github.com/jphill01/HACSim.R>.

Appendix B

Additional Information Accompanying Chapter 4

Supplemental information can be found at <https://github.com/jphill01/PhD-Thesis-Appendix>.

Appendix C

Derivation of Approximate Confidence Interval for Sampling Sufficiency (θ) (Equation 3.3)

The Delta Method permits the approximation of the distribution of a function of a random variable provided said random variable is asymptotically normal.

Using the univariate Delta Method, an approximate large-sample (asymptotic) confidence interval for specimen sampling sufficiency (θ) based on the Central Limit Theorem (CLT) can be derived.

For a single parameter of interest, the Delta Method states that

$$\sqrt{n}(g(X_n) - g(\mu)) \rightarrow_d \mathcal{N}(0, [g'(\mu)]^2 \sigma^2) \quad (\text{C.1})$$

where n is the number of observations and $g(X_n)$ is a function of independent and identically distributed (iid) random variables X_1, \dots, X_n with finite variance σ^2 approximating some unknown parameter μ .

For the problem at hand, both N_i and H^* are constants and H_i is the random variable

of interest.

Writing Equation (3.1) as a function of H_i gives

$$g(H_i) = \frac{N_i H^*}{H_i}. \quad (\text{C.2})$$

Now, differentiating the above expression with respect to H_i using the Quotient Rule, factoring the denominator, and then simplifying leads to

$$g'(H_i) = \frac{-N_i H^*}{H_i^2} = \frac{-1}{H_i} \frac{N_i H^*}{H_i} = \frac{-N_{i+1}^*}{H_i}. \quad (\text{C.3})$$

By the Delta Method, the estimated variance of N^* is given by

$$\widehat{Var}[N_{i+1}^*] = [g'(H_i)]^2 \hat{\sigma}_{H_i}^2 = \left(\frac{-N_{i+1}^*}{H_i} \right)^2 \hat{\sigma}_{H_i}^2 = \left(\frac{N_{i+1}^*}{H_i} \hat{\sigma}_{H_i} \right)^2. \quad (\text{C.4})$$

and its corresponding standard deviation and standard error are respectively

$$\widehat{SD}[N_{i+1}^*] = \sqrt{\widehat{Var}[N_{i+1}^*]} = \frac{\hat{\sigma}_{H_i}}{H_i} N_{i+1}^* \quad (\text{C.5})$$

and

$$\widehat{SE}[N_{i+1}^*] = \frac{\widehat{SD}[N_{i+1}^*]}{\sqrt{N_{i+1}^*}} = \frac{\hat{\sigma}_{H_i}}{H_i} \sqrt{N_{i+1}^*}. \quad (\text{C.6})$$

Finally, a symmetric CI for θ can be constructed, leading to Equation (3.3)

$$N_{i+1}^* \pm z_{1-\frac{\alpha}{2}} \widehat{SE}[N_{i+1}^*] = N_{i+1}^* \pm z_{1-\frac{\alpha}{2}} \left(\frac{\hat{\sigma}_{H_i}}{H_i} \sqrt{N_{i+1}^*} \right). \quad (\text{C.7})$$

where $z_{1-\frac{\alpha}{2}}$ is the $(1 - \frac{\alpha}{2})100\%$ quantile of the Standard Normal distribution and $\hat{\sigma}_H$ is the estimated standard deviation for the number of haplotypes (H) found from sampling N^* specimens. However, there are several issues with this approach. First, the resulting interval is symmetric and, while tight, is likely to be biased, as it is centered on the estimated required sample size (N^*). This is not altogether unexpected due to reliance on the Central Limit Theorem in obtaining an approximate confidence interval for θ . In actuality, N^* would be expected to fall closer to either the lower or upper endpoint of the constructed CI compared to its centre as species' haplotype accumulation curves begin to saturate toward an asymptote (*i.e.*, H^*). Second, the resulting confidence interval is calculated from only a single random sample (*i.e.*, a single run of HACSsim); in reality, any interval estimate should be computed from multiple samples/runs whenever feasible. Methods for producing a non-symmetric interval are currently being investigated. Third, and perhaps most importantly, said confidence interval is unlikely to have desired nominal coverage probability of at least $(1 - \alpha)100\%$ (95% say); a non-symmetric interval may be able to compensate for this discrepancy however. Regardless, calculation of interval estimates for θ is important given the substantial amount of resources (both cost and effort) required to retrieve additional specimens for a given species of interest.